Measurement-Based Characterization of the 5G New Radio Small Cell Propagation Environment

Versão Final Após Defesa

Salomão Manuel Francisco

Dissertação para obtenção de Grau de Mestre em

Engenharia Electrotécnica e de Computadores

(2° ciclo de estudos)

Orientador: Prof. Dr. Fernando José da Silva Velez

julho de 2021

Dedication

I dedicate this dissertation to my family, specially to my children Rebeca Francisco and Rúben Francisco, my wife Cecília Francisco, to my father and mother Ismael Francisco and Georgina Florinda, to my sisters Júlia Francisco, Domingas Francisco, Emília Francisco and to my brother Eduardo Francisco. I also dedicate this Master of Science Work to my godfather Manuel Eduardo Cambinda and my godmother Mariana Ema Chiqquete Cambinda.

Acknowledgements

I want to express my deep gratitude to my advisor Prof. Doctor Fernando José da Silva Velez for all the knowledge and guidance he shared with me during this journey and for the patience he always had to me, especially for showing me the way out in moments when I could not see the way to continue. You left a part of you in me Professor Velez. Thank you, and thank you so much for the ”Tiger PC”, without which it would not be possible to carry out the hard work that culminated in the writing of this Master Science work! I also want to express my deep thanks to Prof. Doctor Jorge Dias Veloso and Escola Superior Pedagógica da Lunda Norte assigned to Universidade Lueji A'Nkonde for his encouragement and support in all aspects from the first to the last day of this stage of journey. Thank you very much Dr. Veloso for believing in me! To Prof. Doctor António Eduardo Vitória do Espírito Santo for the prompt interventions and support during my application to UBI and thank you for the best reception and guidance when I first arrived at UBI. To the engineers Rui Paulo and Rooderson Martines Andrade, thank you for your help with Latex, in the simulations, for helping me in the measurements with srsLTE system and for your patience, especially when I could not do things as they should be and for all you did to make this work a reality today. With you I learned to do science. To Engineer Anderson Rocha Ramos, thank you very much for not letting me give up. Your support was fundamental to this achievement. To Engineer Ricardo Freitas and Mr. Miguel Ângelo Lacerda Dias, thank you very much for your promptness whenever I needed you. To Mr. Rui Barata, thank you very much for your patience and for helping me to manufacture the antennas. To my family, thank you for your support. To my friends and brothers With emphasis on Rodrigo Emediato Fernandes, José Macosso Cumbo, Júlia Chivembe (Sovy), Elias Manuel Muahoca, Avelino Paulo and Arone Inácio Venâncio, thank you for everything you did for me. I also want to thank all the professors of the Departamento de Engenharia Eletromecânica who shared with me their knowledge and to everyone who directly or indirectly supported me so that this work could come to an end today, my most sincere gratitude. Finally, I thank the Supreme God, the creator of the heavens and the earth, for the life, health, courage, wisdom and for all the support he gave me during this journey of my life.

Preface

”You know something you speak when you can measure it. If you cannot measure what you say and express it in numbers your knowledge is of the meager and unsatisfactory type. It may be the beginning of knowledge, but you have barely advanced in yours thoughts to the science stage, whatever the subject.” William Thompson (Lord Kelvin - 1824 - 1907).

Palavras-chave

Ambiente de medição de interior e exterior, LTE-Advanced, 5G, propagação em pequenas células, estação de base, interferência, analisador de espectros, antena dipolo, ondas eletromagnéticas.

Resumo alargado

A investigação de sinais rádio em comunicações sem fios continua a gerar considerável interesse em todo mundo, devido ao seu amplo leque de aplicações, que inclui a troca de dados entre dois ou mais dispositivos, comunicações móveis e via Wi-Fi, infravermelho, transmissão de canais de televisão, monitorização de campos, proteção e vigilância costeira e observação ambiental para exploração. A tecnologia de ondas de rádio é o um dos vários recursos que viabilizam as comunicações de alta velocidade e encurta distâncias entre dois pontos em comunicação. Na realidade, caracterização da comunicação em redes com pequenas células é essencial para obter uma modelização apropriada de ambiente de propagação. Esta dissertação sob o tema "Measurement-Based Characterization of the 5G New Radio Small Cells Propagation Envioronment" foi desenvolvida num ambiente experimental, cujas tarefas foram divididas em fases. A **primeira fase** teve lugar no laboratório do Instituto de Telecomunicações da Covilhã (IT), afeto ao Departamento de Engenharia Eletromecânica. Nela foram feitas as simulações das antenas no software CST STUDIO, versão do estudante que foram utilizadas nos equipamentos durante as medições. Seguiu-se a padronização das mesmas nas faixas dos 2.6 GHz e 3.5 GHz, nas frequências centrais de 2.625 GHz e 3.590 GHZ, usando placas de circuitos impressos. Em seguida, foram feitas as medições do espectro e a caraterização do S11 e da carta de Smith para medir a impedância de entrada e o ganho. As medições foram feitas com recurso ao *Vector Network Analyzer* (VNA). Com base em cálculos matemáticos e considerações sobre a condutividade e permeabilidade do ambiente, as antenas foram construídas para uso em ambientes internos e externos e com ou sem interferentes. As antenas desenvolvidas são caracterizadas por sua largura de banda e suas características de radiação.

A **segunda fase** decorreu nas três salas adjacentes ao laboratório de Telecomunicações, na qual foi montada a topologia com o sistema srsLTE associado aos USRP B210 ligados aos computadores com o sistema operativo Linux com três componentes, nomeadamente uma estação base (BS), que serviu de fonte do sinal de comunicação com um equipamento de utilizador (UE) que o recebe, e dois interferentes. Importa realçar que esta segunda fase foi dividida em duas etapas, das quais uma sem interferente para medir a potência recebida da própria estação base e outra com os interferentes mais próximo e mais afastado da sala do sinal da própria célula. O objetivo desta fase foi o de verificar o modelo de propagação do sinal de comunicação da tecnologia LTE e medir a potência recebida pelo utilizador com recurso ao Analisador de Espectro portátil FSH8 da Rohde & Schwarz capaz de medir de 10 kHz a 8 GHz, feita na frequência central de 2.625 GHz.

Nas medições feitas em ambiente interior, o tamanho de cada uma das três salas é 7.32 × 7.32 metros quadrados. Embora a sala 1 seja a sala de interesse, onde ocorreram as medições teóricas e práticas, as BSs que atuam como nós interferentes também são consideradas separadamente na sala 2 ou na sala 3. Ao variar as posições de UE dentro da sala 1, foi possível verificar que os valores superiores da potência recebida ocorrem próximos à BS central. No entanto, a potência recebida não diminui repentinamente por causa do efeito do ganho reduzido no diagrama de radiação na parte traseira da antena. Além disso, foi demonstrado

que existe um efeito de “atenuação da parede” comprovado pelo aumento da atenuação de trajeto entre a sala 1 e a sala 2 (ou entre a sala 2 e 3). Se considerarmos uma atenuação para cada parede de cerca de 7-9 dB, verifica-se a tendência do modelo WINNER II a 2.625 GHz para a interferência que atravessa as diversas paredes. Trabalhos futuros incluem a investigação da banda de frequência de 3.5 GHz.
Já a **terceira fase** foi realizada nas instalações do antigo aeródromo da Covilhã, e em todas as fases servimo-nos de uma licença concedida pela Entidade Reguladora do Espectro (ICP-ANACOM), que permitiu realizar testes de verificação da propagação do sinal no ambiente livre na faixa de frequência dos 2.6 GHz com 2500 – 2510 MHz (UL - Uplink) e 2620 – 2630 MHz (DL - Downlink). A terceira fase ainda está a decorrer nas instalações do antigo aeródromo da Covilhã, mediante a mesma licença temporária que nos foi atribuída pelo Instituto de Comunicações de Portugal ou Autoridade Nacional de Comunicações (ICP-ANACOM) sendo esta reguladora do espectro. O objetivo é continuar a investigar o comportamento de duas inclinações no cenário UMi. Testes muito iniciais LTE-Advanced foram realizados para verificar a propagação dos dois raios (direto e refletido, com uma reflexão no asfalto) do BS implementado com o sistema USRP B210 e srsLTE, considerando uma célula urbana com um comprimento de 80 metros uma estação base interferente em 320 metros, a operar, provisoriamente, a 2500 - 2510 MHz (na ligação descendente, DL - Downlink, devido à disponibilidade de uma antena direcional específica para esta banda).
Finalmente este trabalho de investigação pode ser resumidamente dividido em três categorias, nomeadamente investigação de análises teóricas e matemáticas relevantes da propagação de ondas de rádio em meios com e sem interferência significativa. Medições para verificar o comportamento do sinal de propagação da tecnologia LTE-Advanced com recursos ao analisador de espectro, simulação das antenas, fabricação e medição das características de radiação das mesmas. Assim, as antenas concebidas com bons resultados foram fabricadas nas instalações da Faculdade de Ciências no Departamento de Física da Universidade da Beira Interior, sendo de seguidas testadas e caracterizadas com o auxílio do *Vector Nettwork Analyzer* disponível no Laboratório de Telecomunicações do Departamento de Engenharia Eletromecânica da Universidade da Beira Interior. E, finalmente, os cálculos estatísticos que incluem o teste de normalidade de Kolmogorov-Smirnov com recurso ao software estatístico SPSS para validar os resultados obtidos seguida da construção dos gráficos no Matlab em 3D, conforme a superfície da sala.

Abstract

The characterization of the wireless medium in indoor small cell networks is essential to obtain appropriate modelling of the propagation environment. This dissertation on ”Measurement-Based Characterization of the 5G New Radio Small Cell Propagation Environment” has been developed in an experimental environment. The underlying tasks are divided into three phases. The **first phase** took place in the laboratory of the Instituto de Telecomunicações – Covilhã, located in the Departamento de Engenharia Electromecânica of Universidade da Beira Interior. During this part of the research, spectrum measurements and the characterization of the S11 parameter (response in the first port for the signal incident in the first port) have been made experimentally through the printed circuit board antennas in the 2.6 GHz and 3.5 GHz frequency bands operating in the 2.625 GHz and 3.590 GHz center frequency, manufactured by us. The fabrication of the antennas was preceded by the simulation in the student version CST STUDIO software. In this phase, the spectrum measurements and the characterization of Smith Chart have been made to measure gain and impedance using the Rohde & Schwarz *Vector Network Analyzer* (VNA) from IT laboratory. Based on mathematical calculations and considerations on the conductivity and permeability of the environment, the antennas were built for use in indoor and outdoor environments. The developed antennas are characterized by their bandwidth and their radiation characteristics.

The **second phase** took place in the three rooms adjacent to the laboratory, in which the srsLTE emulation software was applied to the 4G indoor scenario. The experimental setup includes three elements, namely a base station (BS or 4G eNodeB), which transmits the communication signal and which served as a signal source, a user equipment (UE), and an interfering eNodeB. The size of each room is 7.32 × 7.32 square meters. While room 1 is the room of interest, where theoretical and practical measurements took place, BSs that act as wireless interfering nodes are also separately considered either in room 2 or room 3. By varying the UE positions within room 1, it was possible to verify that the highest values of the received power occur close to the central BS. However, the received power does not decrease suddenly because of the reduced gain in the radiation pattern in the back part of the antenna. In addition, it was demonstrated that there is an effect of “wall loss”proven by the path loss increase between room 1 and room 2 (or between room 2 and 3). If we consider an attenuation for each wall of circa 7-9 dB the trend of the WINNER II at 2.625 GHz model for the interference coming across different walls is verified. Future work includes to investigate the 3.5 GHz frequency band.

The **third phase** is being carried out at the facilities of the old aerodrome of Covilhã which, using a temporary license assigned to us by Instituto de Comunicações Português (ICP-ANACOM) as the two first phases. The aim of this phase is to investigate the two-slope behaviour in the UMi scenario. Very initial LTE-Advanced tests have been performed to verify the propagation of the two ray (with a reflection in the asphalt) from BS implemented with USRP B210 and srsLTE system by considering an urban cell with a length of 80 m and an interfering base station at 320 m, at 2500 - 2510 MHz (DL - Downlink) by now, mainly due to the current availability of a directional antenna in this specific band.

Keywords

Indoor and outdoor measurement environment, Small Cell propagation, LTE-Advanced, 5G New Radio, base station, interfering node, spectrum analyzer, radio dipole antenna simulation, electromagnetic waves

Contents

List of Figures

List of Tables

List of Acronyms

μ	Mean
1 G	First Generation
2 G	Second Generation
3 G	Third Generation
3GPP	3rd Generation Partnership Project
4 G	Fourth Generation
5 G	Fifth Generation
AM	Amplitude Modulation
AMPS	Advanced Mobile Phone Systems
AT&T	American Telephone and Telegraph
BER	Bit Error Rates
BLER	Block Error Ratio
BMS	Broadcast/Multicast Services
BS	Base Station
C/I	Carrier-to interference ratio
CDMA	Code Division Multiple Access
CoMP	Coordinated Multipoint
CP	Ciclic Prefix
CP-OFDM	Cyclic Prefix Orthogonal Frequency Division Multiplexing
CST	Computer Simulation Technology
DFT	Discrete Fourier Transformations
DFTS	Discrete Fourier Transformations Spread
DL	Downlink
DUT	Device Under Test
E	Electric Field
EDGE	Enhanced Data rate from GSM Evolution
EESM	Exponential effective SNR mapping
ELF and VLF	Extremely Low and very low Frequency
eNB	Envolved Node Base
ETSI	European Telecommunications Standards Institute
FCC	Federal Communications Commission
FDD	Frequency Division Duplex
FM	Frequency Modulation
FR	Frequency Range
gnB	generation NodeB
GPRS	General Packet Radio Service
GSM	Global System for Mobile Communications
H	Magnetic Field
HAPs	High Altitude Platform Station
HD	High Definition

HetNet	Heterogeneous Networks
HF	High Frequencies
HPBW	Half-Power Beam Width
ICP-ANACOM	Instituto de Comunicações de Portugal-Autoridade Nacional de Comunicações
IEEE	Institute of Electrical and Electronics Engineers
IT	Instituto de Telecomunicações
KPI	Key Performance Indicator
LAPs	Link Access Protocol
LBT	Listen Before talk
LF	Low Frequencies
LTE	Long Term Evolution
LTE-A	Long Term Evolution Advanced
LTE-Sim	Long Term Evolution Simulate
MATLAB	Matrix Laboratory
MBB	Mobile Broadband
MCC	Mission Critical Communications
MCL	Maximum Coupling Loss
MCN	Macro Cellular network
MCSs	Modulation and Coding Schemes
MIMO	multiple input and multiple output
MMC	Massive Machine Communications
MMS	Multimedia Message Service
mmW	millimeter wave
NMT	Nordic Mobile Telephone
OFDM	Orthogonal Frequency Division Multiplexing
OTA	Over-the-air
PC	Personal Computer
PHY	Physical Layer
Pr	Received Power
PRB	Physical Resources Allocated Blocks
PSA	Portable Spectrum Analyzer
QAM	Quadrature Amplitude Modulation
QNAF	Quadro Nacional de Atribuição de Frequências
QoS	Quality of Service
R & S	Rohde & SChwarz
Rel 15	Release 15
SC	Small Cell
SCS	Subcarrier Spacing
SD	Standard Deviation
SHF	Super High Frequency
SIGINT & EW	Signals Intelligence and tactical electronic warfare
SINR	Signal-to-interference-plus-noise ratio

SMS	Short Message Service
SNR	Signal-to-Noise Ratio
SPSS	Statistical Package of Social Science
srsLTE	Software Radio System Long Term Evolution
sig	statistical significance
symRate	Synchronization Rate
TDD	Time Division Duplex
TRP	Total Radiated Power
TRS	Total Radiated Sensitivity
TV	Television
UE	User Equipment
UMi	Urban Micro Scenario
UHF	Ultra High Frequency
UMiLoS	Urban Micro Line-of-Sight
UL	Uplink
US	Unit State
USA	United State American
USRP	Universal Software Radio Peripherals
V2X	Vehicle-to-vehicle and vehicle-to-infrastructure communications
VHF	Very High Frequencies
VNA	Vector Network Analyzer
VR	Virtual Reality
VSWR	Voltage Standing Wave Ratio
WAP	wireless application protocol
WCDMA	Widband Code Division Multiple Access
WIMAX	Worldwide Inter-operability for Microwave Access

Chapter 1

Introduction

The world is increasingly developing, and its population is growing day after day, giving rise to new challenges to meet the demands at every stage of society making services and interpersonal interactions become increasingly demanding. In today's societies, communication is seen as the most powerful tool, information and communication technologies are and must be increasingly sophisticated in order to answer the real concerns of humanity, science and technology. Thus, it is the task of mankind to improve communication technologies to turn the world more and more into a global village, facilitating interpersonal communications, and the two-way human – machine interaction.

Telecommunications are undoubtedly the main tool to leverages the development of societies as part of the daily life of persons. From the moment when the first international telegraph cable was launched in 1858 until the first wireless telephone transmission by Father Roberto Landell in 1893 to 1894, telecommunications have never stopped evolving and have become more popular in recent years due to the rapid evolution from the first generation (1G) to the fifth generation (5G). These reforms were due to the demands for transmission technologies compatible with the demand for telecommunications services. The word " generation " refers to the nature of the shift in transmission of technologies compatible with the services in the new frequency bands.

By exponential growth of ultra-reliable low latency communication, machine to machine technology, and continues increase in the formations or the demand of applications which needed the high bandwidth, because of this the cellular networks are close to its edge, and this in turn has generated a growing interest in research on the implementation of Small Cellular access points (SC) to ensure extended coverage and link expenses. In this scenario of Heterogeneous Networks (HetNets) there are a variety of short-range cells that support the Macro Cellular network (MCN) and this approach can increase coverage and spatial reuse, allowing cellular systems to provide more data rates while preserving mobility and connectivity [1]. According [2], in 2018, 3GPP finalized the technical specifications for 5G New Radio (NR) and the first commercial 5G network started to operate in the first semester of 2019.

It is expected that the 5G NR technology will allow for significantly faster wireless communication and to will improve the subscribers experiences, by delivering much higher data rates in both uplink and downlink direction. NR employs Cyclic Prefix Orthogonal Frequency Division Multiplexing (CP-OFDM) and Discrete Fourier Transform Spread (DFTS) OFDM based waveforms [3], operating in two sets of frequency ranges identified as frequency range 1 (FR1) and frequency range 2 (FR2). FR1 comprises the sub-6 GHz frequency range (450-6000 MHz) while FR2 is the mmWaves (24250-52600 MHz).

In a saturated network, the average signal-to-interference-plus-noise ratio (SINR) can be mapped into the supported throughput obtained with the implicit function formulation considered in [3]. The only difference in the shape of these curves for the average SINR (also referred to as Carrier-to interference ratio, CNIR) and supported throughput is a transformation that depends on the weights of each value of the physical layer (PHY) throughput that maps the different Modulation and Coding Schemes (MCSs) presented in the different coverage rings of the SC. This Master Science work gives contributions to the fabrication of simple dipole antennas and fundamental aspects of the measurement of spectrum in telecommunications systems to verifies the interference between the average SINR and the supported throughput in a context of 4G, 5G NR SC HetNets, while considering the impact of applying the winner II (indoor) and two-slope urban micro Line-of-Sight (UMiLo propagation models in the optimization process.

1.1 A Brief History about Mobile Communications

The US Federal Communications Commission (FCC) approved in 1946 a first mobile telephony to be operate one year later in 1947 by AT & T. At that time, the equipment were bulky and had to be installed in a vehicle due to the weight and its excessive power consumption. From this point on, more than three decades of cellular communication technology evolution has led to a shift from analog to digital format of communication, going from what was mainly voice to high speed data communication [3].

The first generation of cellular communication (1G) arose in the mid '80s, with mainly voice transmission fuction, grew up using formats such as advanced mobile phone systems (AMPS) in the United State American (USA) and nordic mobile telephone (NMT) in the Scandinavia [3]. These analog formats were later replaced moving to wards 2G with the first digital communication schemes around the mid to late 1990s global system for mobile communications (GSM) in Europe and digital AMPS for the USA. At this point, the short message service (SMS) was introduced, being one of the first widely, used no voice applications for cellular communications. Enhancement 2,5G using enhanced data rate from GSM evolution (EDGE), general packet radio service (GPRS) and code division multiple access (CDMA) sparked the use of mobile data communication and early cellular internet connectivity in the early 2000s. This was an early enabler, which did, however, require a specific protocol, known as Wireless Application Protocol (WAP).

Moving from 2G into 3G in order to meet the increasing demand for cellular access data rate, universal mobile communications systems (UMTS) based on wideband CDMA (WCDMA) technology was introduced by third generation partnership project (3GPP) just around 2000. With advances in mobile user equipment technology, this enabled the user to not only communicate via multimedia message service (MMS), but also stream video content. Transitioning to 4G, long term evolution (LTE) was introduced, which does not only imply major change on the air interface, but was moving from the code division multiplexing to orthogonal frequency division multiplexing (OFDM) and time division duplex (TDD) or frequency division duplex (FDD) [3].

Entering the era of 4G, there were mainly two competing technologies at an early stage These were worldwide inter-operability for microwave access (WIMAX), based on IEEE 802.16m, and LTE Advanced, which is an extension of LTE. LTE-A introduced technology components

such as carrier aggregation and improved support for coordinated multipoint (CoMP) transmissions and heterogeneous network (HetNet) deployment of improving Quality of Service (QoS) in hot-spots and coverage for cell-edge users. Long term evolution advanced (LTE-A) prevailed as the dominant cellular access technology today and has served as basic transition to 5G mobile communications. The transition from 4G to 5G is inspired by new human-centric and machine -centric services[3].
According [4] and [5], the telecommunications systems have growing as follow:

- First Generation (1G) characterized by the use of analog networks, was introduced in the beginnings of 1980's;
- Second Generation (2G) with the introduction of digital multiple access technologies cellular took a big leap towards the progression in wireless cellular technology when launched in 1990's;
- Third Generation (3G) with support to multimedia services, was developed to improve voice services, data throughput, high Quality of Service (QoS) and information security;
- Fourth Generation (4G) user can relish the following service: - High Definition (HD) voice, SMS, MMS, mobile television (TV), wearable devices, HD streaming, Global roaming, gaming services etc;
- Fifth Generation (5G), supports high bandwidth capacity.

1.2 Other Technological Advancements in Telecommunications

The evaluation of wireless systems is used in the process of designing radio networks, e.g., in cellular telephony. Then, terrain locations of wireless network nodes, e.g., base stations, is an important issue for providing different services for mobile users, i.e. providing coverage of an area with network access [6].
As networks become intelligent platforms for innovation, future network security will be key to establishing trustworthiness across future societies. Over the last two decades, technology has been steadily evolving in a variety of domains: machines are endowed with increasingly powerful processors and larger memory capacities; device-to-device communications open the door to new exquisite inventions and realities; the user population grows more dependent upon technological solutions for everyday problems and needs; quality standards display a never-ending tendency to rise; and the cycle goes on.
With 5G networks promoting larger bandwidth for data transmission and lower latency in communications, potential product and services put on standby due to 4G limitations are back in the game, along with some innovative ideas. It is expected that 5G networks will allow the diffusion of VR in real-time applications, since larger bandwidth and lower latency may help solve the problem of motion sickness, while at the same time improving video quality in VR devices.
Small cells are expected to be an important complementary component for 5G (and beyond) communication systems to achieve the goal of global access to the Internet for all to fully

exploit the benefits of the distinct features of various small cells, to inject additional capacity and expand the coverage for underserved areas in a flexible, seamless, and cost-effective manner. It is proposed an integrated airground heterogeneous network architecture and outline its characteristics and potential advantages. Several key enabling techniques for the integrated system are discussed in detail in this Master Science work. In addition, we identify the potential application scenarios where the system can further enhance the performance of traditional terrestrial networks.

1.3 Heterogeneous Networks

LTE-A offers high spectral efficiency, low latency and high peak data rates. LTE-A leverages the economies of scale of 3G, as well as the ecosystem of infrastructure and devices vendors to provide the highest performance in a cost effective. Manner Current wireless cellular networks are typically deployed as homogeneous networks using a macro-centric planned process. A homogeneous cellular system is a network of base-stations in a planned layout and a collection of user terminals, in which all the base-stations have similar transmit power levels, antenna patterns, standardized noise receiver, and similar backhaul connectivity to the (packet) data network. Moreover, all base-stations offer unrestricted assess to user terminals in the network, and serve roughly the same number of user terminals, all of which carry similar data flows with similar QoS requirements.

The locations of the macro base-stations are carefully chosen by network planning, and the base-station settings are properly configured to maximize the coverage and control the interference between base-stations. As the traffic demand grows and the RF environment changes, the network relies on cell splitting or additional carriers to overcome capacity and link budget limitations and maintain uniform user experience.

However, this deployment process is complex and iterative. Moreover, site acquisition for macro base-stations with towers becomes more difficult in dense urban areas. A more flexible deployment model is needed for operators to improve broadband user experience in a ubiquitous and cost effective way. Wireless cellular systems have evolved to the point where an isolated system (with just one base-station) achieves near optimal performance, as determined by information theoretic capacity limits. Future gains of wireless networks will be obtained more from advanced network topology, which will bring the network closer to the mobile users. Heterogeneous networks utilizing a diverse set of base-stations can be deployed to improve spectral efficiency per unit area [7].

So, there is no single solution solution that can effectively satisfy all the needs of universal internet access, global service provision will likely need the inter-working of multiple heterogeneous wireless technologies [7, 8]. In the regions where providing desirable terrestrial assistance is not efficient, various types of aerial platforms can act as a viable alternative to improve performance, agility, and flexibility of 5G and beyond mobile networks in unprecedented ways. Through integrating high altitude platform station (HAPs) and LAP link access protocol (LAPs) into conventional terrestrial networks, the benefits from both air and ground segments can be fully exploited to support multifarious communication services and scenarios [8].

1.4 Challenges in Telecommunications of The XXI Century

On a daily basis, users are often faced with faults or interruptions in the signals of communication systems, whether in urban or in rural areas. These drops or failures of signal can be eliminated or minimized if small cells are installed that can serve as network carriers and fill in the gaps that the base station cannot reach. These small cells can be homogenized with the base station, with the sole purpose of improving the quality of the network signal reaching the user's device and guaranteeing their satisfaction.

It is known that generation (5G) wireless system support data rates up to several Mbps per use because it is operate high data rate at millimeter waves (mmW) about (26.5 GHz - 40 GHz). Improvement is significant compared to currently used LTE networks. One of the first public demonstration for wide audience of the capabilities of 5G networks was open during Winter Olympic Games in Korea [9]. The support of 5G communications system is one of the first wireless backhaul communication operating as wireless last mile system. Systems operating at 60 GHz suffer from a shorter link range than systems operating at 28 GHz. Telecommunications standardization is moving towards a direction where requirements are defined based on radiated power levels.

Conducted measurements have been easier and more robust to perform at the lower frequencies, but will change when 5G communication system with massive Multiple Input Multiple Output (MIMO), radio solutions will come into operation. Conductive measurements for massive - MIMO system will be hard to operate, calibrate, maintain and guarantee the accuracy of the test signal in each of the antenna port.

Since the 1980s, the mobile phone started to be used, telecommunications has undergone significant changes and has experienced a considerable advance. Studies show that the introduction of small cells through low-power base stations for macro - eNBs has been an easy and inexpensive solution to increase capacity at points with low signal and high user demand to fill the coverage gaps and improve network performance and quality of service on 4G and 5G New Radio (NR) networks. The combination of macro molecules with small cells generating a heterogeneous network offers a higher bit rate per unit area [10].

One of the potential outcomes to enhance the network capacity is to enhance the spectral efficiency per unit area by expanding the serving node densities. This is unreasonable on account of present Macro evolved node B (eNB) for which site acquisition is expensive. The idea of heterogeneous network (HetNet) and multi-hop relay (MHR) are extremely prominent in LTE standard, where small cells are deployed along with Macro cell. Small cells are more suitable solution for the coverage and traffic issues experienced by Macro cell users. Because of the high cost and lack of radio resources, a precise and productive HetNet deployment seems uttermost important [10].

As mentioned in the previous section, communication technologies have evolved rapidly from the first generation (1G) to the fifth generation (5G) and each technology and each stage appears with the aim of responding to the real challenges of the time.

The 5G technology is the fifth generation of cellular networks, bringing new capabilities that will create opportunities for people, businesses and society.

1.5 Challenges for this Research

Any theory, however extraordinary and important it may seem, if it is not possible to associate with practice, or if it is principles are not verifiable in practice, it is worth half of what it represents or, a simple theoretical idea with no repercussions on the objective life and does not contribute to science.
The sustained development of communication networks and computers, over time, supports the need for training in communication networks in the context of the Master in Electromechanical Engineering at the University of Beira Interior.
The theme of this work came up in a conversation maintained as a result of the follow-up of the academic relationship between the supervisor and the student, although the initial idea came from the student and which was improved in the academic conversation with the professor, is based on a specific need for laboratory, which consists of having a set of actions that allow to carry out experimental tests to verify and validate a model of propagation of electromagnetic waves with two exponents of propagation (“two-slope”).
The required tests have been carried out by using a portable spectrum analyzer that allows measuring the received power and verifying the frequency spectrum that propagates through the electromagnetic waves in dBm.
The measurements have been made in a real telecommunications environment where two URSP B120 devices were mounted and operated together with the srsLTE system. One of the devices is the base station (BS) and other one are user (UE) or interferers.

1.6 Motivation

The motivation to develop a scientific work is always to contribute to the evolution of science. In this case the motivation is to explore measurement-based approach to characterize indoor small cell propagation environments while improving the experimental radio frequency (RF) skills of the author complemented by other motivations listed below, such as:

- The enormous challenge of studying new mobile radio technologies and tools used in real deployments in the context of telecommunications;
- Experimentation, the anticipation of possible technological risks and the consolidation of all knowledge acquired during the curricular part of this cycle of study, specifically in the ”Communication Systems” curricular unit, are part of the motivations of developing this dissertation with the theme ”Measurement-based characterization of the 5G New Radio small cells propagation environment”;
- Participate in national and international scientific networking events with qualified research work.

1.7 Objectives

One of the several objectives of the Institute de Telecommunicações do Departamento de Engenharia Electromecanica is to create and share knowledge on advanced communication network while in order to provide future professionals with conceptual preparation and dimensioning tools that allow them to integrate multidisciplinary teams in projects where telecommunications systems are one of the relevant components, including fixed wireless, terrestrial or satellite components.
In this context, this Master of Science dissertation work aims to:

1. Develop experimental research work on 5G New Radio through measurements of the radio-frequency spectrum to verify its behavior propagation, and its influence on wireless telecommunications systems;
2. Measure the receiver power by the user and interferer when the signal is emitted from a base station in the srsLTE indoor scenarios;
3. Improving technical tests to prove the applicability of the model of two-slope propagation urban micro Line-of-Sight (UMiLoS).
4. Characterize the small cell propagation environments by at the old Covilhã aerodrome in the 2 x 10 MHz bands, 2500 MHz - 2510 MHz (UL - Uplink) and 2620 - 2630 MHz (DL - Downlink) bands, and for the 3.5 GHz, available 2 x 20 MHz in the frequency bands 3480 - 3500 MHz (UL) and 3580 - 3600 MHz (DL) assigned to us by ICP-ANACOM to prove the applicability of the model of two-slope propagation urban micro Line-of-Sight (UMiLoS).;
5. Verify and validate a propagation model with two exponents ("two-slope") through computational simulations using Linux operative system and two USRP devices built base station and one user.
6. Disseminate results

1.8 Contributions

The main contributions of this Master dissertation is to develop a practical laboratory work using the spectrum measurement instruments available in the Laboratório do Instituto de Telecomunicações da Covilhã (IT). The work facilitates to understand how Software defined radio like Universal Software Radio Peripherals (USRPs) and simple dipole antennas can emulate LTE-Advanced networks and may be used as base station and user equipments (UEs) indoor or outdoor field tests. The research enbles to verify WINNER II propagation modeling for the indoor femtocell environment by considering different classrooms near a common corridor while measuring the received power in UEs (radiated by small eNode B of the own cell and from the interferer cells). These measurements consisted of tens of repetitions in each of the 49 points of the room and have been carrier out either by using the Software Radio System LTE (srsLTE) that emulate the LTE-Advanced network itself or by measuring the

receiver power with a Rohde & Schwarz FSH8 spectrum analyzer. Besides, inicial outdoor filed trial have also been carried out.
The other important contribution of this research includes the submission of two papers with experimental results [11]:
Rooderson M. Andrade, Salomão M. Francisco, Rui R. Paulo and Fernando J. Velez, entitled "**Characterization of Indoor Small Cells Propagation**," submitted to Globecom 2021, Madrid, Spain, December 2021.
Salomão M. Francisco, Rooderson M. Andrade, Rui R. Paulo and Fernando J. Velez, entitled "**Measurement-Based Characterization of Small Cells Indoor Propagation Environments**," submitted to a convened Session from COST CA 20120 "INTERACT" EuCAP 2022, Madrid, Spain, from March 27th to April 1st.

1.9 Outline of the Dissertation

The dissertation sequence is shown in the Figure 1.1. The first part of the present master work has presented brief general aspects related to evolution and of mobile communications, a brief overview of the first to fifth generation and the technical contributions of its launches to the standardization of mobile technologies, heterogeneous networks with small cells. In chapter 2, the state of the art is presented complemented by a study the background of the subject under study, as well as identification the research opportunities on the characterization of the propagation environment of small cell network with a central cell or base tower. The study presented in chapter 2 considers the ways electromagnetic waves propagate and its relations with 5G New Radio, evaluating the capacity of the system considering different radio of cells and equipment from user distances. The properties of the magnetic fields that serve as carriers for small cells and their models are also presented.
In chapter 3, the research methodology of study used for the long term evolution packet level experimentation and algorithms of the measurements are presented. It is used to implement and evaluate measurement considering deployment scenarios with small cells in different frequency bands and the system capacity is evaluated.
In chapter 4, characterizes the propagation of small cells networks and techniques applied in indoor and outdoor field tests are also addressed.
Chapter 5 presents the results followed by its analysis and lessons learned.
Chapter 6 draws conclusions from the work, and concludes a brief overview final of the results obtained together with and suggestions for future work.
Five appendices (A, B, C and D) are presented in the final part of the document.

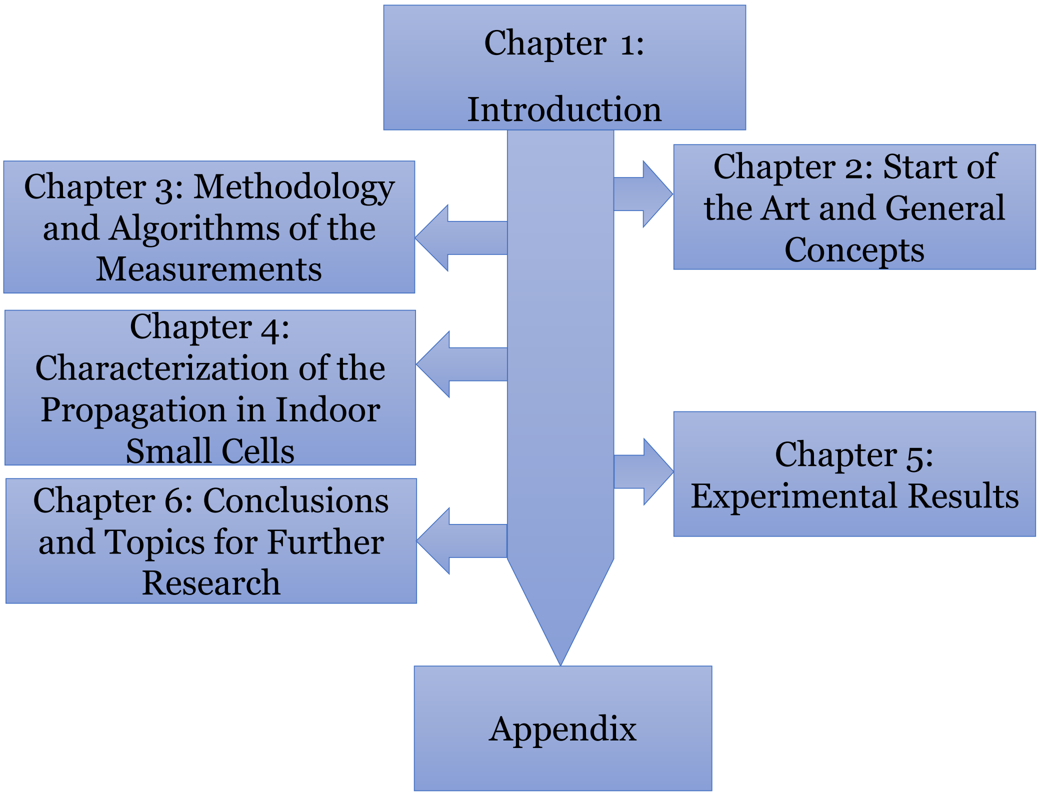

Figure 1.1: Structure of the dissertation

Chapter 2

State of the Art and General Concepts

2.1 Introduction

The latest 5G technology, must operate in backward compatibility LTE/LTE-A in the non-autonomous phase, with cells from both technologies that offer different or equal coverage. Within 5G NR deployment scenarios, among other topologies, is possible to have an eNB LTE/LTE-A (evolved NodeB) as a master node, offering an anchor carrier that can be propelled by a NR gNB (Next-generation NodeB), with aggregated data flow by the evolved package core (EPC) [12].
5G technology shall provide wireless connectivity for anything that can benefit from being connect. To enable a truly networked society, there are three major challenges [12]:

- A massive growth in the number of connected;
- A massive growth in traffic volume;
- A wide range of applications with diverse requirements and characteristics.

To address this challenges, 5G wireless access not only requires new functionalities but also substantially.
The operation of the physical layer of the NR is based on the Orthogonal Frequency Division Multiplex (OFDM) with cyclic prefix (CP) for the downlink and uplink directions. Uplink the communication also supports Discrete Fourier-OFDM Transformations (DFT-physical resources allocated Blocks (PRBs)s-OFDM) and both channels are designed be agnostic about bandwidth, with their capacity being determined by the number of , which are a function of operational bandwidth and subcarrier spacing (SCS)[12].
The choice of radio waveform is the core physical layer of decision for any wireless access technology [13].
After evaluating all proposed waveforms, 3GPP agreed to adopt orthogonal frequency division multiplexing (OFDM) with a cyclic prefix (CP) for downlink (DL) and uplink (UL) transmissions [14].
CP-OFDM defines the low implementation and low cost allowance for broadband operations and multiple input and multiple output (MIMO) technologies.
NR supports the use of discrete Fourier transform (DFT), OFDM scattering (DFT-S-OFDM) in the uplink to improve coverage and operation in spectrum ranges from sub - 1 GHz to millimeter wave bands. Two frequency ranges (FRs) are defined in Rel-15 [15] [16]:

- FR1: 410 MHz–7125 MHz, referred to as sub-6 GHz;
- FR2: 2425 MHz–52.6 GHz, referred to as millimeter-wave.

Table 2.1 shows the frequencies of 5G New Radio.

Table 2.1: NR Frequency Bands, extracted from [16]

NR operating band	Duplex mode	Uplink (UL) operating band	Downlink (UL) operating band
n1	FDD	1920 MHz – 1980 MHz	2110 MHz – 2170 MHz
n2	FDD	1850 MHz – 1910 MHz	1930 MHz – 1990 MHz
n3	FDD	1710 MHz – 1785 MHz	1805 MHz – 1880 MHz
n5	FDD	824 MHz – 849 MHz	869 MHz – 894 MHz
n7	FDD	2500 MHz – 2570 MHz	2620 MHz – 2690 MHz
n8	FDD	880 MHz – 915 MHz	925 MHz – 960 MHz
n12	FDD	699 MHz – 716 MHz	729 MHz – 746 MHz
n13	FDD	777 MHz - 787 MHz	746 MHz - 756 MHz
n14	FDD	788 MHz -798 MHz	758 MHz - 768 MHz
n18	FDD	815 MHz - 830 MHz	860 MHz - 875 MHz
n20	FDD	832 MHz – 862 MHz	791 MHz – 821 MHz
n25	FDD	1850 MHz – 1915 MHz	1930 MHz – 1995 MHz
n28	FDD	703 MHz – 748 MHz	758 MHz – 803 MHz
n34	TDD	2010 MHz – 2025 MHz	2010 MHz – 2025 MHz
n38	TDD	2570 MHz – 2620 MHz	2570 MHz – 2620 MHz
n39	TDD	1880 MHz – 1920 MHz	1880 MHz – 1920 MHz
n40	TDD	2300 MHz – 2400 MHz	2300 MHz – 2400 MHz
n41	TDD	2496 MHz – 2690 MHz	2496 MHz – 2690 MHz
n51	TDD	1427 MHz – 1432 MHz	1427 MHz – 1432 MHz
n66	FDD	1710 MHz – 1780 MHz	2110 MHz – 2200 MHz
n70	FDD	1695 MHz – 1710 MHz	1995 MHz – 2020 MHz
n71	FDD	663 MHz – 698 MHz	617 MHz – 652 MHz
n75	SDL	N/A	1432 MHz – 1517 MHz
n76	SDL	N/A	1427 MHz – 1432 MHz
n77	TDD	3300 MHz – 4200 MHz	3300 MHz – 4200 MHz
n78	TDD	3300 MHz – 3800 MHz	3300 MHz – 3800 MHz
n79	TDD	4400 MHz – 5000 MHz	4400 MHz – 5000 MHz
n80	SUL	1710 MHz – 1785 MHz	N/A
n81	SUL	880 MHz – 915 MHz	N/A
n82	SUL	832 MHz – 862 MHz	N/A
n83	SUL	703 MHz – 748 MHz	N/A
n84	SUL	1920 MHz – 1980 MHz	N/A
n86	SUL	1710 MHz – 1780MHz	N/A
n257	TDD	26500 MHz – 29500 MHz	26500 MHz – 29500 MHz
n258	TDD	24250 MHz – 27500 MHz	24250 MHz – 27500 MHz
n260	TDD	37000 MHz – 40000 MHz	37000 MHz – 40000 MHz
n261	TDD	27500 MHz – 28350 MHz	27500 MHz – 28350 MHz

2.2 Small Cell Environment

To meet the challenges posed by the expected rise in traffic volumes in wireless communication, research on 5G networks is anticipated to intensify in this decade. Rapidly rising demand for radio communication and the explosion in the number of mobile communications service subscribers have led to the need for optimization in the development of next-generation mobile communication systems. The development of competitive the 5G wireless transmission technology and efficient frequency-use research are based on understanding the characteristics of the radio channel. This channel is based on the exact model, including elements of the 5G wireless transmission applications, such as frequency, time, space, and polarization.

Moreover, international standardization organizations such as the IEEE and the 3GPP have considered studies on available bandwidth to present a candidate for each frequency band. From the examination of the candidate frequency bands of 5G New Radio standardization organizations, 3 GHz and 4 GHz bands have been classified as likely to be the most utilized. That involves including only part of the operators on the 3.5 GHz band [17], LTE-TDD; particular areas, such as suburban areas, are often used for fixed wireless [17]

2.3 RF and their Unlicensed Bands at 5G band

RF energy is all around us, the magnetic fields, radio waves, microwaves and wireless signals. Some of the these are just a few applications of this feature as radio, television broadcasting, cellular telephones, satellite communications, microwave ovens, radars, and industrial heaters.

Spectrum sensing is one of the most challenging problems in cognitive radio systems [18]. The spectrum of interest needs to be characterized and unused frequencies should be identified for possible exploitation. This process, however, should be computationally simple and fast in order to catch up with the changing transmission parameters [19]. Besides licensed bands (2.6 and 3.5 GHz bands) our study also visages propagation at 5.62 GHz frequency bands that can be shared in Portugal, accordingo to the QNAF conditions [20]

To study wave-forms propagation, it is necessary beginning by considering Maxwell's contributions in modifying Ampere's law, and then discuss Maxwell's equations, which form the theoretical basis of all electromagnetic phenomena. These equations predict the existence of electromagnetic waves that propagate through space at the speed of light, according to the traveling wave analysis model.

The waves radiated from the oscillating charges can be detected at great distances. Furthermore, because electromagnetic waves carry energy and momentum, they can exert pressure on a surface.

Wavelength is the distance covered by one complete cycle of the electromagnetic wave. Frequency is the number of electromagnetic waves in one second. The unit of frequency is Hertz (Hz). One Hz equals one cycle per second. One megahertz (MHz) equals one million cycles per second. And generally, microwaves are radio frequencies measuring more than 1 GHz.

Table 2.2 shows some properties of the electric and electromagnetic fields and the table 2.3 shows universal constants:

Table 2.2: Field Quantities, adapted from [21]

Symbols for Field	Field quantity	Symbol	Unit
Electric	Electric Field intensity	E	V/m
	Electric Flux density	D	C/m^2
Magnetic	Magnetic flux density	B	T
	Magnetic field intensity	H	A/m

Table 2.3: Universal Constants and unit, adapted from [21]

Universal Constants	Symbol	Symbol	Unit
Speed of light in free space	c	3×10^8	m/s
Permeability of free space	μ_0	$4\pi\times 10^{-7}$	H/m
Permittivity of free space	ε_0	$\frac{1}{36\pi\times 10^{-9}}$	F/m

The Maxwell equations are fundamental to electromagnetic phenomena as Newton's laws are to mechanical phenomena.

2.3.1 Electromagnetic Waves

It is known that there are various types of electromagnetic waves [22]. All forms of the various types of radiation are produced by the acceleration of electric charges.
Therefore, electromagnetic waves have many forms, of which are mentioned [22] the radio waves,microwaves, infrared waves, visible light, ultraviolet waves, X-rays and gamma rays. Therefore, of all the aforementioned rays, the ones that are of great interest for this study are radio waves. Because it is on this type of phenomena that electromagnetic waves are based in our measurement approach include the study of they networks, whose measurements and their influences on small cells propagation systems are analyzed in this Master Science work.

2.3.2 Antenna Radiation

The radio transmitting or receiving antennas are an independent component, but an integral part of any wireless communication system [23, 24]. An antenna acts as a transducer that converts the current or voltage generated by the power-based circuit, such as a transmission line, a waveguide or coaxial cable, into electromagnetic field energy spreading through space and vice versa. In free space, the propagation of the field in the form of spherical waves, whose amplitudes are inversely proportional to their distance from the antenna. Each radio signal can be represented as an electromagnetic wave [23, 24] that propagates in a certain direction.
The strength of the wave field is polarization, and the direction of propagation determines the main characteristic of the operation of an antenna. Antennas can be wire antennas, aperture antennas, reflecting antennas, frequency independent antennas, horn antennas, printed and shaped antennas and so on [23, 24].

When applications require radiation characteristics that cannot be met by a single irradiation antenna, several elements are employed, forming a ”set of antennas”. The arrangements can produce the desired radiation characteristics, appropriately marking each individual element with certain amplitudes and phases. The very same antenna array configurations, when combined with signal production, lead to multi-beam adaptive antennas (witch beam) that offer far more degrees of freedom in a wireless system design than using a single antenna [23, 24].

The direction of the field component of an electromagnetic wave is important because the polarization of the antenna depends on it. The wave can be linearly polarized or plane polarized, which is the oscillation locus of the electric field vector within a plane perpendicular to the direction of propagation forming a straight line. In contrast, when the location of the tip of the electric field of an electric vector forms an eclipse or a circle, it results in an elliptical or circular polarized wave, respectively. There is a tendency to refer to the polarized antenna vertically or horizontally, although it is only the radiations that are polarized.

Therefore, based on mathematical calculations and considerations for the conductivity and permeability of the environment, antennas were developed for use in indoor and outdoor environments. The developed antennas are characterized by their bandwidth and their radiation characteristics. These include narrowband, dual-band and broadband antennas, as well as those with unidirectional, bidirectional and directional radiation characteristics. This research work can be briefly divided into four categories: investigation of relevant theoretical and mathematical analyzes of the propagation of radio waves in media with and without significant interference. It includes the manufacture and measurement of the radiation characteristics of the antennas. Therefore, the manufacture of the antennas designed with good results was carried out at the facilities of the central pole of the Universidade da Beira Interior in the Physics department. The manufactured antennas were tested and characterized with the aid of the spectrum analyzer in the IT Covilhã of the Departamento de Engenharia Eletromecânica da Universdidade da Beira Interior.

Considering the production of electromagnetic waves by a half-wave dipole antenna shown in the Figure 2.1:

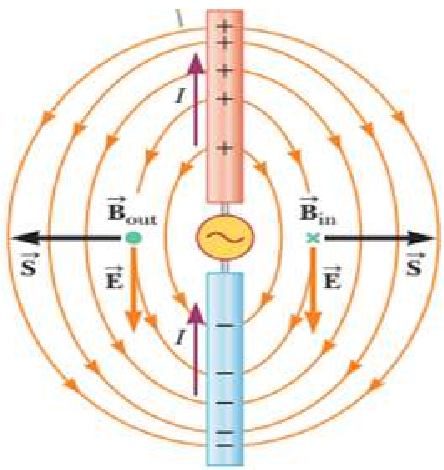

Figure 2.1: A half-wave antenna, extracted from [22]

More mathematical equations of the continuous waveform and other information are presented in Appendix A.

2.4 Characteristics and Measurement Categories

Measurement is an act designed to derive quantitative information about some phenomenon by comparison to a reference and the physical quantity being measured is called the measurand or factor.
The data classes that results from measurements can be divided in two major classes:

- quantitative data;
- qualitative data.

Both categories of measurements are important within the scope of this dissertation based in measurement standard that has been agreed by an International Standards Organization. Measurements can be grouped into three main general categories: direct, indirect and null. The electronic instruments used in the course of the investigation that results in the elaboration of this Master Science work are available based on the three categories.
Broadband access constitutes the "oxygen" for the Internet Era, to which end, the issue of spectrum management is foundational [25].
When it is intended to measure the spectrum of radio in a some region, it is necessarily request the telecommunications regulatory authority of the region where the study is to be carried out, for the proper authorization to avoid interference in the communication system. The radio frequency are characterized according to the communication technology that is intended to be developed. Depending on this scenario, frequencies may be licensed or unlicensed.

2.4.1 Licensed and Unlicensed Frequency Bands

The licence scenario conforms to a single primary network in the licensed band whereas the latter maps to multiple (colocated) networks. The exclusive license model is the operative one for all cellular. Network services, based on the operators belief that exclusive rights to spectrum enables them to offer/tailor desired services, as well as optimize the network/delivery mechanisms so as to extract maximum revenue. The unlicensed model is used by standards, such as Wi-Fi, where the fundamental issue is managing interference, secondary unlicensed interference to primary licensed users and interference between unlicensed secondary users. The rules that govern unlicensed bands have mostly focused on "transmit power" centric rules to ensure limited interference from secondary unlicensed users to primary users (e.g. limits on average transmit power over the band, maximum power spectral density and on out-of-band emission limit using transmit spectral mask) while encouraging the users of "etiquettes," such as listen before talk (LBT) for managing interference between unlicensed secondary users.

Some researchers differentiate between licensed and unlicensed frequency bands, due to the economic value that the two represent for users of the services offered. Thus, while the licensed band is controlled by operators through the established rules, the unlicensed band also needs to be governed by rules for its best use. The unlicensed band is often referred to by researchers as white spaces [25], in the frequency bands assigned by ICP-ANACOM and that which reported in 2.3.
The state of the art study done in this chapter clearly shows that both the approach that starts with Ohm's law and joins the laws of Faraday and James Maxwell and the second approach that supports the propagation of electromagnetic waves based on the Fourier series essentially converge in the interpretation and understanding of electromagnetic waves or radio frequencies, which, as mentioned above, are at the heart of telecommunications systems. The statistical treatment of the data obtained in propagation packages of the measurements allowed to verify that the literature still lacks more approaches and methods for the validation of results, mainly to test their normality.
In our work, besides licensed bands whose use rights were assigned to us by ICP-ANACOM, we have also considered 5G unlicensed band.

2.5 Measurement Quality

In terms of errors, measurements are made to increase knowledge about the reality of the matter and provide the basis for better decisions. The quality of decisions is related to the quality of the measurement results on which they are based. The result of a measurement is different from the result of any product, as there is usually no previously specified value for a measured quantity. The measurement value must be as close as possible to a true, but unknown, value. For correct interpretation and judgment and subsequent decision making, a measurement result must contain two fundamental pieces of information:

- The estimated uncertainty;
- Measurement error

To ensure greater accuracy, it is generally recommended to repeat the measurements or tests a number of times not less than three and, in repeated measurements, particularly on objects under certain conditions, the error can normally have three components [26], random, constant and varies systematically.

2.6 Small Cells Propagation Measurements

There are some studies about the accuracy and the reliability of the measurement at mmW frequencies. Some of them are Over-the-air (OTA). This kind of line-of-sight (LOS), as been used to measure a total radiated power (TRP) and a total radiated sensitivity (TRS) of 2G, 3G and 4G User equipment (UE). The size of shielded anechoic chamber is 1.5 meters and it

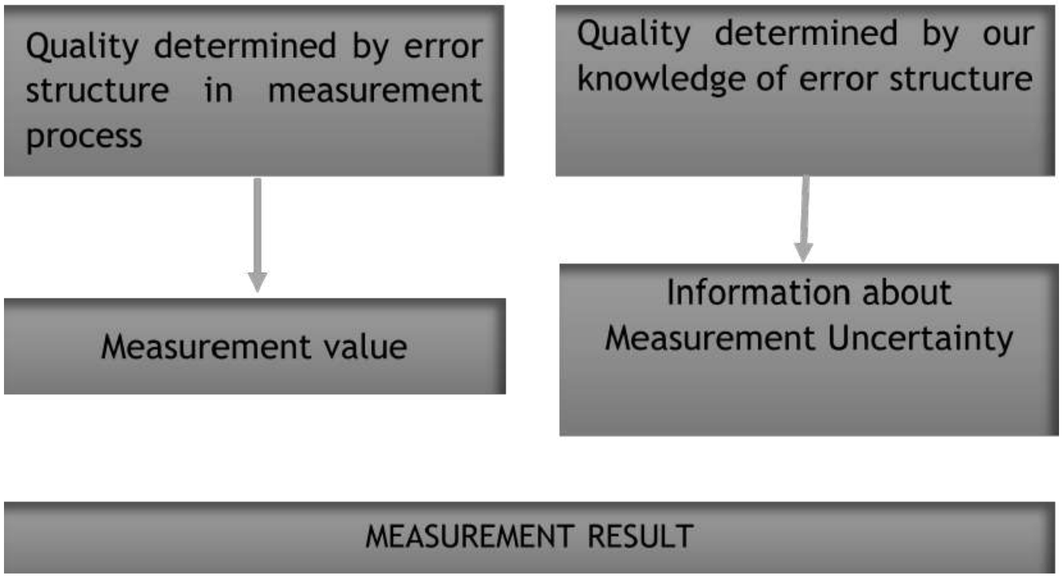

Figure 2.2: Measurement quality process, apdated from [26]

supports power level measurements down to -40 dBm. An alternative method is reverberation chamber that emulates Rayleigh fading radio channel environment. It is not suitable for Los OTA measurements.

According [27], the OTA testing is the preferred method to measure radio performance over a conductive testing and the antenna array consists of 16 sub arrays that are $2x2$ patch element antennas rotated to - 45^0 polarization. The size of array is $90\times$ mm $(W \times L)$ and a diagonal length is 96.2 mm and in test measurements the distance between the field and the antenna is:

$$L \geq \frac{2D^2}{\lambda} \quad (2.1)$$

where D is diameter of the minimum sphere enclosing the antenna, and λ is wavelength of the test signal. Radiating OTA tests at mmW frequencies introduce a new location accuracy challenge between the reference antenna and Device Under Test (DUT) due to short wavelengths [27].

In the literature only few studies are published about a statistical measurement system analysis with a Gage Repeatability and Reproducibility $(R\&R)$ method to applied to radio frequency topics. A study of Statistic Measurement System Analysis of Over- The - Air Measurements of Antenna Array at 28 GHz is presented in [27].

A Spectrum Characterization for Opportunistic Cognitive Radio Systems is presented in [28].

A Spectrum Opportunities for Electromagnetic Energy Harvesting from 350 MHz to 3 GHz [29], and a process to reduce reproducibility error in VNA measurements described in [30].

Fixed positions of the reference antenna and the DUT will overcome the positioning problem and a short wavelength can be used as merit for mmW frequencies since a typical laboratory environment become relatively large at mmW wavelength compared to current sub 6 GHz LTE frequencies. A power level variation in OTA measurement depends on the sphere over the antenna array and the measurement distance. Thus, the variation is given by [31]:

$$\Delta \mathrm{P} = 10 \log_{10}\left(\frac{1+\frac{\mathrm{r}}{\mathrm{R}}}{1-\frac{\mathrm{r}}{\mathrm{R}}}\right)^2 \quad (2.2)$$

where r is radius of the minimum sphere anclosing the antenna, and R is a distance between the reference antenna and the DUT.
The data obtained by the measurement process in the srsLTE scenario within the frequency bands made available by ICP, are processed using the SPSS software to verify the Kolmogorov-Smirnov normality test. They must be normal, according to the theories which support the statistical treatment of whatever the data of a verifiable quantity.

2.7 Statistical Treatment of Data Available in the Literature

In a study with measurement data, normal distribution is an underlying assumption for many statistical procedures. It is also the most commonly used distribution in theory and statistical applications. Hence, when performing statistical analyzes using parametric methods, validating the assumption of normality is a fundamental concern of the analyst. An analyst often concludes that the data distribution is 'normal' or 'non-normal' based on graphical exploration (Q-Q graph, histogram or box graph) and formal test of normality. The graphical method is subjective, as what looks like a "normal distribution" for one may not necessarily be for others. In addition, extensive experience and good statistical knowledge is necessary to interpret the graph correctly. Therefore, in most cases, formal statistical tests are necessary to confirm the completion of the graphical methods [32].
There is a significant number of normality tests available in the literature. Some of these tests are designed to be applied under certain conditions or assumptions. Most of these comparisons were performed using selected normality tests and selected small sample sizes. While some use critical tabulated values, others ones use simulated critical values. Consequently, there are still conflicting results as to which is the ideal test or better, and this can mislead and often confuse practitioners about which test should be used for a given sample size. Of the software presented in table 2.4, we used Statistical Analysis Software (SPSS).

Table 2.4: Normality tests available in statistical software packages, adapted from [32].

	Test									
Software	SW	SF	KS	LL	CVM	AD	JB	CSQ	RJ	SKKU
SAS	x		x		x	x				
SPSS	x			x						
SPLUS	x	x	x					x		
STATISTICA	x		x	x				x		
STATA	x	x								x
STATGRAPHICS	x		x	x	x	x		x		x
MINITAB			x			x			x	
MATLAB		x	x	x	x	x	x	x		
R	x	x	x	x	x	x	x	x		
IMSL Library	x		x	x				x		

Where SW: Shapiro–Wilk test; SF: Shapiro–Francia test; KS: Kolomogorov–Smirnov test; LL: Lilliefors test; CVM: Cramer–Von Mises test; AD: Anderson–Darling test; JB: Jarque–Bera test; CSQ: chi-squared test; RJ: Ryan–Joiner test; SKKU: skewness–kurtosis test.

2.8 Statistical Data

Of the ten normality tests presented in the table 2.4, for the treatment of statistical data, this study uses the Kolmogorov-Smirnov test [33]. The choice of the test is justified by the amount of measured data and its ease of execution and interpretation.

2.9 Introduction to Data Collection Equipment

In order to perform correct measurements of the figure of merit, a set of instruments should be used. These instruments should be jointly capable of identifying the most important parameters of systems and clearly, and without any ambiguity, capturing the correct values to be measured. several types of instrumentation were developed for gathering all these values and thus clearly identifying the quantities to be mearured and specified. For each instrument the quantities to be measured, the internal architecture, de definition of each instrument parameters, and its calibration procedure will be covered. This is done for the main and more important instruments available to microwave and wireless engineers, namely [34]: power meters, spectrum analyzers, vector signal analyzers, real-time signal analyzers, vector network analyzers, nonlinear vector network analyzers, oscilloscopes, logic analyzers and noise-figure meters.

2.10 Radio Signal Generator

Universal Software Radio Peripheral (USRP) was developed for digital radio systems, providing a complete infrastructure for signal processing [35].
This system in the scenario emits signals of the power that can be received by the user, since the tests were performed only in the downlink context.
The tests were done based on the SISO systems that correspond to transmit a signal through a TX anatenna that is in the USRP and the signal is received at another USRP B210 connected to the RX antennas as user.

2.10.1 5G Radio Networks Emulation Bands

With the birth of 5G communication technology, new applicable services have emerged in several areas that can be grouped into 5 categories [36].

- Mobile Broadband (MBB);
- Massive Machine Communications (MMC);

- Mission Critical Communications (MCC);
- Broadcast/Multicast Services (BMS);
- Vehicle-to-vehicle and vehicle-to-infrastructure communications (V2X).

In addition to these services, in the project are identified 9 key performance indicate (KPIs) [36] that are relevant:

Table 2.5: Key Performance Indicator, adapted from [36]

Number	Key Performance Indicator	Services
1	KPI 0	User experienced data rate
2	KPI 1	Traffic density (to achieve high system capacity)
3	KPI 2	Latency
4	KPI 3	Coverage (to provide ubiquitous access)
5	KPI 4	Mobility
6	KPI 5	Connection density
7	KPI 6	Reliability/availability
8	KPI 7	Complexity reduction
9	KPI 8	Energy efficiency

Whose can be summarized as follows: For the non-buffered traffic model, the data rate experienced by the user is 5% of the percentage of the user's throughput. For the same model, the user's throughput during active time is the relationship between the size of a burst and the time between the arrival of the first packet of a overflow and receiving the last overflow packet.

On the other hand, user experience data the rate is defined as the percentage of 5% of the user's spectrum efficiency times the bandwidth for the full buffer traffic model. The efficiency of the 5% user spectrum depends on the number of active users who share the channel.

The radio signals emitted and received reach a certain radial area or radiance of the transmitter (s) where an appropriate level of sensitivity is still available, to ensure that the desired signal is received above or at least at the receiver's reference sensitivity level (applies to both uplink and downlink). Depending on the main service, coverage can also be defined as the Maximum Coupling Loss (MCL) allowed in both uplink and downlink (assuming their goolowest value).

In terms of the difference between the power of the transmitter and the reference sensitivity level of the receiver (taking into account the thermal noise density, the noise figure of the receiver, the interference margin, the occupied channel bandwidth, the required SINR and the receiver's processing gain). Bandwidth is similar to mobility, which represents the user's maximum speed (in km/h) at which a defined QoS can be achieved.

2.11 Frequency Bands for Radio Communication Operation

The main feature for predicting the effectiveness of radio communication links is frequency band. The optimal frequency band for each propagation channel is determined and limited

by the technical requirements of each specific communication system and the radio propagation conditions on each channel. First, consider the radio frequency spectrum and its practical use in various communication channels.
In view of this, the frequencies of service in radio communications can be selected and classified according to the services for which they are intended, which can be [37]:

1. Extremely Low and very low frequency (ELF and VLF);
2. Low frequencies (LF);
3. Hgh frequencies (HF);
4. Very high frequencies (VHF) (or short waves in the wavelength domain);
5. Ultra high frequencies (UHF) (ultra short waves in the wavelength domain).

2.11.1 Frequencies Assigned by ICP-ANACOM

The frequencies on which this study is based, were assigned by the Portuguese regulator communications ICP-ANACOM [20] as a spectrum management entity, granted through the authorization dated 2021 following a request made by the Covilhã Telecommunications Institute for the purpose of research tests.
Certain frequency bands are not accessible to the public due to the services for which they are intended. ICP-ANACOM has reserved certain frequencies for the operation of electronic communications networks and services (reads in the license).
In this context it is possible to distinguish two concepts which are:

1. The need for usage rights that identifies the need to assign usage rights in accordance with article 16 of law nº 05/2004, of 10 February;
2. Mode of operation: duplex, simplex or semi duplex, when applicable, according to the services for which it is intended; Simplex - mode of use by which transmission is possible alternately in both directions of the telecommunication channel of one or two frequencies; Duplex - scanning mode in which transmission is possible simultaneously in both directions of the communication channel using two frequencies; semi-duplex - simplex scanning mode at one end of the communication channel and duplex scanning at the other, using two frequencies.

Table 2.6: Frequency bands assigned by ICP-ANACOM

Frequency bands			
Uplink		Downlink	
2600 GHz	3500 GHz	2600 GHz	3500 GHz
Available			
2 x 10 MHz	2 x 20 MHz	2 x 10 MHz	2 x 20 MHz
2500 MHz - 2510 MHz	3480 MHz - 3500 MHz	2520 MHz - 2530 MHz	3580 MHz - 3600 MHz

Observing the table that presents the study frequencies within the scope of this dissertation authorized by the national telecommunications regulator and spectrum manager ICP-ANACOM, it can be clearly seen that the frequencies contained therein fit Ultra and Super High frequencies suitable for mobile and fixed communications.

2.12 Summary and Conclusions

The radio signal continues to generate great research interest around the world due to its vast utility in communication technologies. Spectrum is becoming increasingly scarce, so researchers are turning their attention to millimeter bands to explore the potential they can offer and continue to guarantee the quality of wireless communication services.
This chapter has discussed propagation characteristics, radiation by simple dipole antennas and spectrum usage opportunities with licensed and unlicensed bands UHF/SHF frequencies, considered the frequencies of choice for LTE/ 4G and 5G New Radio technology.
ICP-ANACOM's license refers to the 2.6 GHz and 3.5 GHz frequency bands with their Uplink and Downlink subbands being the different powers of the transmitter and receiver. The 3.5 GHz frequency band was recently adopted for 5G operator networks deployment alongside millimeter wave bands (mmWaves).

Chapter 3

Methodology and Algorithms for the Measurements

3.1 Introduction

To develop the present study, qualitative and quantitative methods were selected as research methods, using observation, description, interpretation and experimentation. This type of combined investigation (action-research), is characterized by a continuous phase of data collection, planning, experimentation (action), observation, reflection, with the participation not only of the researcher, but also of all researchers in the area , belonging to the Laboratory of Instituto de Telecomunicações da Covilhã (IT) including other engineers who are outside the academic community of UBI.
The methodology used is based on the rules proposed in the official documents, such as, the guidelines of the spectrum management entity, the entity as Institute of Electrical and Electronics Engineers (IEEE), telecommunications operators and in the other research works of published authors.
In the first phase, we sought to identify how wireless communications are designed, to what extent they are in accordance with the assumptions described and what precautions are related to their development.

3.2 Radio Transmitter Measurements

The purpose of a radio transmitter is to generate a radio frequency (RF) signal and to impart information to it so that it can be propagated as radio wave from an antenna.
Although there are several architectures of radio transmitters, in the Figure 3.1 we try to present a basic scheme [38].
Due to its low cost and the low complexity of the infrastructure compared to wired communication systems, the design of wireless communication systems has stood out in the use of wireless since its invention in 1896. One of the advantages is that it does not require construction kilometers of telephone lines with cables such as fiber optics, replacing them with towers of radio antennas strategically positioned with the ability to transmit and connect the entire world, simplifying effort, time and costs. However, today wireless communication systems are being popular due to the high demand for services, it is already intended to allow millions of users to connect simultaneously. Using wireless communication services, we can transfer data, voice, images, videos and more. According to the author [39], four types of wireless or radio communication systems can be identified, mobile phone, basic Bidirectional Radio, point-to-point, Wi-Fi and Wi-Max which is the latest.

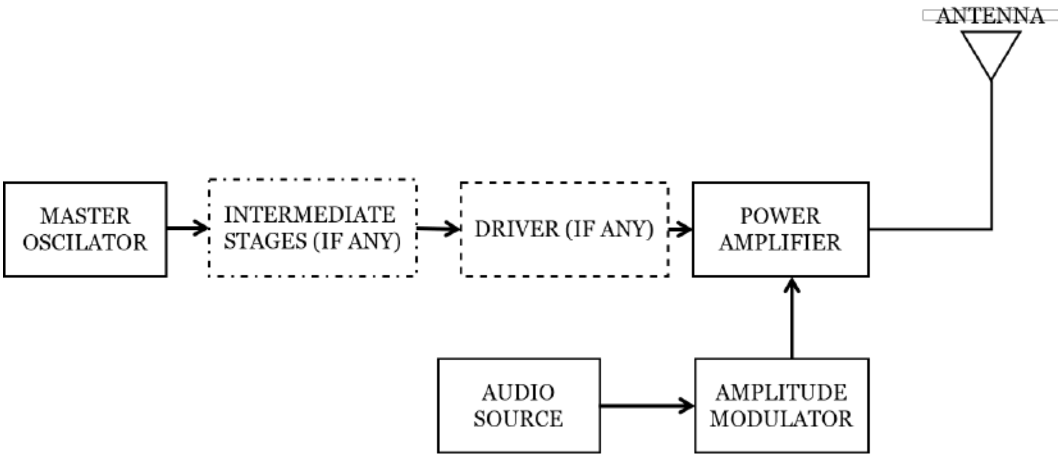

Figure 3.1: Radio transmitter basic scheme, adapted from [38]

And its connectivity services use are known as making Calls, Connecting Devices, accessing the Internet, enhance Security, for Locating and Tracking, as shown in the Figure 3.2.

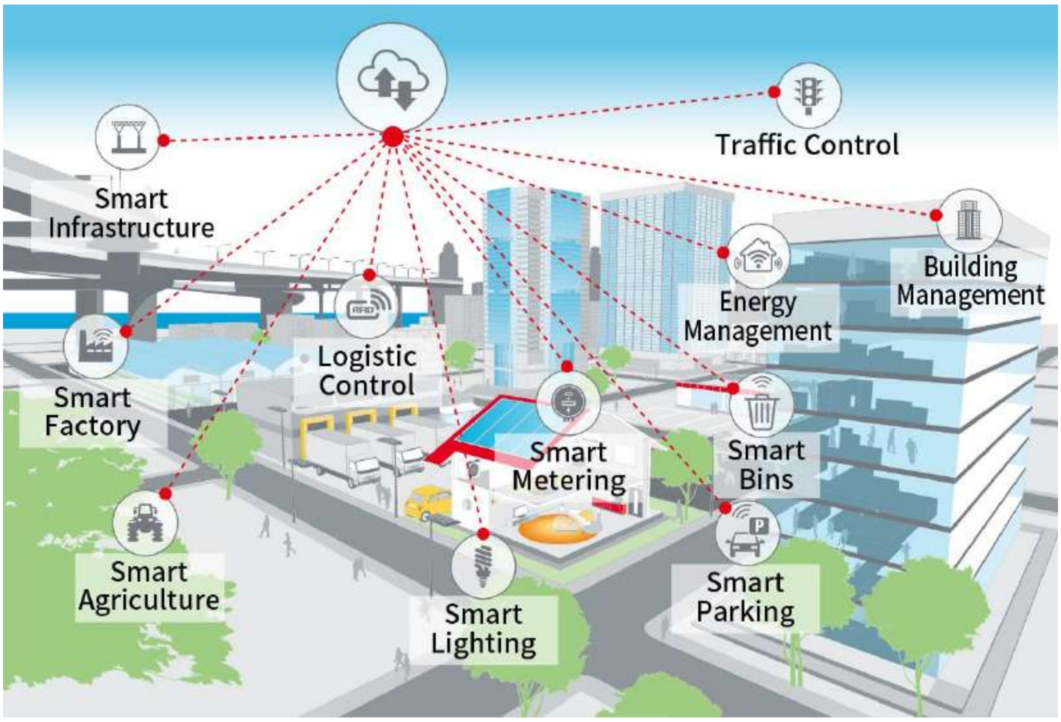

Figure 3.2: Wireless Communication Technologies, extracted from [40].

Frequencies from 3 KHz to 65 MHz range include services such as maritime navigation communications, radio navigation and aeronautical radio communication, analogue AM broadcasting, short wave broadcasting, land mobile communication and fixed services, VHF television broadcasting and amateur radio communication and the measurement procedures and techniques in this range vary according to the frequency and type of service.
In the frequency range from 65 MHz to 300 GHz, the services of VHF frequency modulation (FM) radio, VHF/UHF television and digital, fixed, land mobile/PCS and satellite systems are included. In this frequency range, the wavelengths of the electromagnetic fields are relatively short and the dimensions of the antenna are relatively small. As a result, the measure-

ment sites are usually located in the distant field region and, in general, only electric field (E) measurements are required.
In the region of the distant field, the magnetic field (H) and the electric field (E) are orthogonal and related by a constant. The free space impedance is equal to 377 Ω [41].
In that case, the power density can be derived from $|E|^2$ divided by free space impedance. Consequently, measuring only the E field is sufficient [41].

3.3 Experimental Procedures

In this section, the radio channels of the srsLTE system below 6 GHz are investigated according to the requirements of the 4G and 5G communication scenarios. It presents the methodology used in experimental measurements made in a indoor environment in the telecommunications laboratory of Covilhã, in the Department of Electromechanical Engineering of the University of Beira Interior, and in the old aerodrome of Covilhã in the frequency bands below 6 GHz according to the authorization license assigned to us by ICP-ANACOM.
In order to carry out an experimental work through measurements of the spectrum and the received power by the user, packets of radio communication signals are emitted from a base station (BS) formed by a srsLTE scenario to study the behavior of the received power by the user indoors and outdoors, whose tasks are divided into phases.
The first phase took place at the telecommunications laboratory in Covilhã, allocated to the Departamento de Engenharia Electromecânica.
Spectrum measurements were made experimentally, the characterization of the S11 and Smith Chart [42] to measure the impedance of the antennas in the 2600 GHz range of printed circuit boards manufactured by us preceded by computer simulation.
Based on mathematical calculations and considerations on the conductivity and permeability of the environment, the antennas were built for use in closed and open environments with or without interference. The developed antennas are characterized by their bandwidth, radiation and although they can emit and receive some minimal signals in almost all directions, the antennas developed in the scope of this Master Science work are directional.

3.4 SrsLTE Scenario Implemented with USRP B210

Fourth generation systems are known to provide data transmission rate packages in the order of 5 Mbps in external microcellular environments and up to 10 Mbps in internal microcellular environments [43]. Although broadband services provide high data rates, their installation and maintenance has a very high cost. Therefore, spectrum efficiency is a fundamental factor when choosing a wireless technology. Very wide band systems require complex receivers due to the presence of a large number of resolvable multiple paths [43].
We can identify four access techniques to share the available bandwith in the wireless communication networks [44]:

1. frequency division multiple access (FDMA);

2. time division multiple access (TDMA);
3. code division multiaccess (CDMA);
4. space division multiple access (SDMA).

Taking into account the advantages of high-speed data transmission and dealing with multi-path problems of propagation and bandwidth efficiency, world standard organizations, such as IEEE and ETSI, point to OFDM as the best technique for generations of wireless technology [45].

A tunable transceiver for designing, prototyping and deploying for research radio communication systems is the Universal Peripheral Radio software (USRP B210). Because it is an ideal product for creating wireless prototypes, developing tactical electronic warfare (EW) and strategic signals intelligence (SIGINT) applications and deploying wireless systems [46]. The wireless communication system has a main feature of not needing the physical connection between the transmitter and its corresponding receiver and this fact allows user mobility. However, experiments with these communication systems tend to be done mainly in laboratory, where transmitters and receivers are set up on benches stationary. This prevents the investigator from experiencing fading and other propagation effects associated with mobile communication channels. The Figure 3.3 shows the set up for field trials in the outdoor environment, but can be applier indoor environment.

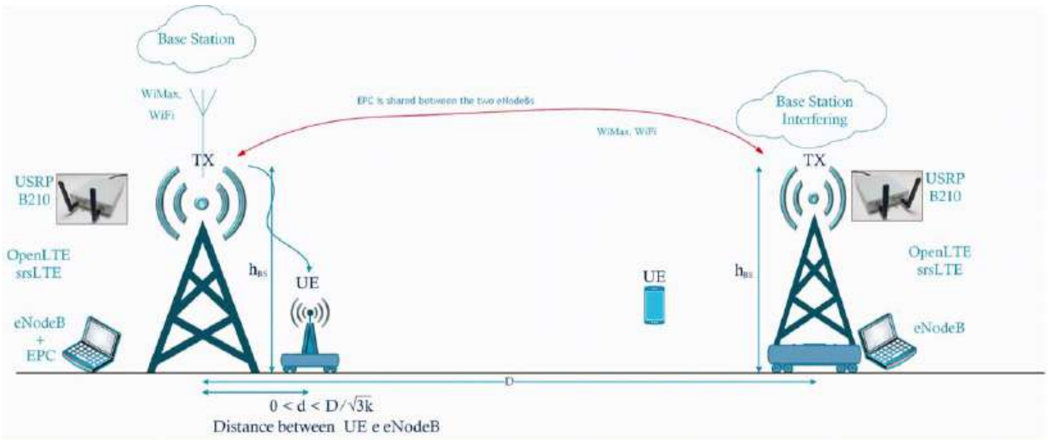

Figure 3.3: Setup for Field Trials, (© 2020 by R. M. Andrade, used with permission. All rights reserved.)

3.5 Measurements in the Indoor Environment

This section presents a wireless mobile communication platform and performs experimental tests indoor environment with fixed and mobile propagation characteristics. The platform used consists of the application of a Universal Software Radio Peripheral (USRP B210) accessible to implement wireless communication between user devices.

With the srsLTE scenario on, the start and end frequencies are configured in the spectrum analyzer, followed by the span to define the scan range.

At the start of each test, the srsLTE EPC and eNB must be synchronized from the downlink (DL) frequency, the cell bandwidth and the number of component carriers must be configured in the eNB, without forgetting ping the eNB and trace to the user (UE) to make it possible to check the communication packets transferred during the connection. Downlink and uplink frequencies are in the range of frequencies assigned by ICP-ANACOM.
To perform the tests, three rooms were selected on Departmento de Engenharia Electromecânica, fourth floor block 8 at Universidade da Beira Interior.
The Figure 3.4 shows the three rooms selected for the tests. In room one, the base station was installed, in room two, interfering one was placed, and in room three, interfering two.

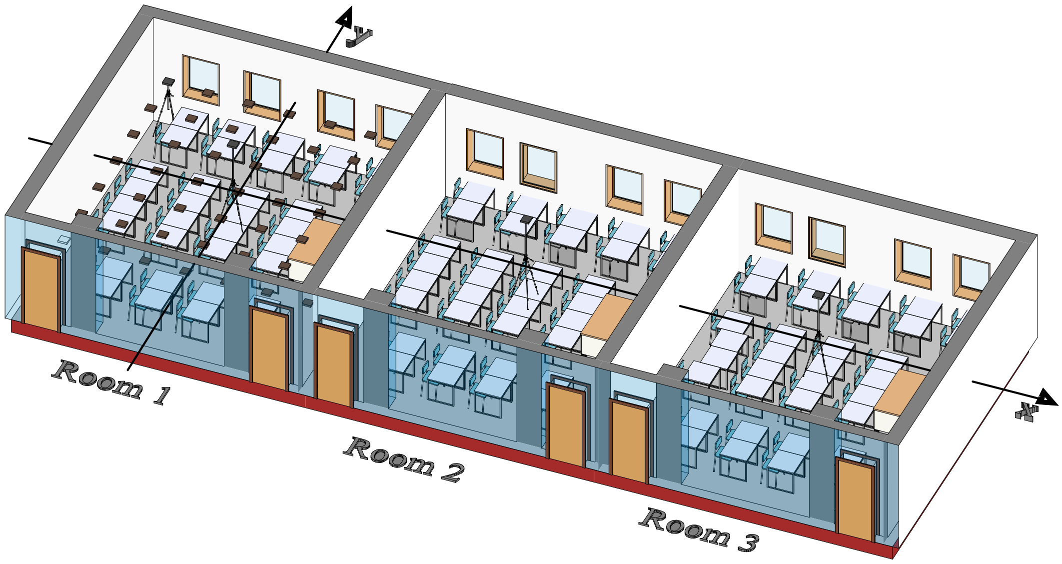

Figure 3.4: Scenario of the three rooms selected for tests, extracted from [11].

The three rooms have dimensions internal equal to 7.32 ×7.32 square metres. Each room was divided into forty-nine points separated by a radius of 1 metre from each other, as shown in the Figure 3.5. At each point, the received power (Pr) by the user was measured, in a time interval and the number of data previously defined in the portable spectrum analyzer FSH8 from Rohde Schwarz.
While room 1 is the room of interest, where theoretical and practical measurements took place, BSs that act as wireless interfering nodes are also separately considered either in room 2 or room 3. By varying the UE positions within room 1, it was possible to verify that the highest values of the received power occur close to the central BS. The third interferer was installed in the room three. The power of the base station was measured in the same room one, where the stage was set up.
The rooms were placed in the two-dimensional Cartesian coordinates to facilitate the location of each of the forty-nine points, as well as to verify the variation of received power at each point, as shown in the Figure 3.5.

3.5.1 Received Power Measurement Mode

Over GNU Radio [11, 47] use executable srsLTE [48, 49] to make use of resources such as the build-in spectrum analyzer. This library supports different types of radio frequency (RF)

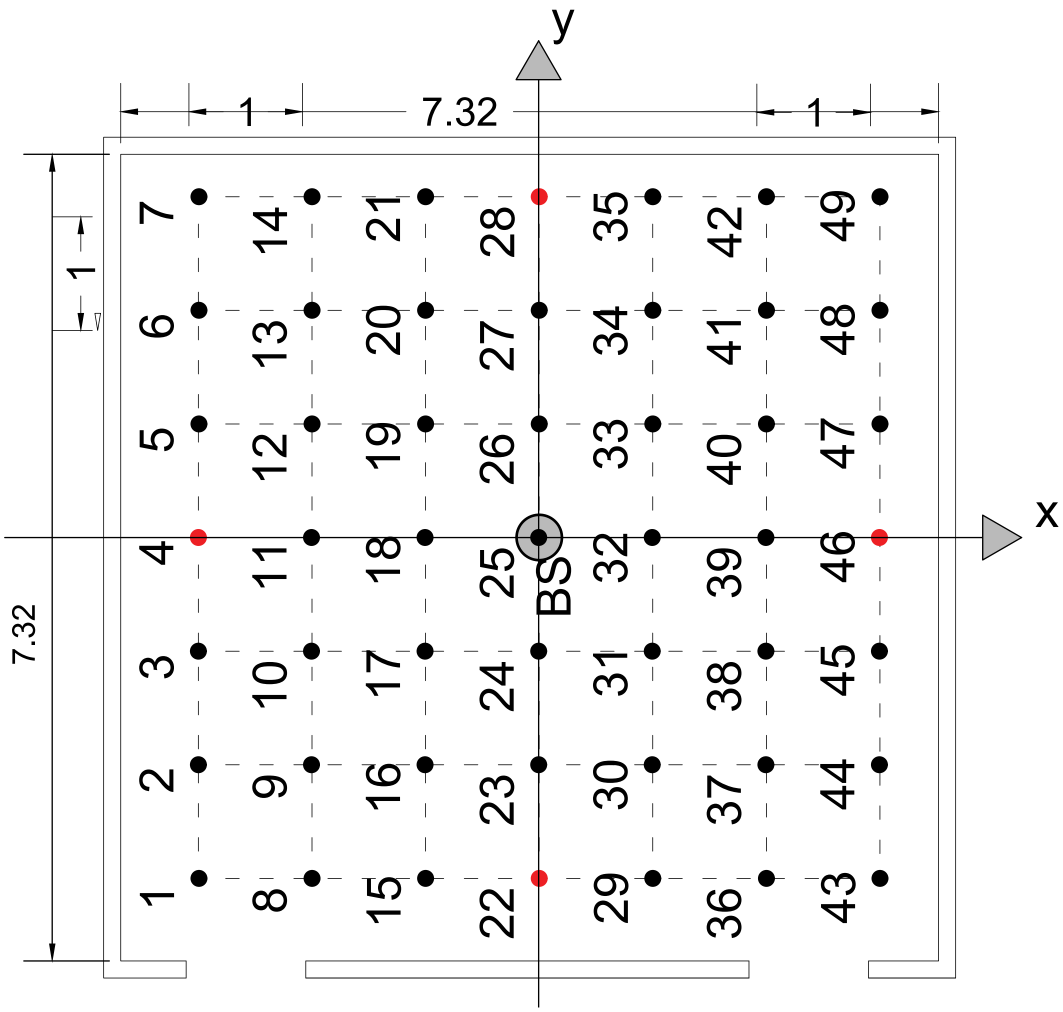

Figure 3.5: Measurement methodology scenario UE distribution 49 points, extracted from [11].

front-ends [50] and is organized in modules with the objective of creating a structure where each part can be changed and replaced without altering or having to modify the rest of the structure. The supported bandwidths are the 1.4, 3, 5, 10 and 20 MHz [51]. During the tests, it was possible to verify that the srsLTE calculates the Block Error Ratio (BLER) performance as a function of the signal-to-noise ratio (SNR) in all channel interactions for a specific channel model, in real time.

Rooms are characterized by the ceilings height at 3 m and are made by mineral fiber boards, glass windows, and projected plaster walls. The main base station was at room 1 while, the interferers was at rooms 2 or and rooms 3. Base stations were fixed close to the ceiling, at the center of the room. The UE was positioned at a height of 1.5 m, as shown in Figure 4.2.

One USRP B210 was used as signal generators and other one was used as (UE), while the spectrum analyzer was used as equipment for measuring the received power by the user. With the srsLTE system on, the start and stop frequencies are configured in the spectrum analyzer, followed by the span to define the range, the report intervals and the number of data are also previously defined.

The choice of the srsLTE scenario with URSP B210 results in a moderate overall cost for the radio hardware required by the platform, which can be easily programmed using open source software, such as GNU Radio, Linux - Ubuntu operating system and software packages such as Matlab or LabView. The user and the issuer are managed from three computers equipped with the tools to execute the code, in order to allow the communication/connection of the two USRPs B210 which are the own cell and an interferer. The transmission of the power signal through the rooms of the indoor measurement environment was carried out with the help of a student from IT - Covilhã telecommunications institute as part of his doctoral thesis.

3.6 Conceptual Aspects of Antenna

An antenna acts as a transducer that converts the current or voltage generated by the power-based circuit, like a transmission line, a waveguide or a coaxial cable, into electromagnetic field energy propagating through space and vice versa [52].

Whether it is a transmitter or receiver, a radio antenna is an independent component, but it is an integral part of any wireless communication system.

Antennas can be manufactured in such a way that they operate in time domain or frequency domain. Since the antennas manufactured by us are tested with a Vector Network Analyser, they give signals in the frequency domain.

An antenna has the basic parameters known as the radiation diagram, the radiation power density and the gain. Figure 3.6 show the radiation pattern of dipole antenna designed by us.

Electromagnetic waves are used to transport information through a wireless point to another. It is then natural to assume that there is power and energy associated with electromagnetic fields.

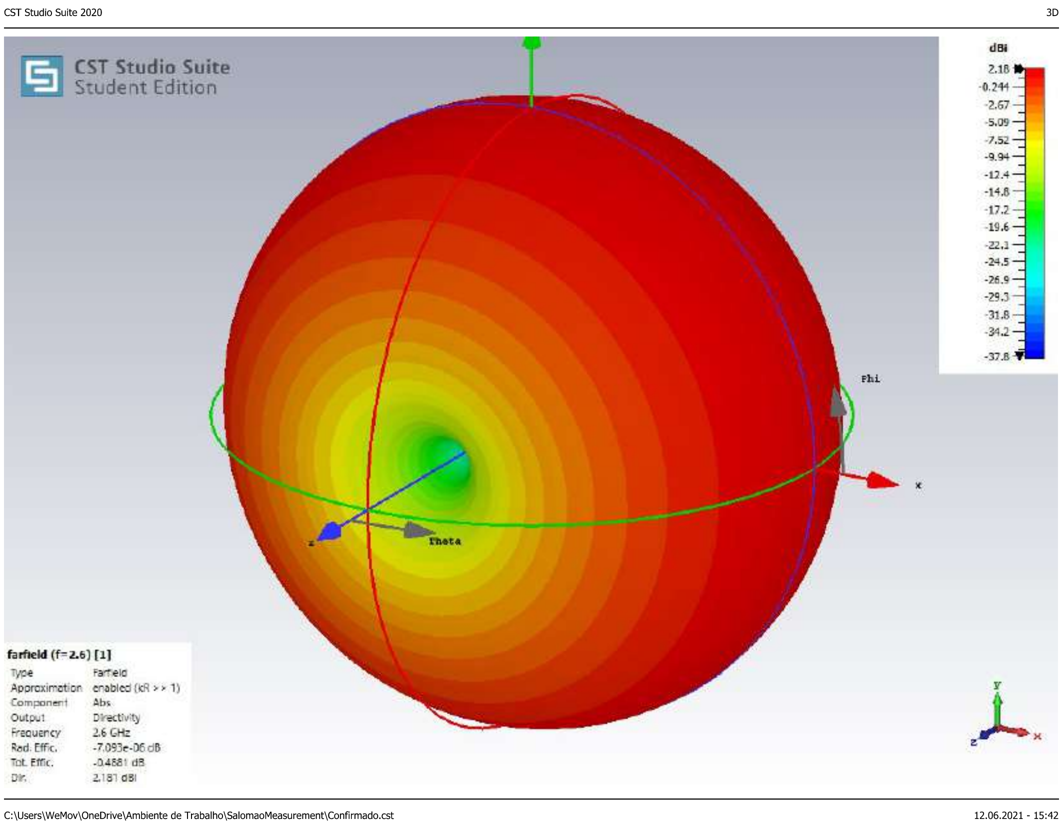

Figure 3.6: Radiation pattern of an antenna

3.7 Antennas Used in the Tests

The antennas used in the USRP 210 in the srsLTE scenario are dipole-type half wave antennas manufactured by the writer of this Master Science work with the help of the laboratory technician of the Departamento de Física da Faculdade de Ciências da Universidade da Beira Interior.
The manufacture of antennas was based on the theory of printed circuits in the central frequencies of 2625 MHz and 3590 MHz in accordance with the temporary license from ICP-ANACOM.

3.7.1 Simulation on CST STUDIO and Tests on VNA

The antenna simulation was done in the Computer Simulation Technology (CST STUDIO Software with the parameters presented in the table 3.1.

Table 3.1: Simulated antenna parameter for 2.625 GHz center frequency

Magnitude name	Symbol	Value	Unity
Radius of Dipole	R	1.5	mm
Length of Dipole	L	57.15	mm
Length of Dipole	L	$L * a$	mm
Feed of Dipole	F	10	mA
Input of Impedance	Z	50	Ω
S11 setting parameter	a	2.3345/2.625	dB

Table 3.2: Simulated antenna parameter for 3.590 GHz center frequency

Magnitude name	Symbol	Value	Unity
Radius of Dipole	R	3	mm
Length of Dipole	L	41.75	mm
Length of Dipole	L	L ∗ a	mm
Feed of Dipole	F	10	mA
Input of Impedance	Z	50	Ω
S11 setting parameter	a	3.448/3.590	dB

For the correctness of the desired frequency (study frequency), the calculations were made using the following formulas followed by its frequency hit:

$$\mathrm{d} = \frac{\lambda}{2} \quad (3.1)$$

$$\lambda = \frac{\mathrm{c}}{\mathrm{f}} \quad (3.2)$$

It is intended to operate in the frequency band 2600 MHz at the central frequency 2625 MHz, which results in $\lambda = 114.3\mathrm{mm}$, by the formula 3.2.

The Figures 3.16, 3.17 and 3.18 show the S11 parameter in the 2600 MHz frequency band, and the S11 parameter in the 2625 MHz frequency center and the Smith Chart of simulated.

The dielectric medium to be used to fill the guide will be air. The propagation constant this dielectric and are in the table 2.3 given in chapter 2.

The antenna model under construction is shown in Figure 3.7

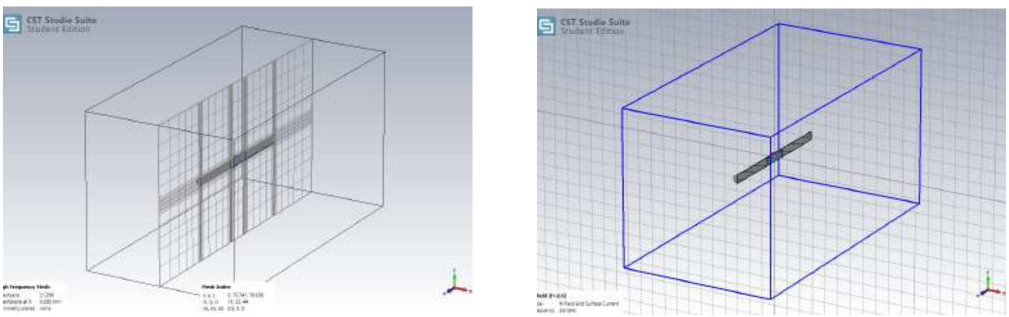

(a) Simulation 2625 MHz frequency center (b) Simulation 3590 MHz frequency center

Figure 3.7: Simulation of the antenna in the 2.625 GHz and 3.590 GHz frequencies bands.

3.7.2 Results Obtained in the Manufacture of Antennas

The Figures 3.11, 3.12 show the manufacturing process of dipole antennas operating in the 2.6 GHz and 3.5 GHz frequency bands.

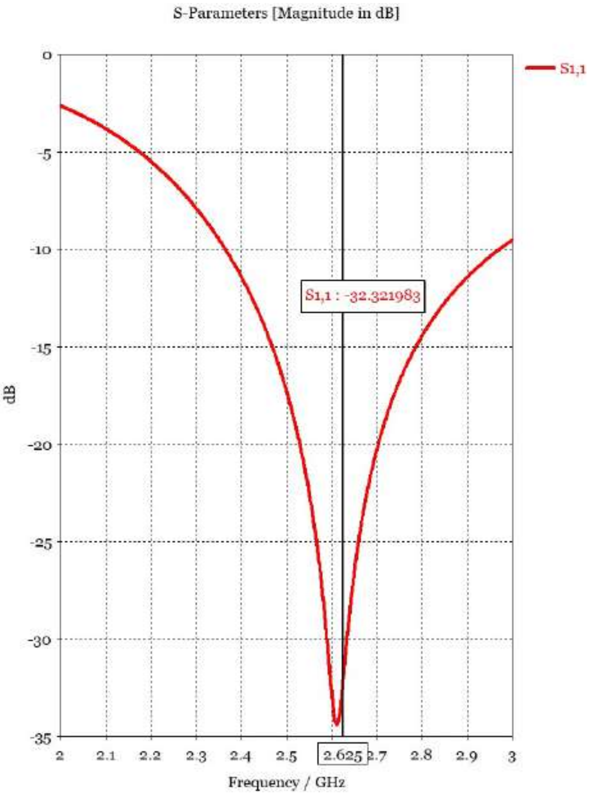

Figure 3.8: S11 parameter from CST Studio at the frequency center 2625 MHz

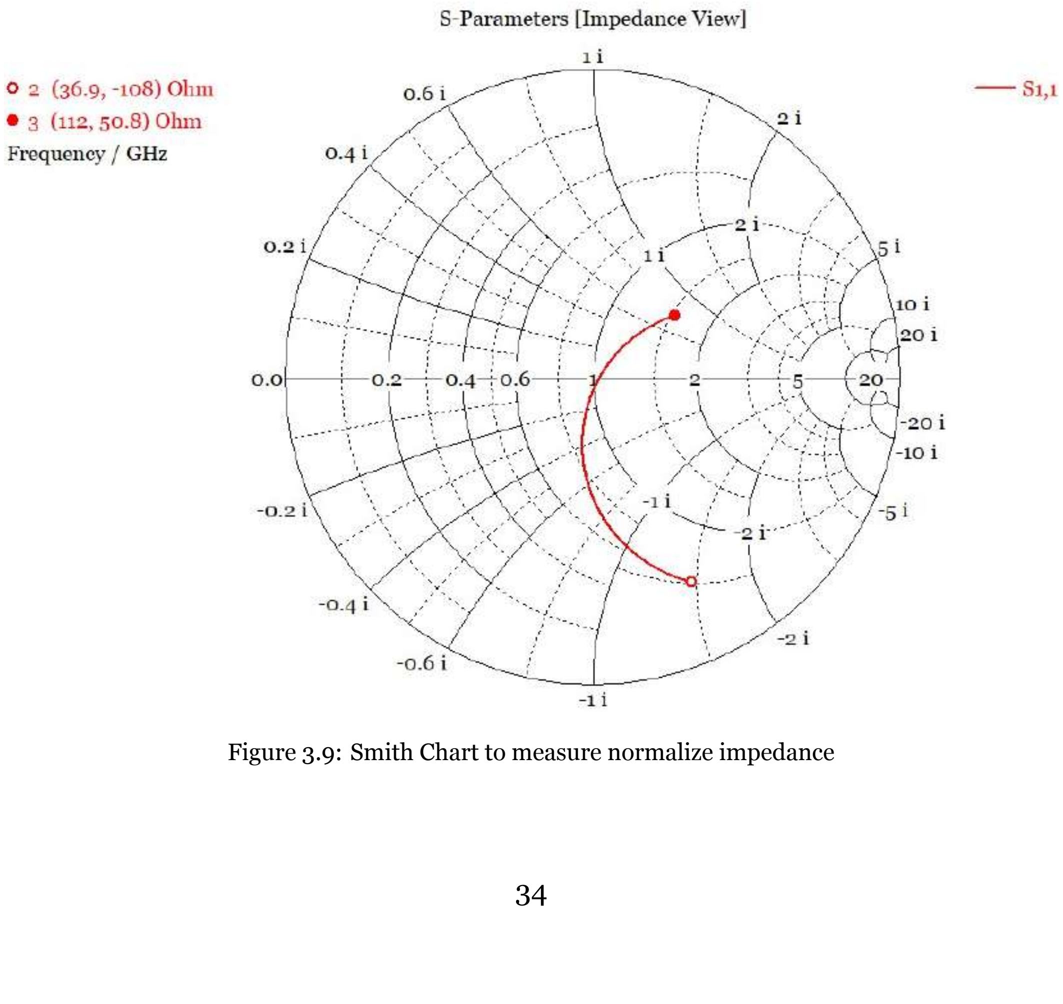

Figure 3.9: Smith Chart to measure normalize impedance

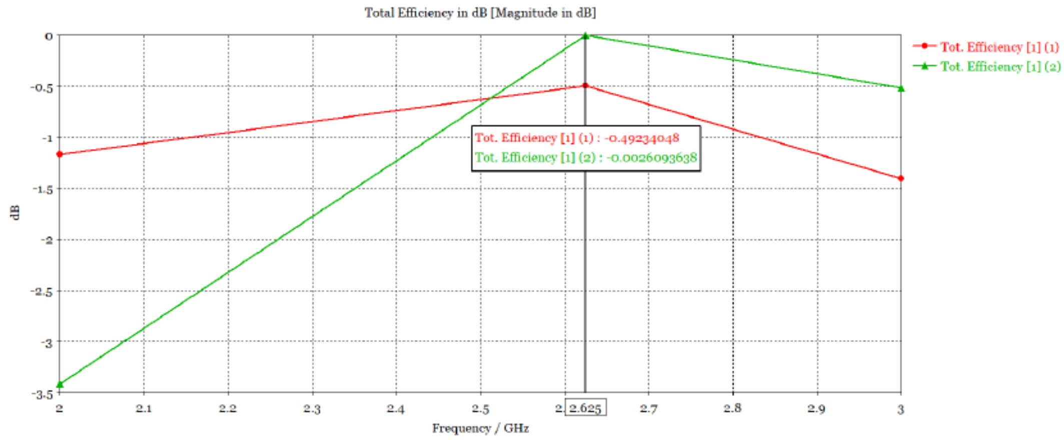

Figure 3.10: Total efficiency

(a) Washing in the NH_4^+

(b) Cleaning in the R_3COH

Figure 3.11: Manufacturing process of antennas in 2.625 GHz and 3.590 GHz frequency bands.

(a) Cutting and with 1mm drill

(b) Component Welding

Figure 3.12: Simple dipole antennas printing, cutting and welding process.

(a) Final model

(b) Final model

Figure 3.13: Final stage of the manufactured dipole antenna.

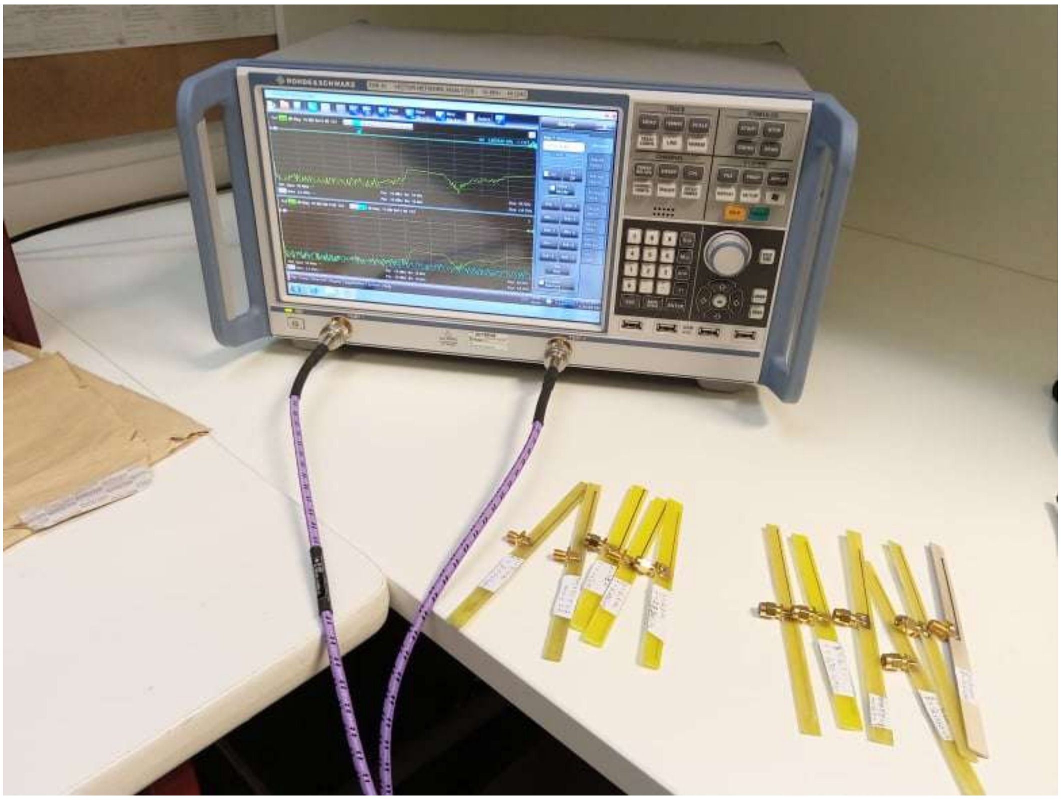

Figure 3.14: Measuring S11 parameter with VNA in the 2.625 GHz frequency center.

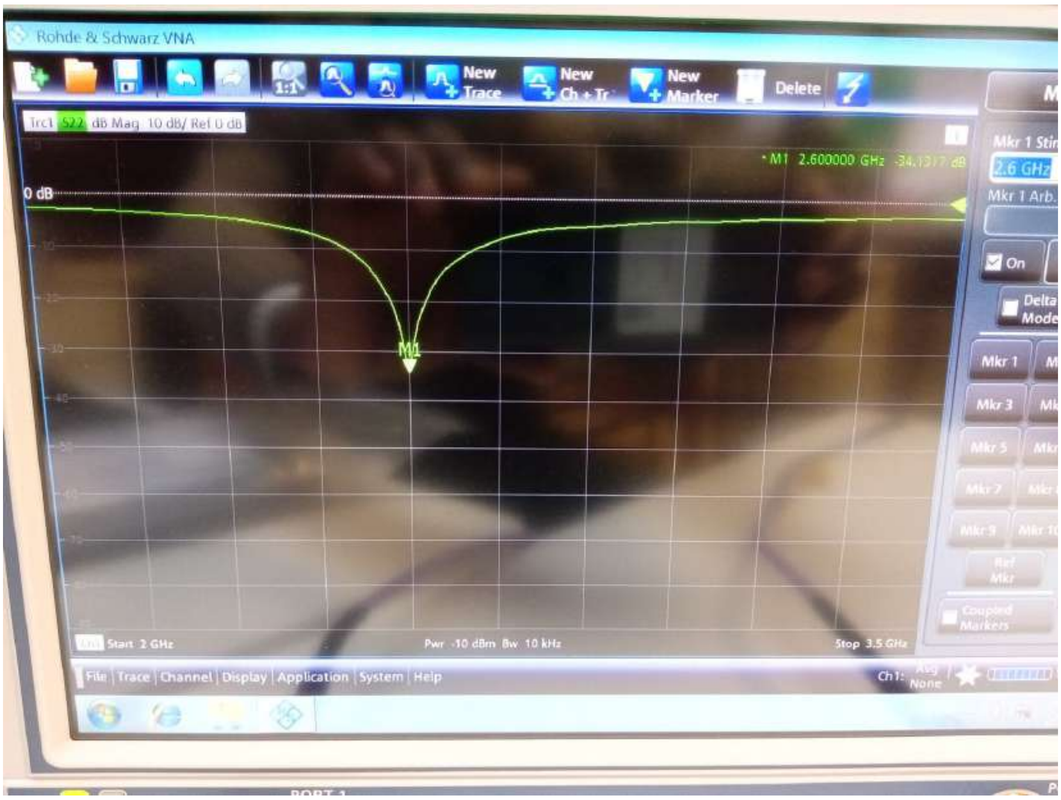

Figure 3.15: Measuring S11 parameter with VNA in the 2.625 GHz frequency center.

3.7.3 VNA Test Results

The result of the tests with the VNA in the antennas operating at 2625 MHz frequency center is shown in Figures 3.16, 3.17 and 3.18.

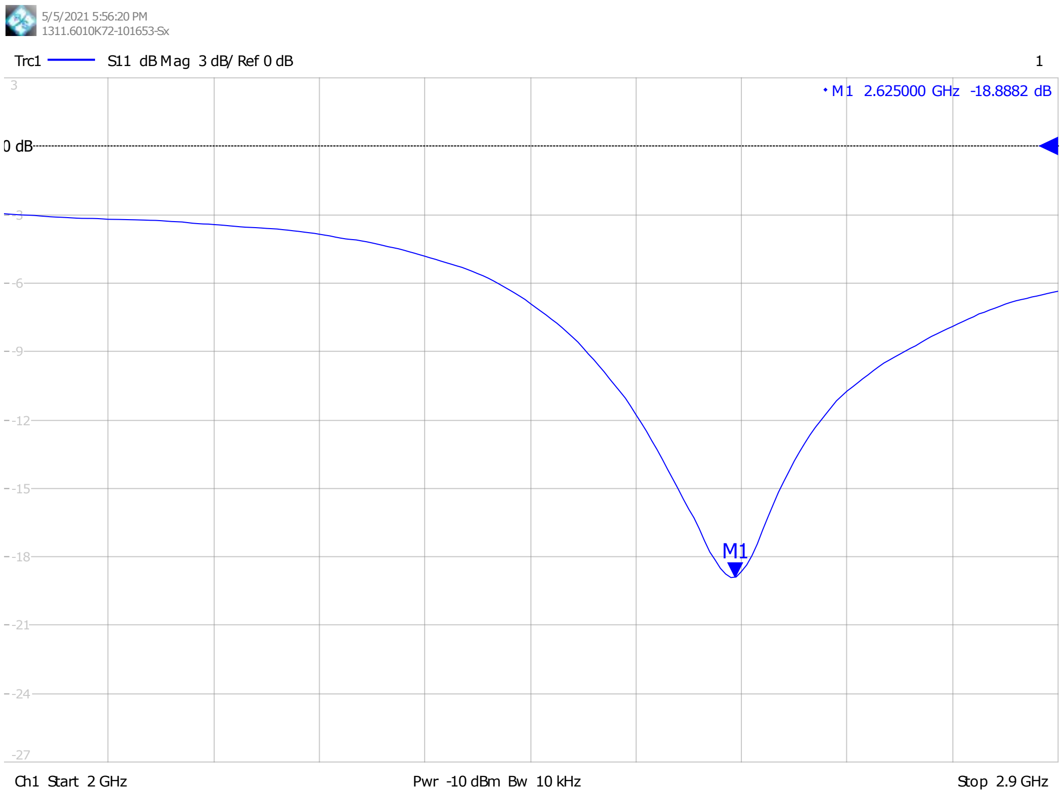

Figure 3.16: Parameter S11 tests result with the VNA in the 2625 MHz frequency center.

3.7.4 Voltage Standing Wave Ratio

This term indicates the degrees of deviation between the impedance of the load connected to the transmission line and the characteristic impedance of the transmission line and indicates the deviation in the termination, based on the modules of the maximum and minimum values. The desirable value for the VSWR is obtained if the line is properly terminated and there are no reflections. Any VSWR greater than one indicates a deviation and the greater the VSWR, the greater the deviation. VSWR as a figure of merit, can be considered as having an acceptable value, if it oscillates between 1 and 1.1 [53].

$$\mathrm{VSWR} = \frac{1+|\Gamma|}{1-|\Gamma|} \quad (3.3)$$

3.8 Antenna Radiation Pattern

The structure of antennas proposed in the scope of this Master Science work is based on a dipole antenna that is wire-shaped, flattened at different angles. Angle rotations are limited from 0 degree to 90 degrees. A corresponding basic dipole antenna is represented by 90

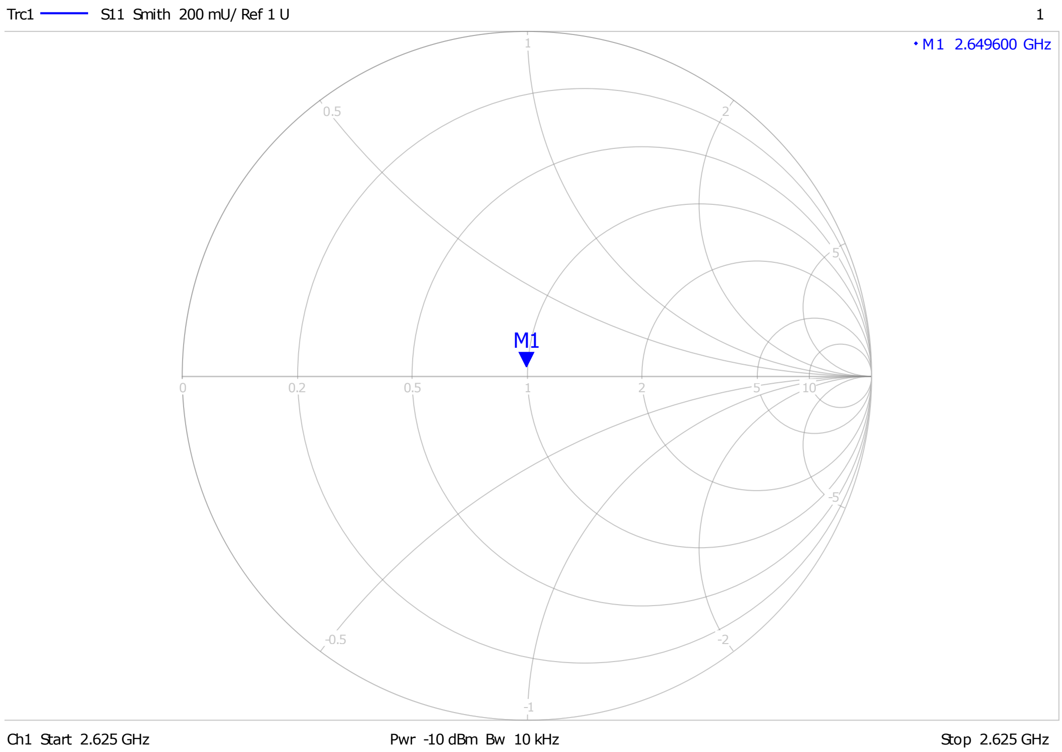

Figure 3.17: S11 from VNA test in the 2625 MHz frequency center, the normalise impedance.

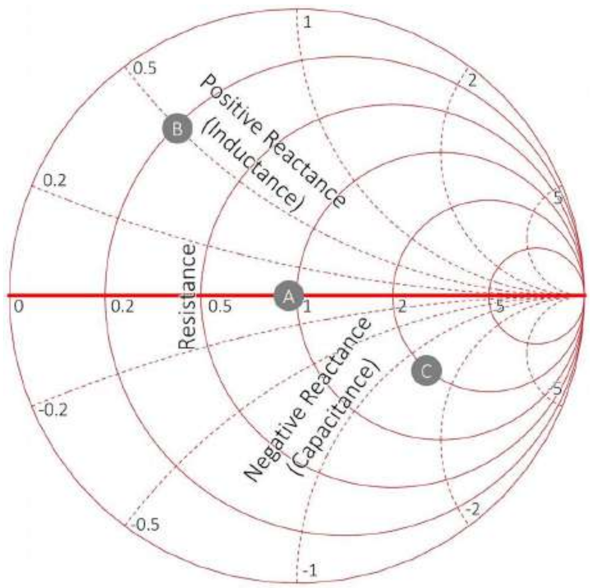

Figure 3.18: Parameter S11 for normalized impedance.

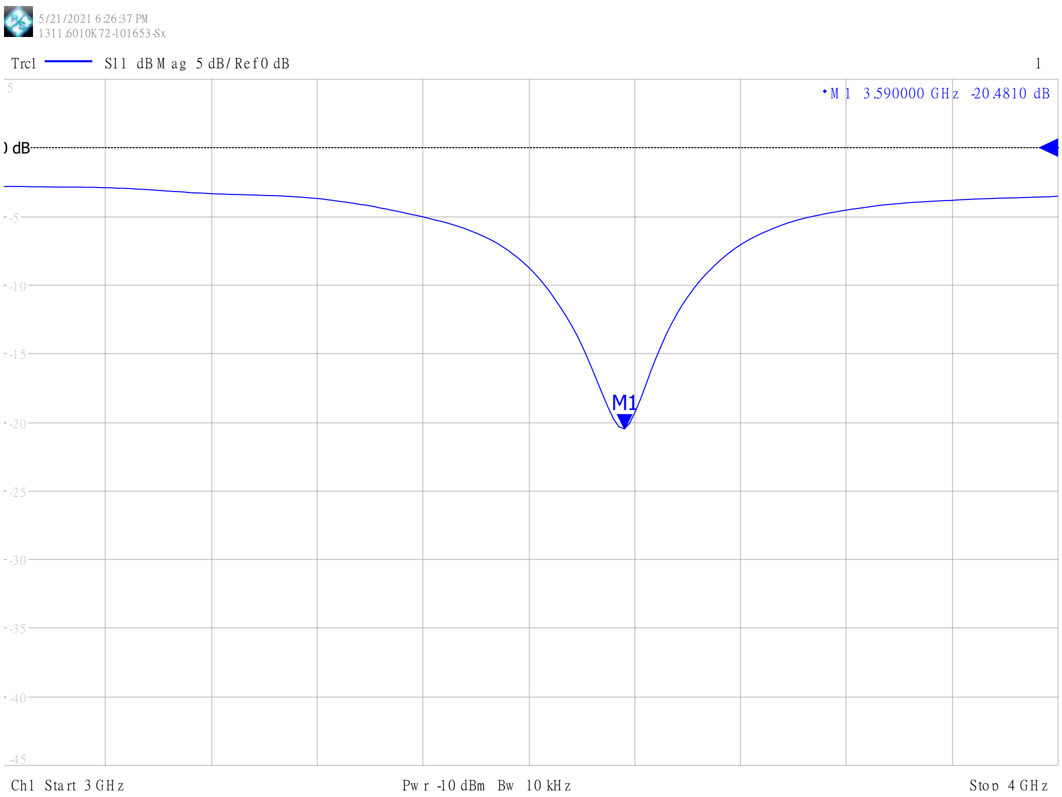

Figure 3.19: Parameter S11 for 3.590 GHz frequency band, measured with VNA.

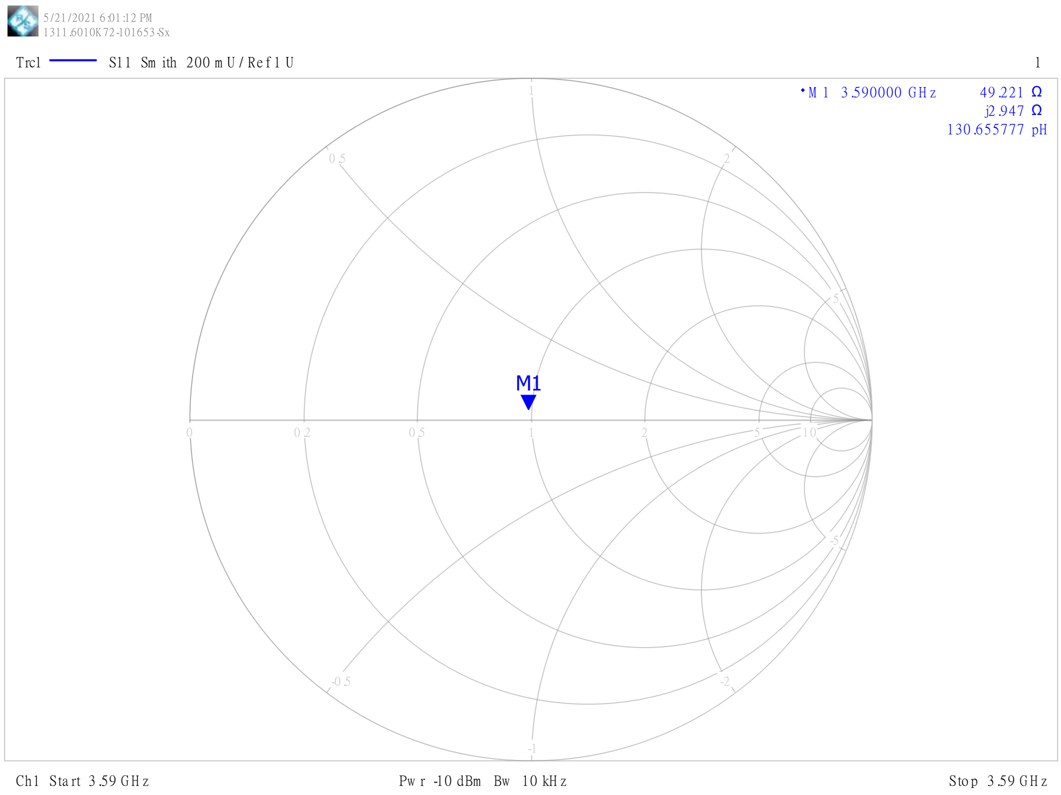

Figure 3.20: Parameter S11 for 3.590 GHz frequency band, measured with VNA.

degrees [52]. And because it is a dipole, the total length of the proposed antennas is $\lambda/2$. The result shows that the increase in the angle results in a reduction in the half-power beam width (HPBW) of the radiation pattern and, consequently, increases the directivity of the antenna, as shown in the Figure 3.21. Although it has a maximum angle of 90 degrees, our antenna's greatest gain is achieved at 30 degrees.

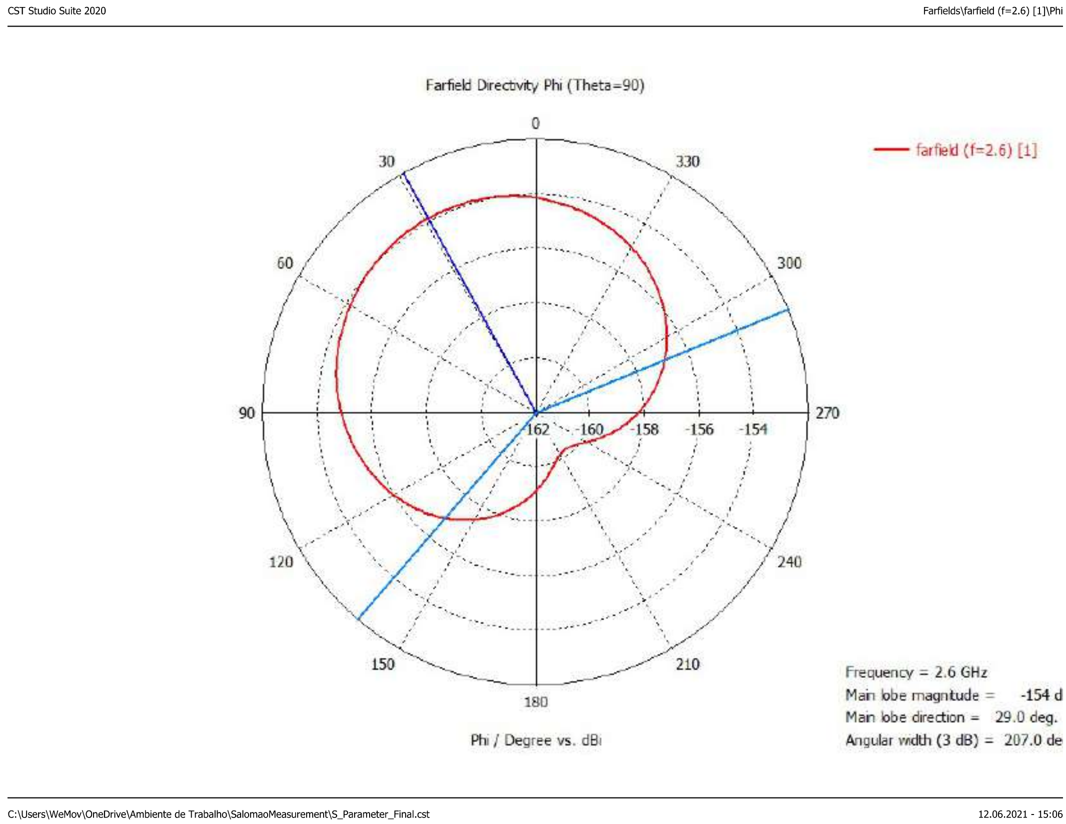

Figure 3.21: Horizontal dipole antenna radiation angle.

HPBW is an angular width measured in degrees from the main lobe of an antenna radiation pattern at half power points, that is, the points where the signal strength is half its peak value. In other words, a (HPBW) indicates the angular separation where the magnitude of the radiation pattern decreases by 50 % (or -3 dB) from the peak of the main beam.

During measurements, we have to use the antennas manufactured by us coupled to the USRP B210 and were positioned in such a way that they could be pointed and well aligned with the other antenna that was coupled to the spectrum analyzer. When this assumption was not fulfilled, the power received by the user and measured by the spectrum analyzer was very low, on the order of -94 dBm on average.

3.9 Summary and Conclusions

Thus, in any scientific research work, the methodology used counts a lot to obtain the best results, so it is up to the researcher to select the methodology that best suits the reality of his research problem. In our case, the method of dividing the tests into phases allowed us to make the tests with the greatest focus at each phase. On the other hand, the choice of three

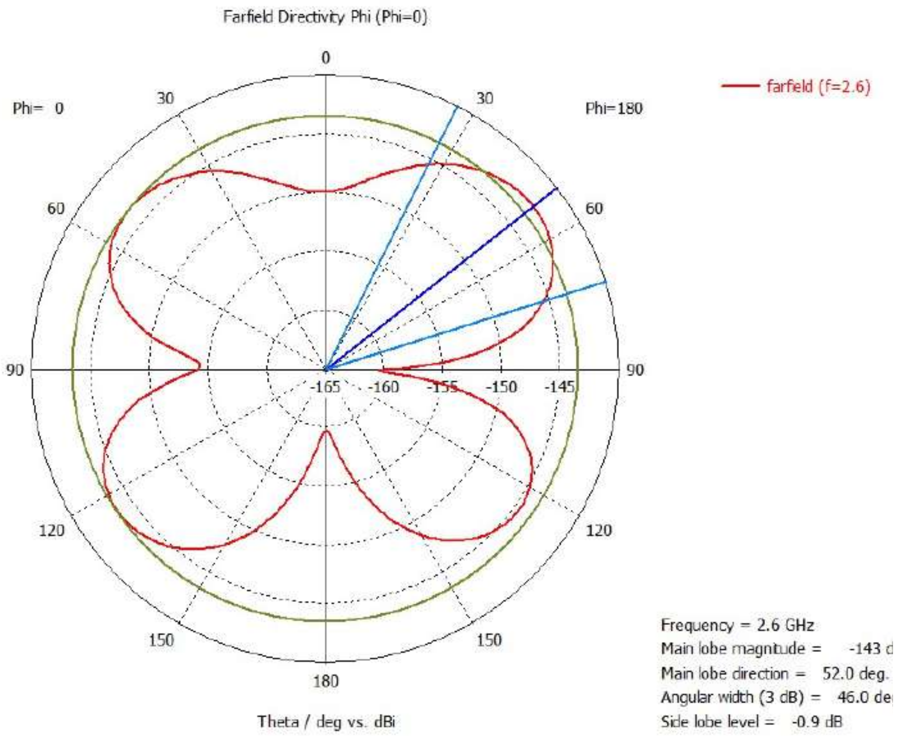

Figure 3.22: Vertical dipole antenna radiation angle.

rooms to set up the scene and apply the srsLTE system and perform the measurements in the room divided into forty-nine points allowed us to obtain the greatest possible precision in the results. In addition, our data collection method is interesting when compared to other methods that the literature presents, because, by dividing the classroom into forty-nine, squares 1 meter apart, it allowed us to accurately assess the distribution of the power received by the user and its variation in each point of the room. Obtaining 3D graphics was only possible because to the coordinates drawn in the measurement room. The manufacture of antennas in the 2.625 GHz and 3.590 GHz frequency bands was also an important issue to consider in our study, as this fact helped us to use antennas that operate at the same frequencies bands as those assigned to us by ICP-ANACOM.

The impedance of the simulated antenna is shown in the Smith Chart, by the point of intersection between the real axis and the imaginary axis. This point of intersection is point 1 pointed by the marker and corresponds to 50 Ω, as reported in [54, 55]. Counterclockwise, above point 1 is the imaginary axis and corresponds to the inductive component equal to $z = 1 + j1$, while below the real axis is the capacitive part given by $z = 1 - j1$. It should be noted that on the real axis, the impedance is zero in the extreme left part of the Smith Chart $(g < 1)$ and increases as it moves towards the center, being infinite in the generator core. At the Appendix B is shown other components of the dipole antenna under study as impedance, gain, radiation, and other parameters.

Chapter 4

Characterization of the Propagation in Indoor Small Cells

4.1 Introduction

Researchers explore the spatial properties of the 5G propagation channel to mitigate interference. Design and analysis of communication systems need transmission simulations to test the transmission and reception algorithms and to obtain system performances such as bit error rates (BER). These simulations require realistic radio channel modeling [56].
Measuring a quantity is comparing it with another that is taken as a standard to allow knowing the real value and the meaning of the magnitude to be measured.

4.2 Indoor Environment Modeling

In this section we present the indoor environment modeling approaches. Our model is designed for a specific building and calibrated with measurements valid for the field, as we use it in outdoor tests.

4.2.1 Average Room Size

Figure 3.4 shows the plan of three 3D classrooms located in the building of the Faculdade de Engenharia da Universidade da Beira Interior in which the tests were carried out. The building has four floors and is large. We modeled the interior of the three rooms by extracting some building plan information. The USRP B210 was placed in the center of the room at the maximum height (3 m) of the mosaic up to the ceiling height. The directive antenna pattern shown in Figure 3.6 was used in simulations and was first mechanically directed to 90° in the vertical plane towards the entrance to the interior of the rooms.

4.2.2 4G Network Emulation

The signal was emitted from a base station (BS) and received by a user (UE) in the srsLTE system consisting of two USRP B210 connected via USB 3.0 - ROHS cables to two computers equipped with the Linux operating system.
The URSP of the BS was mounted at a height of 3.0 m and the UE's was installed at a height of 1.5 metre from the ground. The Figure 4.1 shows the real scenario set for the emission by BS and the reception of power by the UE.
In the Figure 4.1 it is possible to see the equipment used in the tests. The spectrum analyzer was mounted at the same height as the UE (1.5 metre), to guarantee the approximation and allow the best measured signal of the received power.

Figure 4.1: srsLTE set up with USRP B210

4.3 Experimental Measurements in the Indoor Environment

The experiments were carried out in two stages. In the first, measurements were made of the signal emitted by the BS and received by the UE. The performance of the experimental measurements in the second stage was focused on measuring the power signal from the interferer at two different distances from the emitting station.
Using the portable spectrum analyzer from Rohde & Schwarz, it was possible to measure and obtain the numerical data packages of the received power by the user and emitted from the base station as shows in the Figure 4.2. The Figure 4.3 shows receiver power measurement set up interferer one of the room two, while the Figure 4.4 shows the receiver powers measurement of the interferer two mounted in the room three.

Figure 4.2: Base station received power measurement in the room 1.

4.4 Procedures

It should be noted that during our research we went through a measurement phase in which after we concluded and processed the data, we discovered that the graphics were not com-

Figure 4.3: Interferer one power measurements from room 2

Figure 4.4: Interferer two power measurements from room 3

patible with the expected results. Well, the power peaks of the interferers one and two were similar. Which clearly didn't make sense to have equal interference for different distances. This event was due to the fact that the spectrum analyzer could not measure the power peaks (lower and higher), due to the initial configuration of the measurement parameters that we had imposed on it, shown in Appendix D, Table D.1. The results of measurements with these parameters, including in the Table of statistical data shown in the Table D.2 and the normality test shown in the Table D.3.
Once this was verified, we had to change the parameters of the spectrum analyzer according to the table 4.1 to measure a wider range of received power from the highest to the lowest, in order to get better results and conclude our study.
The srsLTE scenario was put into operation and the spectrum analyzer was mounted on a tripod connected to the computer using a USB 2.0 m SHIELDED HIGHSPEED cable. At each of the forty-nine points, 30 data of the power received by the UE were measured. While the tripod that supported the spectro analyzer was moved around the room depending on the successive measurement points, the srsLTE scenario was fixed, as shown in the Figures 4.4, 4.2 and 4.3.

4.5 Resources Used in Measurements

The measurements were made using the devices available in Laboratório de Telecomunicações da (IT) - Covilhã laboratory in order to obtain the expected results and achieve the recommended objectives.

4.5.1 Equipment Used

- A VNA from Rohde & Schwarz, ZNB 40 version from 10 MHz to 40 GHz, to measure the operating frequencies of the antenas, S11 and Smith chart;
- Three USRP B210, namely base station, user and two interferers;
- A Spectrum Analyzer from Rohde & Schwarz FSH8 portable from 100 KHz to 8 GHz;
- A 7th Generation Core i7 branded portable computer with the Windows 10 operating system equipped with R & S InstrumentView software that allowed direct access to the device and programmed the time and number of measurements for each point;
- Two computers with the LinuxUbuntu operating system with the code access to the USRP B210 of the Scenario srsLTE;
- Three cables USB 3.0 m, E330337, AWM 2725 ROhS 30 V;
- One USB 2.0 m SHIELDED HIGHSPEED cable;
- Three tripods, two of them supports 50 kgs and other one for 7 kgs.

4.5.2 Useful software

- Computer Simulation Tecnology (CST - STUDIO), in the student version to simulate manufactured antennas;
- Statistical Package for the Social Sciences (IBM SPSS Statistics), version 27 (IBM Corporation, Armonk, New York), for calculating dispersions in relation to the average because of simple tool use and it is a powerful statistical software platform that offers a robust feature set that allows the organization and processing of data.
- Matrix Laboratory (MATLAB), version R2019b, to plot the graphics;
- R & S InstrumentView.

To measure the intensity of the receiver power the user and the power of each of the interferers for the subsequent statistical treatment, we selected the portable Spectrum Analyzer FSH8 from Rohde & Schwarz capable of measuring frequencies in time demon from 100 KHz to 8 GHz.
Our choice was due to the fact that this device is easy to use and to take sense it is portable allows determining the occupied bandwidth and tracking sources of interference [57].

4.6 Spectrum Analyzer configuration Parameters

Based on the temporary license assigned to us by ICP-ANACOM, the spectrum analyzer was configured to measure the received power by the user at the central frequency of 2625 MHz. The other parameters are shown in the table 4.1.

Table 4.1: FSH8 spectrum analyzer configuration parameters.

Spectrum analyzer FSH8 parameters	
Start Frequency	2620 MHz
Center Frequency	2625 MHz
Stop Frequency	2630 MHz
Bandwidth	3 MHz
Span	10 MHz
Sweep Time	20 ms
Reference	-40 dBm
Range	90 dB
Measure	30
Time interval	1s

We had keep them invariable the parameters of the table 4.1 during measurements in the three sessions of measurements of the power of the base station and of the both interferers to guarantee the principle of equilibrium of experimental[58]. Further Research work in Small Cell Urban Environments two-slope model

4.7 Measurements and Environment Calibration

Before setting up the srsLTE scenario, we had to remove the white board in the classrooms so as not to create an environment with metal interference.
The received power by the user varies with the point and the room from where the measurement was made in relation to the point of the scenario. Thus, it is expected that in room one where the BS scenario was set, the power received is greater. In the remaining two rooms, the power of the interferer is lower in room two and even lower in room three, due to the distance between each one and the measurement room or interest room.

4.8 Further Research Work in Small Cell Urban Environments

Following the experiments in the indoor environment to verify the WINNER II propagation characteristics, ongoing work consists of performing received signal measurements in the old airfield from Covilhã, where a section with circa 410 m of asphalt remains. The aim is to verify the two-slope behaviour of the propagation at UHF/SHF bands in an environment where there is a direct ray and a ray reflected onto the ground. Appendix D.3 briefly presents the urban environment scenario for the field tests to verify the urban micro (UMi) propagation model with two-slope behaviour. Towers with USRP equipment and antennas were mounted for performing experimental tests with srsLTE in 4G/5G like small cell networks at the former Covilhã Aerodrome, as shown in Figure 4.5.

(a) (b)

Figure 4.5: Towers mounted on the antigo aeródromo da Covilhã to carry out tests at 2.6 GHz and 3.5 GHz frequencies ban.

Chapter 5

Experimental Results

5.1 Introduction

The real demonstration of a theory is to put it into practice. In this perspective, the challenge to develop this Master Science work arose, being a practical work based on experimental tests. Through measurements around radiofrequency, it was possible to detect the received power by a user when the signal is emitted from radio communication packets that propagate through small cells.

After the tests with the own cell and interferers, there is required to organize the data for better interpretation and understanding by the reader.

5.2 Statistical Analysis of the Data

To organize the data obtained experimentally through the measurements, namely to analyze, to interpret the observations and to determine the correlations between them, to guarantee conclusions of our investigation, it was necessary to resort to the knowledge of Statistical Inference.

Currently, statistical data are obtained, classified, and stored on digital media and made available in various information systems accessible to researchers [59], who in turn can use them in the development of their scientific activities mainly.

In an experimental measurement work, the data set constitutes a collection of individual and inseparable cases [60]. The knowledge of Statistical Inference helped us to summarize the set of observations and provide simple information with the highest possible quality.

5.3 Sample Size

In each of the forty-nine points in the room, thirty data of the sample of received power were measured (stop after 30 sweep updates) in a time interval equal to one second previously defined in the spectrum analyzer. The choice of the sample number equal to thirty (N = 30), is justified by the fact that it is assumed that the larger the sample size, the better the results obtained [61].

However, there are other factors that intervene in the accuracy of the results. In addition, this choice of the sample number fits the empirical non-probabilistic method, being a convenience sample [61].

5.4 Kolmogorov-Smirnov Normality Test

Considering the size of our sample ($N = 30$), we used the Kolmogorov-Smirnov normality test [62, 63]. The normality test was performed and fulfilled to assess the type of distribution and validate the null hypothesis ($H0$) [63].
Now, in this phase of measurements the results of the Kolmogorov-Smirnov normality test led us to calculate the statistical characteristics and produce the graphics in two ways [64]:

1. Using the median which is the closest value to the real mean of our data;
2. Using the mean and confidence interval which are the more commonly used measure statistical.

Thus, the graphics produced from the data obtained using the spectrum analyzer are paired, being calculated with the median (graphics on the left side) and with the mean and confidence interval (graphics on the right side), in the Figures 5.1, 5.2, 5.3, 5.4 and 5.5.
The results of the normality tests are shown in table 5.1.
In the table 5.2 we present the statistical distribution of the received power measured in dBm. P_r [dBm].

5.5 Dispersion of Measurements

To show the dispersion of the data within the selected sample in relation to the mean (μ), we calculated the variance (S^2) and standard deviation (SD). To measure the variation of the sample mean in relation to the population, we calculated the standard error (SE) and the confidence interval, the values of the minimum and maximum powers, respectively.
For $N = 30$, the variance, standard deviation, and the carrier-to-interference ratio (C/I), respectively were calculated [65], as shown in Appendix C.
Thus, because we used confidence level equal 95 %, z^* value is equal to 1.96 ($z^* = 1.96$) [66].
To interpret the mean confidence interval, we assume that the sample values were selected for the convenience of a population with normal distribution with mean μ and S^2 variance and the level of statistical significance was carefully established at $p < 0.005$.
The level of significance of 5% corresponds to the value of the percentile equal to 1.96, which allowed the construction of a confidence interval that has a 95% probability of containing the real average of the power measured by the spectrum analyzer.
In the data of the measurements made, we tried to keep the uncertainty at low and tolerable levels to guarantee reliability to the results.
By observing the tables D.2, 5.1 and 5.2 and the respective generated graphics, it is clearly concluded that the powers received by the user and measured by the spectrum analyzer in the two measurement phases are different and those of the second phase are more effective we thought. The results of the second phase are more accurate and offer us greater confidence, since, as mentioned above, the spectrum analyzer had a greater range of measurements in the second phase. However, the data result from Kolmogorov-Smirnov normality test, with the significance set at 0.005 and for this reason we used the median in addition to the mean

Table 5.1: Kolmogorov-Smirnov normality test results from SPSS.

Variable	Sig. 1 room	Sig. 2 rooms	Sig. 3 rooms
Point 1	0.001	0.000	0.200
Point 2	0.000	0.000	0.200
Point 3	0.024	0.000	0.083
Point 4	0.000	0.000	0.200
Point 5	0.009	0.000	0.200
Point 6	0.000	0.000	0.200
Point 7	0.000	0.000	0.137
Point 8	0.000	0.000	0.200
Point 9	0.000	0.004	0.200
Point 10	0.000	0.000	0.013
Point 11	0.000	0.21	0.004
Point 12	0.000	0.000	0.146
Point 13	0.000	0.000	0.200
Point 14	0.000	0.000	0.103
Point 15	0.000	0.000	0.200
Point 16	0.000	0.000	0.048
Point 17	0.000	0.000	0.150
Point 18	0.000	0.000	0.200
Point 19	0.000	0.000	0.016
Point 20	0.000	0.004	0.200
Point 21	0.000	0.000	0.016
Point 22	0.000	0.000	0.076
Point 23	0.000	0.000	0.200
Point 24	0.000	0.000	0.021
Point 25	0.000	0.000	0.200
Point 26	0.000	0.000	0.200
Point 27	0.000	0.000	0.200
Point 28	0.000	0.000	0.200
Point 29	0.000	0.000	0.189
Point 30	0.000	0.000	0.200
Point 31	0.000	0.000	0.114
Point 32	0.000	0.000	0.200
Point 33	0.000	0.000	0.117
Point 34	0.000	0.001	0.200
Point 35	0.000	0.000	0.105
Point 36	0.000	0.000	0.200
Point 37	0.000	0.000	0.145
Point 38	0.000	0.000	0.200
Point 39	0.0004	0.000	0.200
Point 40	0.000	0.000	0.200
Point 41	0.000	0.000	0.156
Point 42	0.000	0.000	0.200
Point 43	0.002	0.000	0.134
Point 44	0.000	0.000	0.006
Point 45	0.001	0.002	0.147
Point 46	0.001	0.000	0.198
Point 47	0.009	0.000	0.065
Point 48	0.000	0.000	0.027
Point 49	0.000	0.000	0.200

Table 5.2: Statistical distribution of P_r [dBm] in srsLTE scenario.

Statistical Measure	1 room	2 rooms	3 rooms
Sample Size	30	30	30
Mean	-74.2448	-81.2079.	-87.8724
Median	-73.7150	-81.1400	-88.2300
Min	-91.8400	-91.3300	-92.1100
Max	-47.6500	-57.8000	-78.6600
SD	12.5153	7.9185	2.1528
CI	3.2029	3.2988	1.1033
Standard error	0.3264	0.2065	0.0561

and the confidence interval to obtain and compare the graphics of the received power from own cell and from interferers in 3D.

5.6 Experimental Results

The rooms were framed in orthogonal coordinates and at each point where the power was measured, it corresponds to an ordered pair of coordinates in the plane. The ordered pairs for the coordinates associated with the received power allowed to generate the graphs that reflect the distribution of signal propagation throughout in the room.
Tests have been performed with a video streaming running in the transmitter mode and being received in the UE. Measurements have been made by collecting data during thirty seconds in each of the forty-nine points. First, we have extracted results for a topology without any interferer, i.e., with only one transmitter node in room 1. The position of the UE varies inside the room in the considered (x,y) coordinates. A typical quadrature amplitude modulation (QAM) in use is 64-QAM.
The graphic of the Figures 5.1 shows that the power received by the user when measuring the signal from the base station is the highest in the whole srsLTE scenario. This result is appropriate for the research objectives proposed for this Master Science work. The own cell is the central element of investigation from the interfering nodes. The spectrum analyzer was installed in the same room where the signal was being transmitted signal of its, i.e., the room of interest corresponds to the same room of the experimental tests.
Despite this, it is still possible to observe some points with low received power, due to external factors that result from the change in the characteristics of the room.
The tests carried out in the signal emission rooms, in addition to gaining proximity to the base station, allowed to verify the directions of the Tx and Rx antennas and to kill them in the same direction face to face throughout the process. This procedure resulted in obtaining the highest power since we used directional type antennas.
As the room of interferer move away from spectrum analyzer room the power signal measured decreased in intensity, until it reached very low levels. Figure 5.3 shows a lower power level than that of the base station due to the distance between rooms two where interferer one was mounted and room one where its power was being measured.
The carrier-to-interference ratio C/I graphics characterizes the ratio between the average

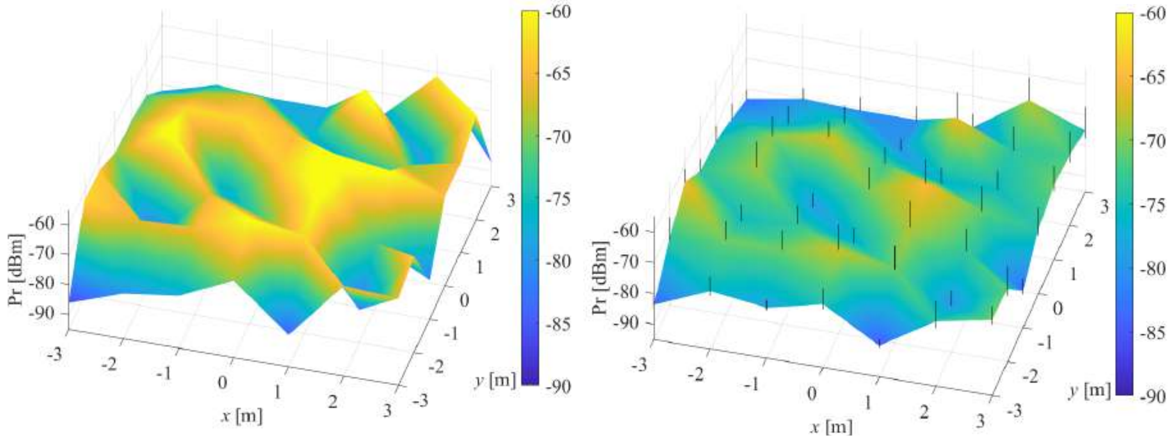

(a) With median (b) With confidence interval

Figure 5.1: Received power from base station in the 2.6 GHz frequency band.

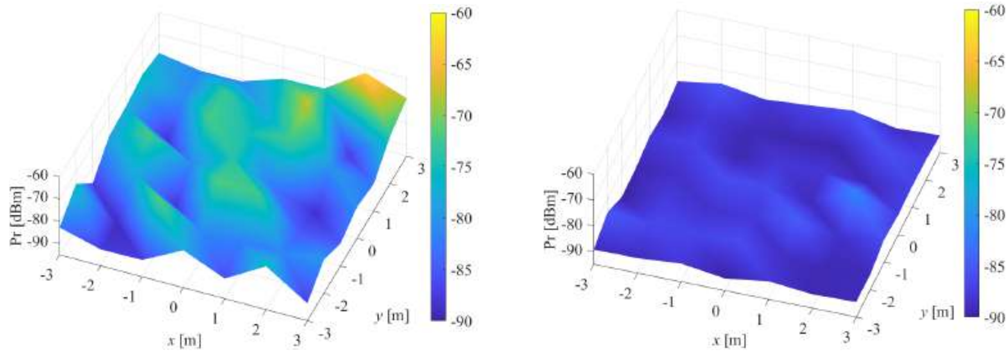

(a) 2 rooms (k=1) (b) 3 rooms (k=2)

Figure 5.2: Received interferer power with median in the 2.6 GHz frequency band.

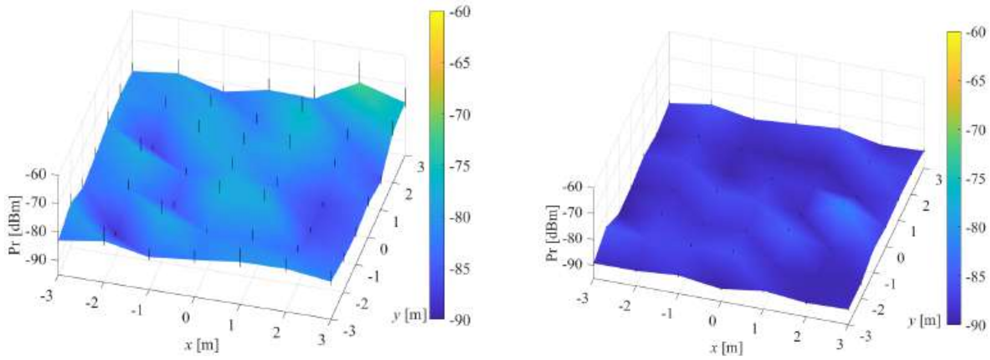

(a) 2 rooms (k=1) (b) 3 rooms (k=2)

Figure 5.3: Received interferer power with confidence interval in the 2.6 GHz frequency band.

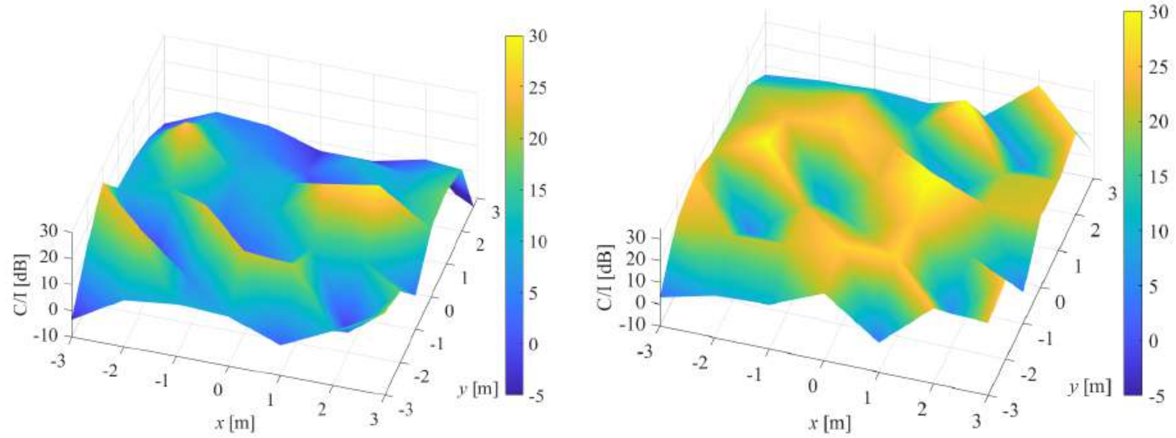

(a) 2 rooms (k=1) (b) 3 rooms (k=2)

Figure 5.4: Average C/I with median in the 2.6 GHz frequency band.

power received from the base station of interest and the average power received power from the interfering base station to the interference. Since the received power at the base station on average is greater than that of the interfering nodes, the difference in both results consists of positive values with decreased confidence intervals.

The power received from the base station and the two interferers is expressed in dBm. Due to the logarithm of the quotient [67], this operation results in subtraction. The measured power of the base station is numerically close to the interfering power of room two. However, the result of the difference between the two is almost null. For this reason, the C/I view graphic for the interfering node in Figure 5.5 circa zero.

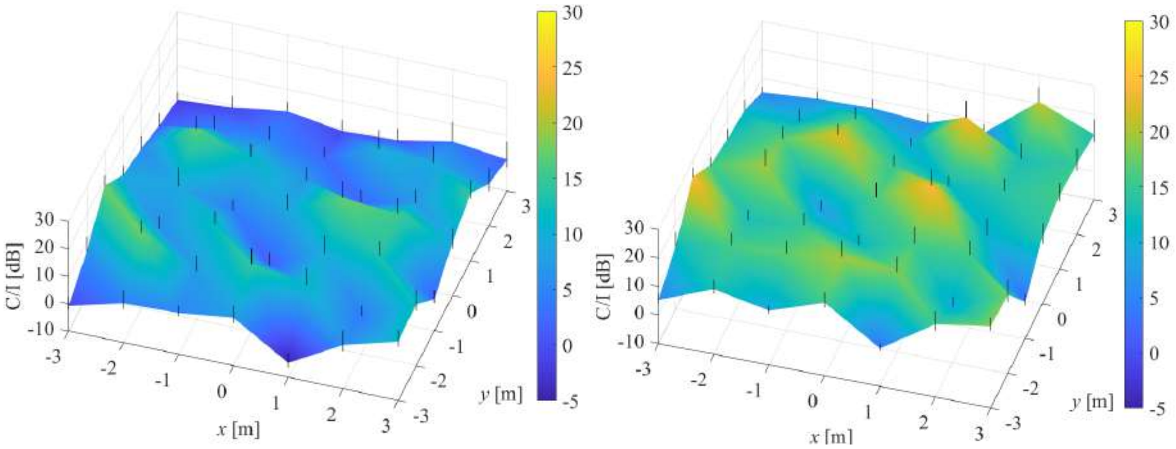

(a) 2 rooms (k=1) (b) 3 rooms (k=2)

Figure 5.5: Average C/I with the confidence interval in the 2.6 GHz frequency band.

The average of C/I for the ninety-nine points in Figure 5.5b (interference from room 3) is circa 14 dB. The difference results of C/I obtained when the interfering is in room 2 (C/I circa 7 dB), because of the lowest received power by the UE from the interfering node.

Essentially the received power from the base station is the highest on average with -74.2448 dBm, that of interferer one is -81.2079 dBm, while the power of interferer two is the lowest

with -87.8724 dBm.
These results were to be expected because of the variation in the distance between the base station and the rooms of interferers in relation to the room where the tests were carried out (the room of interest). On the other hand, the characteristics of the room are a fundamental element that during the testing process, since they cannot be changed.
When taking measurements with interferer at room 3, we try to match the characteristics of the room in such a way that the results are not differentiated by the furniture in the room. However, the reflections on the walls, the type of wall, the mosaic, the whiteboard on the walls and the very movement of the men who carried out the experiments influenced results. In practice, it is almost impossible to keep the three rooms homogeneous.
Although it is very difficult to keep the characteristics of the rooms homogeneous, but during the tests, in addition to removing the whiteboard from the rooms, we tried at all costs to keep the three rooms with the same characteristics. When it was to measure a point, we put the devices to measure and we left the room to ensure that the scenario did not change.

5.7 Attenuation of Room Walls

Looking carefully at the table 5.2 that shows the statistical distribution of the power of the three rooms and associating the results of the graphs, it is possible to see that the wall exerts some influence on the results. Thus, for the same sample size, the average power received by the user in room one is circa 7-9 dBm higher than the average received power measured from the room two, is higher than that in room three. From what is said, it can be concluded that for the tests with the spectrum analyzer, the wall attenuation is circa -7 dB.

5.8 Comparison of Between Experimental and Simulation Results

Fig. 5.6 shows the simulation results for effective exponential of SNR (EESM) by simulation. The representation of the EESM in a single graph simplifies the problem of grouping the vector of SNRs into a single equivalent SNR. A new statistical model for EESM with only two parameters based on the Beta distribution [68], is motivated by the approximation of the central limit for the sum of random variables with finite support.
Results obtained directly in the srsLTE system and those obtained in the simulation are presented in the graphics 5.6, 5.7, 5.8.
The lowest values of EESM are obtained for the case with two rooms, as shown in Fig. 5.6a. The lowest values where obtained near the wall that is common with the neighbor room.
Fig. 5.8 presents results of the comparing for path loss model Winner II, USRP, LTE-Advanced and spectrum analyser.
Indoor propagation scenarios can be mounted in all indoor environments that can be interior corridors, offices, classrooms, urban or rural microcell. The concept also includes transmission from indoors to outdoors and vice versa. In small cell propagation scenarios, the WIN-

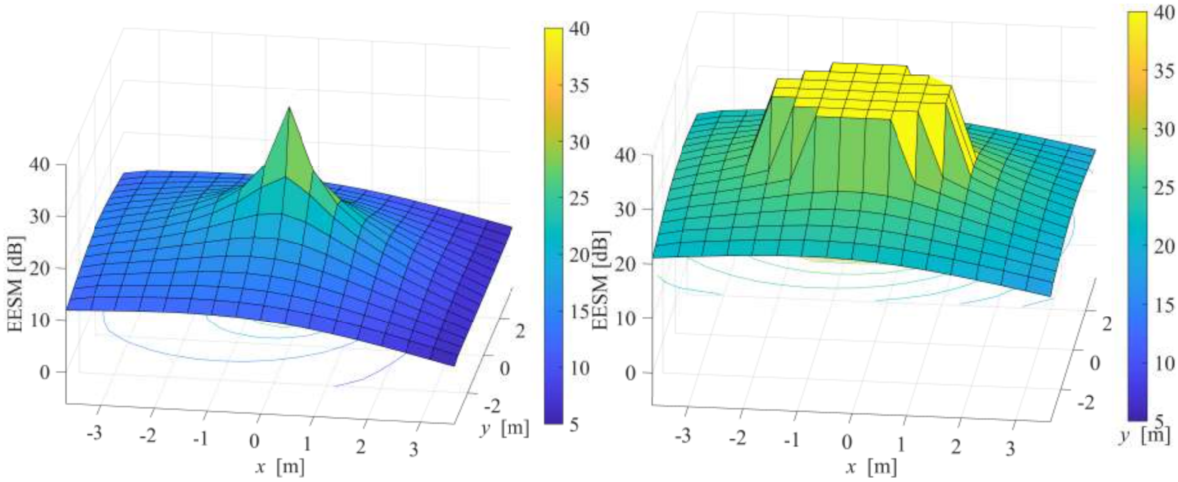

(a) 2 rooms (k=1)

(b) 3 rooms (k=2)

Figure 5.6: EESM for a frequency band of 2.6 GHz with 10 MHz frequency bandwidth, extracted from [11].

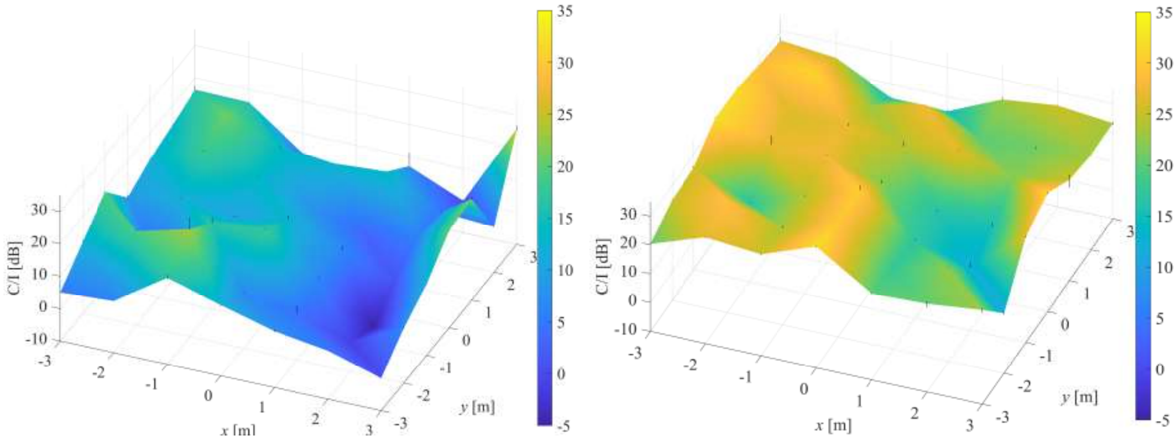

(a) Interferer in room 2, (k=1)

(b) Interferer in room 3, (k=2)

Figure 5.7: C/I for a frequency band of 2.6 GHz measured with USRP B210 extracted from [11].

NER II model [69] represents signal path loss. It has stochastic channel modeling based on geometric configuration that allows the creation of a dual-way (Tx and Rx), directional radio channel model. The channel of the WINNER II model can be built by summing the ray distributions with the specific parameters that include delay, power and the emission and reception angles [70].

The UE is within or outside the building. Since this PLM did not consider the number of walls the WINNER II path model [22] is considered and stands as [71]:

$$\mathrm{PL_{Tx}(x,y)[dB]} = \mathrm{A} * \log_{10}(\mathrm{d}) + \mathrm{B} + \mathrm{C} * \log_{10}(\frac{\mathrm{f_c}}{5}) + \mathrm{X}. \quad (5.1)$$

Here the effects of considering different system frequency is considered and is expressed by fc, in GHz. The fitting parameter A includes the path loss exponent, parameter B is the intercept, parameter C describes the path loss frequency dependence.

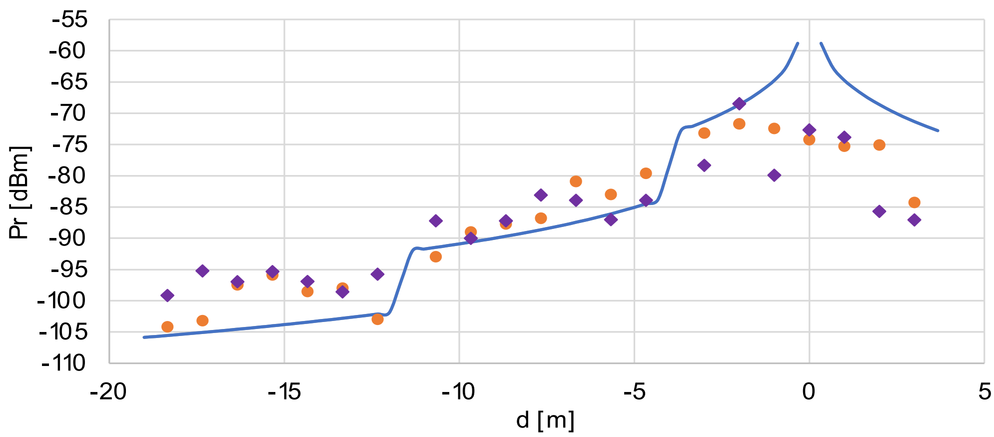

Figure 5.8: Comparison of the WINNER II path loss model with the measurement results.

The view graphics 5.6, 5.7, 5.8, show that both the direct test results and those obtained by simulation and by the srsLTE are similar with those obtained in the measurements with the FSH8 spectrum analyzer. This clearly shows the consistency of our results.

Figure 5.8 compares the received power measured with USRPs (and srsLTE itself) with results obtained with the Winner II path loss model, over the straight line in the centre of the room (y = 0) common to all the BSs. Measurement results with an FSH8 R&S spectrum analyzer are also presented (with purple dots). Results with the orange color represents the power measured directly by the srsLTE system, while the blue line represents the analytical data. As measurements have been taken simultaneously, differences between FSH8 and USRPs measurements were caused by a shadowing from a device to the other. All the results correspond to the 2.6 GHz frequency band made in the 2625 MHz frequency center.

5.9 Outdoor Test Results

As part of the IT research project for the determination of the two-slope behaviour in the UMi scenario, initial LTE-Advanced tests have been performed to verify the propagation of the two ray (with a reflection in the asphalt) from BS implemented with USRP B210 and srsLTE system in the old aerodrome form Covilhã, with the parameters from Table 5.3. We have considered a cell with a length of 80 m and an interfering base station at 320 m. Figure 5.9, shows the initial results of the behavior of the measurements at 2505 MHz (10 MHz bandwidth - this frequency was chosen because of the availability of a directive antenna in this band) of the received power by the user equipment in a straight line between the own cell base station and the interfering base station, for a distance that varies from 0 up to 115 meters, when the tilt of the antenna was circa 7°, in order to have enhanced coverage up to 80-100 m. By the end of this thesis writing the need for further improving the tilt of the BS antenna (and cope with the tilt of the UE antenna) was identified. It should be noted that the power results complies with the Kolmogorov-Smirnov normality test, as shown in Table 5.4.

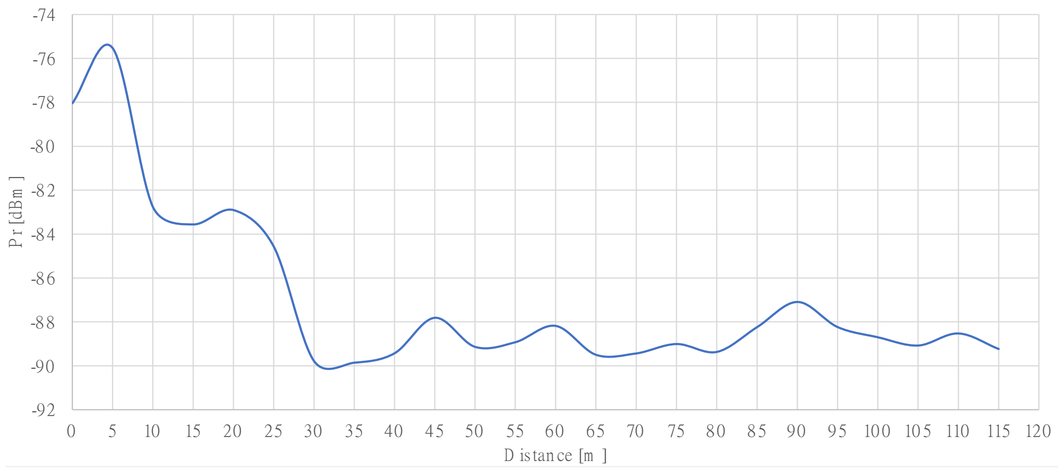

Figure 5.9: Experimental Outdoor Measurements in the 2.505 GHz central frequency.

Table 5.3: Statistical distribution of P_r [dBm] in srsLTE scenario.

Statistical Measure	Pr [dBm]
Sample Size	30
Mean	-83.0093
Median	-88.8400
Min	-91.44
Max	-58.88
SD	3.7524
CI	1.9230
Standard error	0.685

Table 5.4: Kolmogorov-Smirnov normality test results from SPSS by Outdoor.

Variable	Significance
Point 5	0.200
Point 10	0.200
Point 15	0.200
Point 20	0.200
Point 25	0.200
Point 30	0.200
Point 35	0.250
Point 40	0.240
Point 45	0.000
Point 50	0.003
Point 55	0.000
Point 60	0.000
Point 65	0.024
Point 70	0.200
Point 75	0.200
Point 80	0.061
Point 85	0.000
Point 90	0.000
Point 95	0.000
Point 100	0.200
Point 105	0.129
Point 110	0.000
Point 115	0.200

Chapter 6

Conclusions and Topics for Further Research

6.1 Conclusions

Considering the challenges presented, this work explored the concepts of Small Cells Propagation, using experimental tests through the srsLTE scenario in the 2.6 GHz frequency band and the LTE-Sim packet level simulator in the 3.5 GHz frequency band, analytical formulations previously developed by researchers from the Instituto de Telecommunicações da Covilhã [72]. We have considered 4G indoor coverage on a floor with adjacent classrooms of our Departamento de Engenharia Eletromecânica da Universidade da Beira Interior. The size of each of the three rooms is 7.32 × 7.32 square meters. While room 1 is the room of interest, where theoretical and practical measurements took place, BSs that act as wireless interfering nodes are also separately considered either in room 2 or room 3. The method we used allowed us to verify the received power at each of the 49 points in the room. By varying the UE positions within room 1, it was possible to verify that the highest values of the received power occur close to the central BS. However, compared to the WINNER II propagation model, the received power does not decrease suddenly because of the effect of the reduced gain in the radiation pattern in the back part of the antenna. In addition, it was demonstrated that there is an effect of “wall loss”, as the path loss increases between room 1 and room 2 (or between room 2 and 3). If an attenuation for each wall of circa 7-9 dB is considered the trend of the WINNER II model for the interference coming across different walls is verified. Future work includes to analyze in detail results with the spectrum analyzer while considering upper frequency bands that are being considered for 5G New radio and will allow for supporting larger bandwidths, e.g., at the 3.5 GHz and 5.8 GHz frequency bands. In developing this work, we verified that the mm wave spectrum is more valuable as the interferers move away from the base station. So, on the other hand, it was demonstrated that the power from interferer in the room 2 is two low, when compared with that which measured in the room of interest.
In the 5G network emulator srsLTE scenario, signal propagation and data exchange between the base station and the user is efficient for the 2.6 GHz frequency band.

6.2 Future Research

The main feature explored in this work is Small Cells Propagation in Indoor Environment. This study explored small cell propagation using srsLTE in the 2.6 GHz frequency band. The work carried out demonstrated the advantages of applying srsLTE to connect two USRP B210s being a base station and a user. The values of the power of the own cell and of the interferers are different, being those of the own cell higher, having been shown that the study has a positive impact in this regard.

For future activities of this investigation, one of the possibilities is to implement the tests in srsLTE with two interferers connected simultaneously to evaluate the behavior of the received power in this new scenario.
In the implementation of the LTE-based network built on the OpenLTE/srsLTE protocol stack using USRP B210 devices that works as eNodeB and User Equipment which is one of the research projects of the Laboratório de Telecomunicações da Covilhã, the protocol stack can be adjusted to work with higher frequency bands in 5G from the 3.5 GHz band, which was explored for the simulation results. As shows in the Figure 4.5 this will allow research to be carried out studies is to develop experimental tests in srsLTE in the higher frequency bands from 3.5 GHz to also invert different small cell propagation scenarios to better understand the propagation behavior in this scenario both indoor and outdoor. It is the case of the study already started by the Laboratorio do Instituto de Telecommunicações da Covilha at Antido Aeródromo da Covilhã whose photographs are in Appendix D.

References

[1] A. R. Ramos, B. C. Silva, M. S. Lourenço, E. B. Teixeira, and F. J. Velez, "Mapping between Average SINR and Supported Throughput in 5G New Radio Small Cell Networks," in *2019 22nd International Symposium on Wireless Personal Multimedia Communications (WPMC)*, Nov 2019, pp. 1–6. 1

[2] M. G. Kibria, G. P. Villardi, K. Nguyen, K. Ishizu, and F. Kojima, "Heterogeneous Networks in Shared Spectrum Access Communications," *IEEE Journal on Selected Areas in Communications*, vol. 35, no. 1, pp. 145–158, Jan 2017. 1

[3] A. Zaidi, F. Athley, J. Medbo, U. Gustavsson, G. Durisi, and X. Chen, *5G Physical Layer: Principles, Models and Technology Components*. Elsevier Science, 2018. [Online]. Available: https://books.google.pt/books?id=mtJKDwAAQBAJ 1, 2, 3

[4] Q. K. Ud Din Arshad, A. U. Kashif, and I. M. Quershi, "A Review on the Evolution of Cellular Technologies," in *2019 16th International Bhurban Conference on Applied Sciences and Technology (IBCAST)*, 2019, pp. 989–993. 3

[5] A. R. Ramos, "Cellular planning and optimization for 4g and 5g mobile networks," in *Cellular Planning and Optimization for 4G and 5G Mobile Networks*, 2019. 3

[6] J. M. Kelner, M. Kryk, J. Łopatka, and P. Gajewski, "A Statistical Calibration Method of Propagation Prediction Model Based on Measurement Results," in *INTL JOURNAL OF ELECTRONICS AND TELECOMMUNICATIONS, 2020, VOL. 66, NO. 1, PP. 11-16*, 2020, pp. 1–5. 3

[7] A. Khandekar, N. Bhushan, J. Tingfang, and V. Vanghi, "LTE-Advanced: Heterogeneous networks," in *2010 European Wireless Conference (EW)*, 2010, pp. 978–982. 4

[8] I. Bor-Yaliniz, M. Salem, G. Senerath, and H. Yanikomeroglu, "Is 5G Ready for Drones: A Look into Contemporary and Prospective Wireless Networks from a Standardization Perspective," *IEEE Wireless Communications*, vol. 26, no. 1, pp. 18–27, February 2019. 4, 5

[9] J. Horwitz. (2018) PyeongChang will host first major 5G video demonstrations for Olympics viewers. [Online]. Available: https://venturebeat.com/2018/01/31/pyeongchang-will-host-first-major-5g-video-demonstrations-for-olympics-viewers/ 5

[10] M. Arthi and P. Arulmozhivarman, "A Flexible and Cost-Effective Heterogeneous Network Deployment Scheme for Beyond 4G," in *King Fahd University of Petroleum and Minerals 2016*, 2016, pp. 1–18. 5

[11] R. M. Andrade, R. R. Paulo, S. M. Francisco, and F. J. Velez, "Characterization of Indoor Small Cells Propagation," Dec. 2021, submitted to, 2021 IEEE Global Communications Conference (GLOBECOM). 8, 29, 30, 58

[12] Chih-Ping Li, Jing Jiang, W. Chen, Tingfang Ji, and J. Smee, "5G ultra-reliable and low-latency systems design," in *2017 European Conference on Networks and Communications (EuCNC)*, 2017, pp. 1–5. 11

[13] X. Lin, J. Li, R. Baldemair, J. T. Cheng, S. Parkvall, D. C. Larsson, H. Koorapaty, M. Frenne, S. Falahati, A. Grovlen, and K. Werner, "Unveiling the Essentials of the Next Generation Wireless Access Technology," *IEEE Communications Standards Magazine*, vol. 3, no. 3, pp. 30–37, 2019. 11

[14] L. Laine, "Performance Management of 3rd Generation Partnership Project Long Term Evolution," Ph.D. dissertation, AALTO UNIVERSITY, 2011. 11

[15] "3GPP Global Initiative 5G," https://www.3gpp.org/release-15, accessed: 2021-06-03. 11

[16] sqimway. NR frequency band. [Online]. Available: https://www.sqimway.com/nr_band.php=(accessed:28.01.2021) 11, 12

[17] B. J. Lee, J. P. Cho, I. H. Ra, and K. S. Kim, "Propagation Characterization Based on Geographic Location Variation for 5G Small Cells," in *Mobile Information Systems*, 2017. 13

[18] M. Joshi and S. D. Borde, "Comprehensive analysis of various Energy detection parameters in spectrum sensing for cognitive radio systems," in *2014 International Conference on Advances in Communication and Computing Technologies (ICACACT 2014)*, Aug 2014, pp. 1–4. 13

[19] J. Tavares, N. Barroca, H. M. Saraiva, L. M. Borges, F. J. Velez, C. Loss, R. Salvado, P. Pinho, R. Goncalves, and N. Borges Carvalho, "Spectrum opportunities for electromagnetic energy harvesting from 350 MHz to 3 GHz," in *2013 7th International Symposium on Medical Information and Communication Technology (ISMICT)*, 2013, pp. 126–130. 13

[20] ANACOM. (2020) Autoridade Nacional de Telecomunicações. [Online]. Available: https://www.anacom.pt/ 13, 22

[21] O. Aboderin, "Antenna Design for Underwater Applications," Ph.D. dissertation, Faculdade de Engenharia da Universidade do Porto, 2019. 14

[22] R. A. S. . J. W. J., *Physics for Scientists and Engineers with Modern Physics*. Mary Finch & Charlie Hartford, 2008. 14, 15, 74

[23] N. B. . C. G. C., *Radio Propagation and Adaptive Antennas Wireless Communications Networks*. John Wiley & Sons, Inc., Hoboken, New Jersey, 20014. 14, 15

[24] M. G. Hill. Mobile Communications Engineering. [Online]. Available: https://www.accessengineeringlibrary.com/content/book/9780070371033=(accessed:30.01.2021) 14, 15

[25] R. Ramjee and S. Roy, "A CRITIQUE OF FCC'S TV WHITE SPACE REGULATIONS," *Proceedings of the IRE*, vol. 1, no. 20, pp. 1–25, 2016. 16, 17, 73, 74, 77, 79

[26] metrology. Applications of Statistics in Measurement & Testing. [Online]. Available: https://metrology.wordpress.com/statistical-methods-index/basic-theory-of-measurement-and-error/:02.02.2021) 17, 18

[27] M. E. Leinone, M. Sonki, and A. Parssinen, "Statistic Measurement System Analysis of Over- The - Air Measurements of Antenna Array at 28 GHz," *12^a European Conference on Antennas and Propagation (EuCAP 2018)*, vol. 5, no. CP741, pp. 1–5, 2018. 18

[28] T. Yucek and H. Arslan, "Spectrum Characterization for Opportunistic Cognitive Radio Systems," in *MILCOM 2006 - 2006 IEEE Military Communications conference*, 2006, pp. 1–6. 18

[29] H. Arslan and M. E. Sahin, "Cognitive UWB-OFDM: Combining Ultrawideband with Opportunistic Spectrum Usage," in *2006 IEEE Sarnoff Symposium*, 2006, pp. 1–4. 18

[30] J. M. Peterson and B. Grossman, "A process to reduce reproducibility error in VNA measurements," in *2010 76th ARFTG Microwave Measurement Conference*, 2010, pp. 1–5. 18

[31] W. Fan, I. Carton, P. Kyosti, A. Karstensen, T. Jamsa, M. Gustafsson, and G. F. Pedersen, "A Step Toward 5G in 2020: Low-cost OTA performance evaluation of massive MIMO base stations," *IEEE Antennas and Propagation Magazine*, vol. 59, no. 1, pp. 38–47, Feb 2017. 19

[32] B. W. Yap and C. H. Sim, "Comparisons of various types of normality tests," *Journal of Statistical Computation and Simulation*, vol. 81, no. 12, pp. 2141–2155, 2011. [Online]. Available: https://doi.org/10.1080/00949655.2010.520163 19

[33] GeeksforGeeks. (2020) Kolmogorov-Smirnov Test in R Programming. [Online]. Available: https://www.geeksforgeeks.org/kolmogorov-smirnov-test-in-r-programming/ 20

[34] N. B. C. D. S., *Microwave and Wireless Measurement Techniques*. Cambridge University Press, New York, 2013. 20

[35] Ettus. (2021) Research a National Instrument Brand. [Online]. Available: https://www.ettus.com/product-categories/usrp-bus-series/ 20

[36] K. Tsagkaris. Flexible Air iNTerfAce for Scalable service delivery wiThin wIreless Communication networks of the 5th Generation (FANTASTIC-5G). [Online]. Available: https://onlinelibrary.wiley.com/doi/full/10.1002/ett.3050=(accessed:11.01.2021) 20, 21

[37] P.-C. Huang, J.-Y. Tang, C.-H. Feng, P.-Y. Cheng, and L.-S. Jang, "Influences of Extremely Low Frequency Electromagnetic Fields on Germination and Early Growth of Mung Beans," in *2018 IEEE International Conference on Consumer Electronics-Taiwan (ICCE-TW)*, May 2018, pp. 1–2. 22

[38] J. C. Joseph, *Practical Radio Frequency Test and Measurement*. British Library, 2002. 25, 26

[39] WatElectronics.com. Different Types of Wireless Communication Technologies. [Online]. Available: https://www.watelectronics.com/different-types-wireless-communication-technologies/=(accessed:08.02.2021) 25

[40] muRata. (2020) Ultra-Compact, Low-Power-Consumption Cellular LPWA Modules, Enabling All Kinds of Internet Connections. [Online]. Available: https://article.murata.com/en-eu/article/small-low-power-cellular-lpwa-module-1 26

[41] ic.gc.ca. GL-01 — Guidelines for the Measurement of Radio Frequency Fields at Frequencies From 3 kHz to 300 GHz. [Online]. Available: https://http://www.ic.gc.ca/eic/site/smt-gst.nsf/eng/sf01451.html=(accessed:08.02.2021) 27

[42] J. Kretzschmar and D. Schoonaert, "Smith chart for lossy transmission lines," *Proceedings of the IEEE*, vol. 57, no. 9, pp. 1658–1660, 1969. 27

[43] H. J. Taha and M. Salleh, "Multi-carrier transmission techniques for wireless communication systems: A survey," *Wseas transactions on communications*, vol. 8, no. 5, pp. 457–472, 2009. 27

[44] H. Elgala, R. Mesleh, and H. Haas, "Indoor optical wireless communication: potential and state-of-the-art," *IEEE Communications Magazine*, vol. 49, no. 9, pp. 56–62, 2011. 27

[45] N. Yuan, "An equalization technique for high rate OFDM systems," Ph.D. dissertation, University of Saskatchewan, 2003. 28

[46] E. Research. Supporting a variety of development environments on an expansive portfolio of high-performance RF hardware. [Online]. Available: https://www.ettus.com//=(accessed:09.02.2021) 28

[47] G. R. project. (2021) GNU Radio. [Online]. Available: https://www.gnuradio.org/ 29

[48] srsLTE. (2020) Software Radio Systems - srsLTE 20.10.1 Documentation. [Online]. Available: https://docs.srslte.com/en/latest/ 29

[49] srsLTE_git. (2020) Software Radio Systems "srsLTE: Open Source LTE. [Online]. Available: https://github.com/srsLTE/srsLTE 29

[50] N. Nikaein, "OpenAirInterface Simulator/Emulator," 2015. 31

[51] I. Gomez-Miguelez, A. Garcia-Saavedra, P. D. Sutton, P. Serrano, C. Cano, and D. J. Leith, "SrsLTE: An Open-Source Platform for LTE Evolution and Experimentation," in *Proceedings of the Tenth ACM International Workshop on Wireless Network Testbeds, Experimental Evaluation, and Characterization*, ser. WiNTECH '16. New York, NY, USA: Association for Computing Machinery, 2016, p. 25–32. [Online]. Available: https://doi.org/10.1145/2980159.2980163 31

[52] E. Kusumawati, W. Gunawan, Y. Pramono, and A. Rubiyanto, "The effect of various angles of v-shaped cps on the antenna characteristics," vol. 11, 11 2016. 31, 41

[53] C. Y. Chiu, K. M. Shum, C. H. Chan, and K. M. Luk, "Bandwidth enhancement technique for quarter-wave patch antennas," *IEEE Antennas and Wireless Propagation Letters*, vol. 2, pp. 130–132, 2003. 38

[54] J. R. Pereira and P. Pinho, "Using Modern Tools to Explain the Use of the Smith Chart," *IEEE Antennas and Propagation Magazine*, vol. 52, no. 2, pp. 145–150, 2010. 42

[55] C. Zelley, "A spherical representation of the Smith chart," *IEEE Microwave Magazine*, vol. 8, no. 3, pp. 60–66, 2007. 42

[56] P. Laspougeas, P. Pajusco, and J.-C. Bic, "Radio propagation in urban small cells environment at 2 GHz: experimental spatio-temporal characterization and spatial wideband channel model," in *Vehicular Technology Conference Fall 2000. IEEE VTS Fall VTC2000. 52nd Vehicular Technology Conference (Cat. No.00CH37152)*, vol. 2, Sep. 2000, pp. 885–892 vol.2. 43

[57] T. Web. Overview Of Spectrum Analyzer Measurement. [Online]. Available: https://www.tutorialsweb.com/rf-measurements/spectrum-analyzer.htm=(Lastaccessedon2021May17) 47

[58] M. I. Skolnik, "Theoretical Accuracy of Radar Measurements," *IRE Transactions on Aeronautical and Navigational Electronics*, vol. ANE-7, no. 4, pp. 123–129, 1960. 47

[59] T. G. Nick, "Descriptive statistics," *Topics in biostatistics*, pp. 33–52, 2007. 51

[60] L. Statistics. Descriptive and Inferential Statistics. [Online]. Available: https://statistics.laerd.com/statistical-guides/descriptive-inferential-statistics.php=(Lastaccessedon2021April14) 51

[61] G. McPherson, *Statistics in scientific investigation: its basis, application, and interpretation*. Springer Science & Business Media, 2013. 51

[62] S. J. Walters, M. J. Campbell, and D. Machin, *Medical Statistics: A Textbook for the Health Sciences*. John Wiley & Sons, 2020. 52

[63] P. Action. TESTE DE KOLMOGOROV-SMIRNOV. [Online]. Available: http://www.portalaction.com.br/inferencia/62-teste-de-kolmogorov-smirnov=(Lastaccessedon2021May17) 52

[64] C. . EU. (2021) Stuck in the middle – mean vs. median. [Online]. Available: https://www.clinfo.eu/mean-median/ 52

[65] G. Fasano and A. Franceschini, "A multidimensional version of the Kolmogorov–Smirnov test," *Monthly Notices of the Royal Astronomical Society*, vol. 225, no. 1, pp. 155–170, 03 1987. [Online]. Available: https://doi.org/10.1093/mnras/225.1.155 52, 89

[66] D. J. Rumsey. Creating a Confidence Interval for the Difference of Two Means with Known Standard Deviations. [Online]. Available: https://www.dummies.com/education/math/statistics/creating-a-confidence-interval-for-the-difference-of-two-means-with-known-standard-deviations/=(Lastaccessedon2021May17) 52

[67] E. Koelink and W. V. Assche. Leonhard Euler and a q-analogue of the logarithm. [Online]. Available: https://www.ams.org/journals/proc/2009-137-05/S0002-9939-08-09374-X/home.html=(Lastaccessedon2021May17) 56

[68] J. Francis and N. B. Mehta, "EESM-based link adaptation in OFDM: Modeling and analysis," in *2013 IEEE Global Communications Conference (GLOBECOM)*, Dec 2013, pp. 3703–3708. 57

[69] G. Couillard, G. Dahman, G. Poitau, and F. Gagnon, "Quantifying range extension capability of mimo: a simulation study based on winner ii model," in *2019 IEEE Canadian Conference of Electrical and Computer Engineering (CCECE)*, 2019, pp. 1–3. 59

[70] A. Karttunen, J. Jarvelainen, A. Khatun, and K. Haneda, "Radio propagation measurements and winner ii parameterization for a shopping mall at 60 ghz," in *2015 IEEE 81st Vehicular Technology Conference (VTC Spring)*, 2015, pp. 1–5. 59

[71] M.-D. Kim, J. Liang, J. Lee, J. Park, and B. Park, "Path loss measurements and modeling for indoor office scenario at 28 and 38 ghz," in *2016 International Symposium on Antennas and Propagation (ISAP)*, 2016, pp. 64–65. 59

[72] E. Teixeira, S. Sousa, F. J. Velez, and J. M. Peha, "Impact of the propagation model on the capacity in small-cell networks: Comparison between the UHF/SHF and the millimeter wavebands," *Radio Science*, vol. 56, no. 5, pp. 1–13, May 2021. 63

[73] O. Aboderin, "Antenna Design for Underwater Applications," Ph.D. dissertation, Porto University, 2019. 76, 77, 78

[74] S. R. Saunders and A. Aragón-Zavala, *Antennas and propagation for wireless communication systems*. John Wiley & Sons, 2007. 77

[75] A. J. Schwab and P. Fischer, "Maxwell, Hertz, and German radio-wave history," *Proceedings of the IEEE*, vol. 86, no. 7, pp. 1312–1318, July 1998. 77

[76] D. Zhang, "Wavelet transform," in *Fundamentals of Image Data Mining*. Springer, 2019, pp. 35–44. 81

[77] A. Arneodo, G. Grasseau, and M. Holschneider, “Wavelet Transform of Multifractals,” *Phys. Rev. Lett.*, vol. 61, pp. 2281–2284, Nov 1988. [Online]. Available: https://link.aps.org/doi/10.1103/PhysRevLett.61.2281 81

[78] “Página de Álvaro Silva,” https://paginas.fe.up.pt/ ee99051/pstfc/diagrama.html. 81

[79] . M. T. Ami Rida, & Li Yang, *RFID-Enabled Sensor Design and Applications*, 1st ed. Artech House, 2010. 81, 82

[80] C. A. Balanis, *Antenna Theory*, 4th ed. Jhon Wiley & Sons, Inc., Hoboken, New Jersey, 2016. 81

[81] S. K. A. Rahim, A. Abdulrahman, T. A. Rahman, and M. U. Islam, “Measurement of wet antenna losses on 26 GHz terrestrial microwave link in Malaysia,” *Wireless Personal Communications*, vol. 64, no. 2, pp. 225–231, 2012. 83

[82] N. C. Karmakar, *Handbook of smart antennas for RFID systems*. John Wiley & Sons, 2011. 83

[83] M. Deshpande and M. Bailey, “Input impedance of microstrip antennas,” *IEEE Transactions on Antennas and Propagation*, vol. 30, no. 4, pp. 645–650, July 1982. 83

[84] R. Meys and F. Janssens, “Measuring the impedance of balanced antennas by an S-parameter method,” *IEEE Antennas and Propagation Magazine*, vol. 40, no. 6, pp. 62–65, Dec 1998. 83

[85] H. T. F. Sergei A.S., *Antennas*. New York. John Wiley & Sons, INC., 1952. 84

[86] H. T. Friis, “A Note on a Simple Transmission Formula,” *Proceedings of the IRE*, vol. 34, no. 5, pp. 254–256, 1946. 85

[87] T. INSTRUMENTS. Everything RF. [Online]. Available: https://www.everythingrf.com/rf-calculators/friis-transmission-calculator=(accessed:19.03.2021) 85

Appendix A

Mathematical Equations of Continuous Wave forms

One of the mysteries for scientists for a long time was the nature of radiation. Communication technologies take place, generally making use of electromagnetic waves. A device, for example, can include a transmission unit, a dielectric waveguide and a receiving unit. The transmission unit can be configured to transmit electromagnetic waves through a first waveguide. The dielectric waveguide can be configured to direct the electromagnetic wave from the first waveguide to a second waveguide. In addition, the receiving unit can be configured to receive the electromagnetic wave from the dielectric waveguide through the second waveguide.
Electromechanical waves are vibrations that propagate in material medium or in a vacuum but the medium itself doesn't move [25]. Individual atoms and molecules oscillate around their equilibrium positions, but their average position does not change. As they interact with neighbors, they transfer some of their energy to them. In turn, neighboring atoms transfer energy to the next neighbors, in sequence. In this way, energy is transported through the medium, without any material being transported.
Ampere's law is valid only if any electric fields present are constant in time. James Clerk Maxwell recognized this limitation and modified Ampere's law to include time-varying electric fields.
Hertz performed experiments that verified Maxwell's prediction, using apparatus to generate and detect electromagnetic waves. In the 18th century James.C. Maxwell proposed that energy travels through space in the form of an oscillatory field composed of an electrical and magnetic disturbance in the direction perpendicular to the disturbances [25].
In the Figure above, it can seeing oscillations in the electric field (red), and in the magnetic field (blue), which are orthogonal to each other - the electric field is in the XY plane; the magnetic in the XZ plane. The wave is moving in the X direction. An electromagnetic wave can be defined in terms of its oscillation frequency, designated by (ν). The wave moves in a straight line with a constant speed (the speed of light, c); the distance between successive peaks is the (λ), which is equal the ratio between its speed by its frequency, (λ) = c/n.
The electromagnetic spectrum covers a huge range in wavelengths, from very short to very long, as shown in the Figure below.

A.1 Continuous Waveforms Equations

Electromagnetic waves are radiated around 100 MHz frequency [25], as a result of the oscillation of free charges in the transmitter circuit. To generate the prediction of plane electromagnetic waves, we start with Faraday's law, Equation:

$$\oint \vec{E} \cdot \vec{dS} = -\frac{d\Phi_B}{dt} \quad \text{(A.1)}$$

Considering the three directions perpendicular plane XYZ, and each one corresponding one field (electric, magnetic and speed of light), as shown in the Figure A.1.

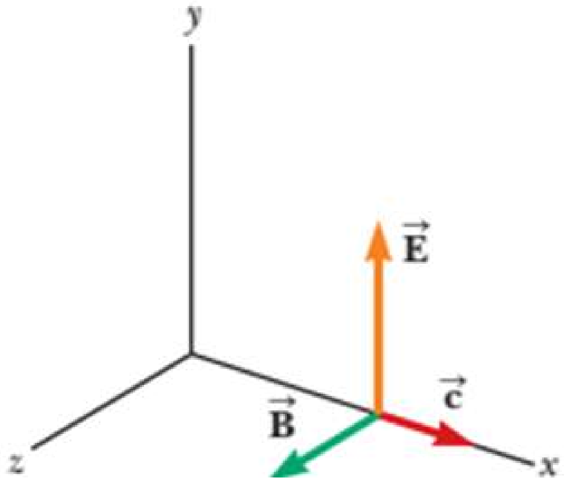

Figure A.1: Plane electromagnetic waves, adapted from [25]

Lets apply this equation to the wave as shown in Figure A.1; the electric field on the right side of the rectangle can be expressed by [22]:

$$E(x + dx) \approx E(x) + \frac{dE}{dx} |_{tconstant}\, dx = E(x) + \frac{\partial E}{\partial x} dx \quad \text{(A.2)}$$

where E(x) is the field on the left side of the rectangle at this instant. Therefore, the line integral over this rectangle is approximately:

$$\oint \vec{E} \cdot \vec{dS} = [E(x + dx)]\ell - [E(x)]\ell \approx \ell(\frac{\partial E}{\partial x})dx \quad \text{(A.3)}$$

Taking the time derivative of the magnetic flux gives:

$$\frac{d\Phi_B}{dt} = dx\frac{d\Phi_B}{dt} |_{xconstant} = \ell dx \frac{\partial B}{\partial t} \quad \text{(A.4)}$$

Substituting Equations A.3 and A.4 into Equation $\oint \vec{E} \cdot \vec{dS} = -\frac{d\Phi_E}{dt})dx$, gives

$$\ell \frac{\partial E}{\partial x} = -\ell dx \frac{\partial E}{\partial t} \quad \text{(A.5)}$$

$$\frac{\partial E}{\partial x} = -\frac{\partial B}{\partial t} \quad \text{(A.6)}$$

$$\frac{\partial E}{\partial x} = -\frac{\partial B}{\partial t} \quad (A.7)$$

the line integral over this rectangle is found to be approximately:

$$\oint \overrightarrow{B} \cdot \overrightarrow{dS} = [B(x)]\ell - [B(x + dx)]\ell \approx -\ell(\frac{\partial B}{\partial x}) \quad (A.8)$$

The electric flux through the rectangle is Φ_E = Edx, which when differentiated with respect to time, gives:

$$\frac{\partial \Phi_E}{\partial t} = \ell dx \frac{\partial \Phi_E}{\partial t} \quad (A.9)$$

Substituting Equations A.8 and A.9 into Equation $\oint \overrightarrow{B} \cdot \overrightarrow{dS} = \mu_0 I + \in_0 \mu_0 = \frac{\partial \phi_E B}{dt}$, derive the result in order the time, gives:

$$\frac{\partial^2 E}{\partial x^2} = \mu_0 \in_0 \frac{\partial^2 E}{\partial t^2} \quad (A.10)$$

taking the derivative of Equation A.9 with respect to x,

$$\frac{\partial^2 B}{\partial x^2} = \mu_0 \in_0 \frac{\partial^2 B}{\partial t^2} \quad (A.11)$$

Equations A.9 and A.10 both have the form of the linear wave equation with the wave speed v replaced by c, where

$$c = \frac{1}{\sqrt{\mu_0 \in_0}} \quad (A.12)$$

c = $\frac{1}{\sqrt{(4\pi.10{-}7.m/A8.85419.10{-}12C^2)}} = 2.99792.10^8$ m/s

Let's evaluate this speed numerically equal c = 2.99792310^8 m/s.

Because this speed is precisely the same as the speed of light in empty space, we are led to believe (correctly) that light is an electromagnetic wave.

The problems related to the concern of the behavior of the propagation of an EM wave in a region free of source and also when there are no external sources of current can be solved by Fourier equations in the other way in which ro and J are equal to zero. Therefore, Maxwell's curl equations in phasor form are written:

$$\nabla \times \mathbf{E} = -j\omega\mu\mathbf{H}, \quad (A.13)$$

$$\nabla \times \mathbf{H} = \mathrm{j}\omega\mu\mathbf{E}, \quad \text{(A.14)}$$

$$\nabla \times \mathbf{E} = 0, \quad \text{(A.15)}$$

$$\nabla \times \mathbf{H} = 0 \quad \text{(A.16)}$$

If only two unknowns **E** and **H** are considered in the equations, they can be resolved to **E** or **H**. So further analysis of these equations will involve take the winding of these equations and combine them separately for one equation in each field. Therefore, in field E, the resulting equation is given by [73]:

$$\nabla \times \mathbf{E} = -\mathrm{j}\omega\mu\nabla \times \mathbf{H} = \omega^2\mu\varepsilon\mathbf{E} \quad \text{(A.17)}$$

Applying vector properties in $\nabla \times \nabla \times \mathbf{P} = \nabla(\nabla.\mathbf{P}) - \nabla^2\mathbf{P}$, it can be written:

$$\nabla(\nabla\mathbf{E}) - \nabla^2\mathbf{E}) = \omega^2\mu\varepsilon\mathbf{E}. \quad \text{(A.18)}$$

Where, substituting A.15 and attending properly A.18, obtain:

$$\nabla^2\mathbf{H} + \omega^\mu\varepsilon\mathbf{H} = 0 \quad \text{(A.19)}$$

The equations A.18 and A.19 are known as Helmoltz equation or wave equation in **E** and **H** field respectively.

Continuing with analyzing the previous equations one can arrive at the equations that produce the wave propagation speed in the medium of as:
$\frac{1}{\sqrt{\mu\varepsilon}}$. where:

$$\mu = \mu_0\mu_\mathrm{r}, \quad \text{(A.20)}$$

$$\varepsilon = \varepsilon_0\varepsilon_\mathrm{r}, \quad \text{(A.21)}$$

μ, ε, magnetic permeability and electric permittivity of free space defined among the universal constant in Table 2.2. In free space μ_r = ε_r = 1 and the resultant parameter is the third element among the universal constant, which is the speed of light. The propagation constant or wave number is another important parameter that can be derived from A.18 and A.19, and is defined as k = $\omega\sqrt{\mu\varepsilon}$. Thus, the equations A.18 and A.19 are re-written as:

$$\nabla^2\mathbf{E} + \mathrm{k}^2\mathbf{E} = 0, \quad \text{(A.22)}$$

$$\nabla^2\mathbf{H} + \mathrm{k}^2\mathbf{H} = 0, \quad \text{(A.23)}$$

Thus, by squaring the propagation constant k, the result satisfies the $\overrightarrow{\mathrm{E}}$ component in equation A.18.

A.2 Maxwell Equations

As was discussed above, the fundamental phenomena for describing electromagnetic induction are simply summed together in four equations which are known as Maxwell's equations and presented as follows [74, 75]:

$$\nabla \times \overrightarrow{\mathrm{E}} = -\frac{\partial\overrightarrow{\mathrm{B}}}{\partial \mathrm{t}} - \overrightarrow{\mathrm{M}}, \quad \text{(A.24)}$$

$$\nabla \times \overrightarrow{\mathrm{H}} = -\frac{\partial\overrightarrow{\mathrm{D}}}{\partial \mathrm{t}} + \overrightarrow{\mathrm{j}}, \quad \text{(A.25)}$$

$$\nabla \times \overrightarrow{\mathrm{D}} = \rho, \quad \text{(A.26)}$$

$$\nabla \times \overrightarrow{\mathrm{B}} = 0 \quad \text{(A.27)}$$

where $\overrightarrow{\mathrm{M}}$ is the fictitious magnetic current density $\mathrm{V/m^2}$, $\overrightarrow{\mathrm{j}}$ is the electric current density in $\mathrm{A/m^2}$ and ρ is the electric charge density in $(\mathrm{C/m^3})$.

Equations A.24, A.25 A.26 and A.27 are the Faraday law of electromagnetic induction, Ampere circuital law, Gauss'law and law of magnetism, respectively [25, 73], which are otherwise known as Maxwell's equations in differential form. The Maxwell equations with the continuity equation and the Lorentz force equation are the foundation of the electromagnetic theory. Also, the constitutive relations are given as:

$$\overrightarrow{D} = \varepsilon\overrightarrow{\varepsilon}, \quad (A.28)$$

$$\overrightarrow{B} = \mu\overrightarrow{H}, \quad (A.29)$$

Here the ε and μ are the permittivity and permeability of the medium respectively. These equations can be converted into integral form by using various vector integral theorems as shown in A.1

So, the Maxwell equations can be written as:

$$\oint_c \overrightarrow{\varepsilon}.\overrightarrow{dl} = -\frac{\partial}{\partial t}\int_s \overrightarrow{B}\overrightarrow{ds} - \int_s \overrightarrow{M}\overrightarrow{ds}, \quad (A.30)$$

$$\oint_c \overrightarrow{H}.\overrightarrow{dl} = -\frac{\partial}{\partial t}\int_s \overrightarrow{D}\overrightarrow{ds} + \int_s \overrightarrow{j}\overrightarrow{ds}, \quad (A.31)$$

$$\int_s \overrightarrow{B}.\overrightarrow{ds} = 0, \quad (A.32)$$

$$\int_s \overrightarrow{D}.\overrightarrow{ds} = \int_v \rho dv = Q, \quad (A.33)$$

Q is the total charge in the close volume V.

In a steady state sinusoidal time dependence, $\overrightarrow{\varepsilon}$ and $\overrightarrow{H}$ will transform as:

$$\overrightarrow{\varepsilon}(x, y, z, t) = \mathbf{E}(x, y, z)e^{j\omega t}, \quad (A.34)$$

$$\overrightarrow{H}(x, y, z, t) = \mathbf{H}(x, y, z)e^{j\omega t}, \quad (A.35)$$

where ω is the angular frequency in radians/second. Assuming linear and isotropic media and taking into consideration an $e^j\omega t$ time dependence, time derivatives in A.34 to A.35 can be replaced by $j\omega$. The output of these are Maxwell's equations in phasor form given as [73]:

$$\nabla \times \mathbf{E} = -j\omega\mathbf{B}, \quad (A.36)$$

$$\nabla \times \mathbf{H} = -\mathbf{J} + j\omega\mathbf{D}, \quad (A.37)$$

$$\nabla \times \mathbf{D} = \frac{\rho}{\varepsilon}, \quad (A.38)$$

$$\nabla \times \mathbf{B} = 0 \quad (A.39)$$

A.3 Fourier Series

Another mathematical approach to study the propagation of electromagnetic waves is with respect to the application of the Fourier series. As already discussed in A, electromagnetic waves propagate in the void with the same speed as light and obey other parameters such as wavelength and the frequency in Hertz.
Any electromagnetic wave function, whether continuous or discontinuous, of a variable y = f(x) could be represented by the Fourier series of the form: It has direct application in the areas of electrical, acoustic, optical engineering, signal processing and image processing. The latter is the one that concerns this study.
Where: f is the frequency in Hertz; ω is the angular frequency $(2\pi f)$
and

$$\frac{1}{\pi}\sum_{n=1}^{\infty}\frac{1}{n}\sin\frac{n\pi\chi}{L} \quad (A.40)$$

Once again, we can see that electromagnetic waves can be transverse or longitudinal waves (compression), depending on whether the displacement of atoms or molecules is perpendicular to the direction of the wave's movement or parallel to the wave's movement respectively. The principle of overlapping waves establishes that two or more waves can move in the same environment with different speeds for different frequencies. When the waves overlap, they create an interference given by the equation [25]:
The recent suggestion that children might in some way be more susceptible to some radiation both because their body are developing and in
There are suspicion that radiation may have undesirable effect on people taking some types of drugs for medical conditions. The fact that the thermal effects of Radiation (if such exist) may eventually prove to adverse effects on human health.

Appendix B

Antenna Simulation, Construction and Measurements

In order to carry out the intended experimental tests, for use in the USRP B210 and to study the behavior of the power received by the user, the antennas in the 2600 MHz band were designed, simulated, built and tested.

B.1 Radio Antennas

A function can be converted in the time domain to the frequency domain using the "integral transformed" operator, e.g Fourier transform that decomposes a function in the sound of a number of potentially infinite sinusoidal components producing a frequency spectrum. There are also transforms that allow conversion to a mixed domain of time and frequency at the same time, such as the Wavelet transform [76].
In the free space, the fields propagate in the form of spherical waves and provide amplitudes inversely proportional to the distance of the antenna. Each radio signal can be represented as an electromagnetic wave [77] that propagates in a certain direction, as discussed in chapter 2.

B.2 Brief Antenna Parameters

Among many others that can be pointed out, an antenna can have the following basic parameters [78]:
The amount used to describe the associated power to an electromagnetic wave is the Poynting vector defined by [79]:

$$\mathrm{W} = \mathrm{E} \times \mathrm{H} \quad \text{(B.1)}$$

where W = Poynting Vector $(\mathrm{W/m^2})$,
E = Electric field strength (V/m),
H = Magnetic field strength (A/m).
Because of the shape of their Radiation diagram, the antennas can be classified into [80]:

- Isotropic;
- Directional;
- Omnidirectional;

B.2.1 Directivity

Is given by the quotient between the radiation intensities in a given direction and the average in all directions (U), (U0), respectively. The average radiation intensity in all directions corresponds to the total power radiated by the antenna and generally its value is expressed in dBi and represents the gain in decibels compared to an isotropic radiator.
The directivity of a half-wave dipole (l=l/2) is given by [79]:

$$\mathrm{D} = \frac{\mathrm{U}}{\mathrm{U}0} = \frac{4\pi}{\mathrm{P_{rad}}} \quad \text{(B.2)}$$

Its value can be approximated by: D = $\mathrm{D_0} \sin^3 \theta = 1.67 \sin^3 \Theta$
The maximum directivity of the dipole occurs in $\theta = \pi/2$ = 1.67;

B.2.2 Gain

The gain is the parameter that allows to evaluate the performance of an antenna and is given by:

$$\mathrm{G} = \frac{\mathrm{Radiationintensity}}{\frac{\mathrm{inputpower}}{4\pi}} = \frac{4\pi \mathrm{U}(\theta,\phi)}{\mathrm{P_{in}}} \quad \text{(B.3)}$$

The total radiated power (Pr) is related to the power supplied to the antenna (Pin), as follows:

$$\mathrm{P_r} = \mathrm{e_{cd}} \mathrm{P_{in}} \quad \text{(B.4)}$$

where $\mathrm{e_{cd}}$ is antenna radiation efficiency.

$$\mathrm{G}(\theta,\phi) = \frac{4\pi \mathrm{U}(\theta,\phi)}{\frac{\mathrm{P_{rad}}}{\mathrm{e_{cd}}}} = \mathrm{e_{cd}}[4\pi \frac{\mathrm{U}(\theta,\phi)}{\mathrm{P_{rad}}}] \quad \text{(B.5)}$$

B.2.3 Radiation Efficiency

When designing an antenna, you have to take into account a very important parameter, which is its radiation. This in turn totals the losses present in the antenna, since not all the power delivered to the antenna is radiated. The radiation efficiency $(\mathrm{e_{cd}})$ is expressed by the quotient between the radiated powers and delivered to the antenna, respectively.
Radiation efficiency is also a measurement of losses at the terminals and the structure of the antenna. These losses may be due to:

- reflections due to mismatch between the line of transmit and an antenna;
- losses in conductors and dielectric.

In an antenna there are three essential losses; due to mismatch $(\mathrm{e_r})$, losses in the conductors $(\mathrm{e_c})$ and in the dielectrics $(\mathrm{e_d})$. So that the total efficiency of the system $(\mathrm{e_0})$, takes the form [81]:

$$\mathrm{e_0 = e_r e_c e_d = e_{cd} er} \quad \text{(B.6)}$$

Here, $\mathrm{e_0}$ is total efficiency, $\mathrm{e_r}$ is adaptation efficiency, $\mathrm{e_c}$ is driver efficiency, $\mathrm{e_d}$ is dielectric efficiency and ρ is voltage reflection coefficient.

B.2.4 Resonance Frequencies

The resonance frequency is the ability of an antenna to transmit or receive electromagnetic waves more efficiently in some frequencies than in others, depending on its design e.g size, shape, configuration, and so on. [82].

B.2.5 Polarization

The polarization of an antenna is the polarization of the wave electromagnetic emitted or received by the antenna. The polarization of the radiated energy varies with the direction to the antenna center, which makes different parts of the radiation diagram may have polarizations many different.

The polarization of a radiated electromagnetic wave is the how the electric field oscillates along the direction propagation.

The polarization of an antenna can be classified as linear, circular or elliptical according the trajectory of the vector that describes the electric field is finds over a line, an ellipse our circular. Linear and circular polarizations are particular cases elliptical polarization.

$$\mathrm{e_0 = e_r e_c e_d} \quad \text{(B.7)}$$

B.2.6 Input Impedance

The input impedance is the antenna impedance at its terminals and is given by:

$$\mathrm{Z_a = \frac{V_{in}}{I_{in}} = R_a + jX_a} \quad \text{(B.8)}$$

Where $\mathrm{Z_a}$ is input impedance in the antenna terminals, $\mathrm{R_a}$ is the real part impedance of antenna or resistence and $\mathrm{X_a}$ is the imaginary part of the antenna impedance or reactance.

The real part of the antenna $(\mathrm{R_a})$ is composed of the radiation resistances $(\mathrm{R_r})$, used to represent the radiation by the antenna, and the resistance loss (RL), used to represent dielectric and conduction losses, or the power dissipated in the antenna [83, 84].

$$R_a = R_r + R_L \quad (B.9)$$

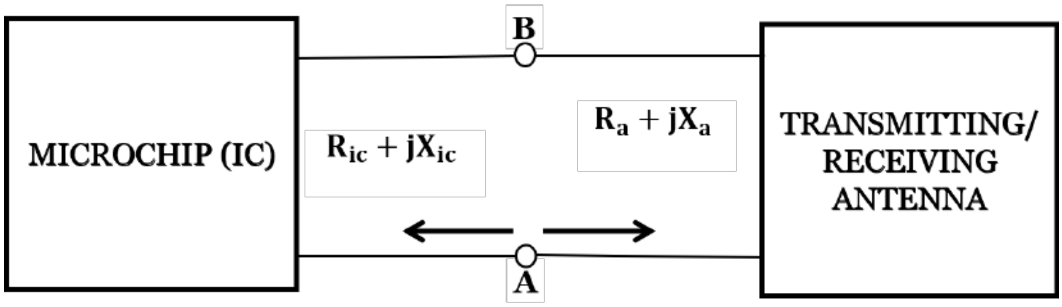

Figure B.1: Antenna model in receive and transmit mode, adapted from [85]

where V_g is the peak voltage of the generator. Thus, the power delivered to the radiation antenna is follows:

$$P_r = \frac{1}{2}|I_g|^2 R_r = \frac{|V_g|^2}{2(R_r + R_L + R_g)^2 + (X_A + X_g)^2}. \quad (B.10)$$

The antenna receives maximum power when
$R_r + R_L = R_g$ and $X_A = -X_g$, for such,

$$P_r = \frac{|V_g|^2}{2}[\frac{R_r}{4(R_r + R_L)^2}] = \frac{|V_g|^2}{8}\frac{[R_r}{(R_r + R_L})\quad (B.11)$$

And, as such, the power dissipated in the antenna is:

$$P_A = P_r + P_L = \frac{|V_g|^2}{8}[\frac{R_r + R_L}{R_r + R_L}] = \frac{|V_g|^2}{8}[\frac{1}{R_r + R_L})] \quad (B.12)$$

The reflection coefficient (ρ) is the parameter that quantifies the adaptation of the antenna and relates the impedance of the chip to the impedance of the antenna at its terminals.

$$\rho = \frac{Z_{in} - Z_0}{Z_{in} + Z_0} \quad (B.13)$$

$$Z_{in} = R_{in} + jX_{ic} \quad (B.14)$$

When the antenna impedance is a conjugate complex of the chip ($\rho = 0$), there is maximum energy transfer and the necessary condition is:

$$R_a = R_{in} \cap X_a = X_{in} \quad (B.15)$$

Usually input impedance is represented as a function of frequency or using antenna simulation programs such as Computer Simulation Technology that we used in this dissertation.

B.2.7 Radiation Efficiency

A metal bar with length l and section A has a resistance for direct current given by:

$$e_{cd} = \frac{R_r}{R_r + R_r} \quad (B.16)$$

Due to the skin effect, the resistance increases with increasing frequency and at high frequencies the resistance can be written as:

$$R_{af} = \frac{1}{P}\sqrt{\frac{\omega\mu_0}{2\rho}} \quad (B.17)$$

where, P is perimeter of the lateral section;
ω = angular frequency, μ_0 is magnetic permeability of the void and
rho is metal conductivity.

B.2.8 Friis Transmission Equation

If two antennas are associated in order to obtain maximum radiation and reception (powers received and emitted), an equation known as the Friis transmission equation is obtained, whose mathematical expression is[86, 87]:

$$\frac{P_r}{P_t} = \left(\frac{\lambda}{4\pi R}\right)^2 G_{0t}G_{0r} \quad (B.18)$$

B.3 Antenna Simulation With CST Studio Software

To simulate an antenna, it is necessary to take into account different basic operating principles, that present different modeling techniques and the simulation tool should offer this flexibility. And, because around of the antenna is the magnetic field and other interferences, since the antenna work system is not isolated, the software used in the simulation must take into account other elements of the system such as the circuit, the power supply and the waveguides.
But the simulation is always accompanied by a margin of error, so testing of the S11 with with another equipment is required. In our case, after the antennas were manufactured,

we performed S11 tests with the vector network analyzer to check the bandwidth and the impedance of the antenna.
On the other hand, around an antenna there are always elements that are part of the system from the human body, the lamps, an aircraft, or another body like a satellite for example.
The set of factors mentioned above makes the antenna simulation process more challenging, requiring the use of more robust software.

B.3.1 Parameters of Simulation

Quantum and Classical Mechanics can describe the electromagnetic orbital angular momentum. Although an antenna cannot generally be described in quantum language, its field characteristics can be redefined in the radio regime. The carriers of circular antennas in phase can generate the fields, in which the several elements of the matrix are distributed around the perimeter of the circle and made such that are phased such that the phase difference between each element is $\delta\Phi = \frac{2\pi l}{N}$.
It should be noted that during the simulation it is necessary to define the material to be used, Whatever copper, gold, tin, or another material.
The performance of installed antenna can be calculated in a reasonable time and standard desktop hardware.

Appendix C

Statistical Treatment Data Formula

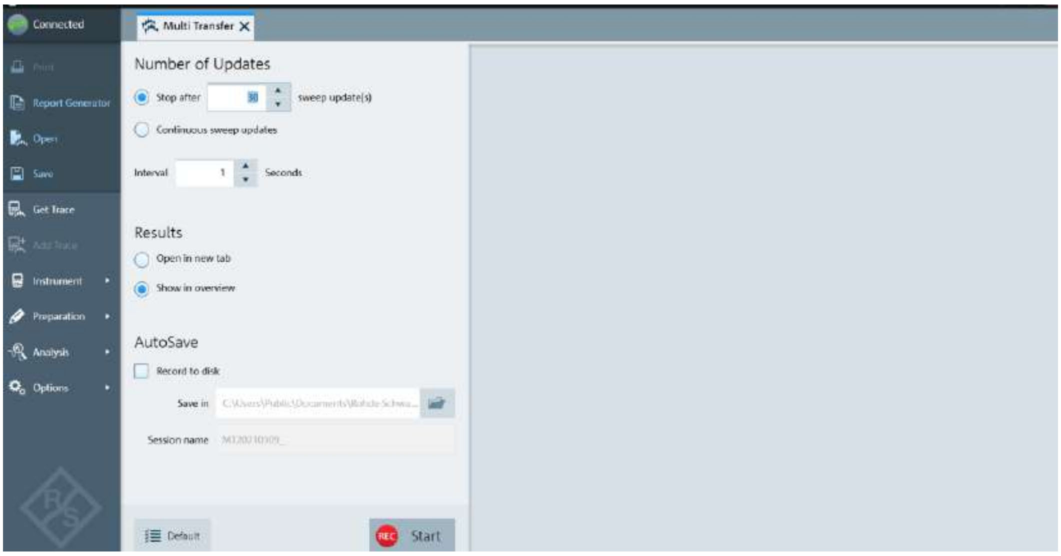

Figure C.1: Sample size

Figure C.2: Adding files

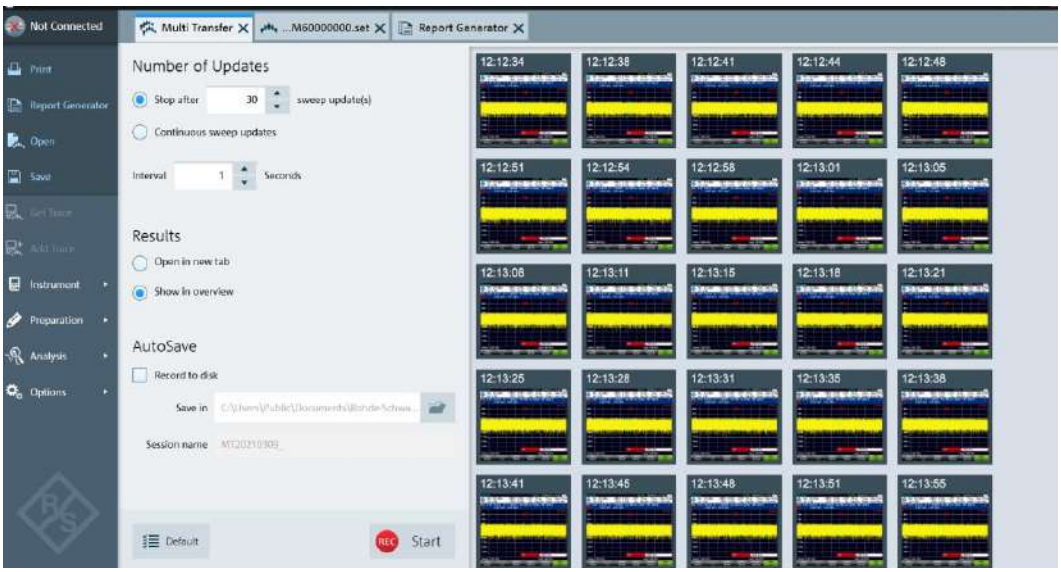

Figure C.3: Real time recording

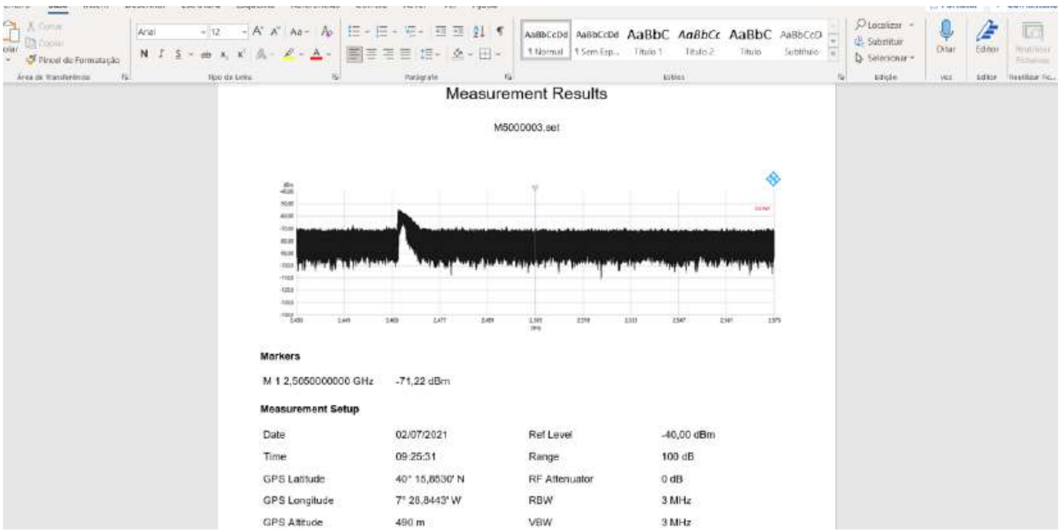

Figure C.4: Spectrum view

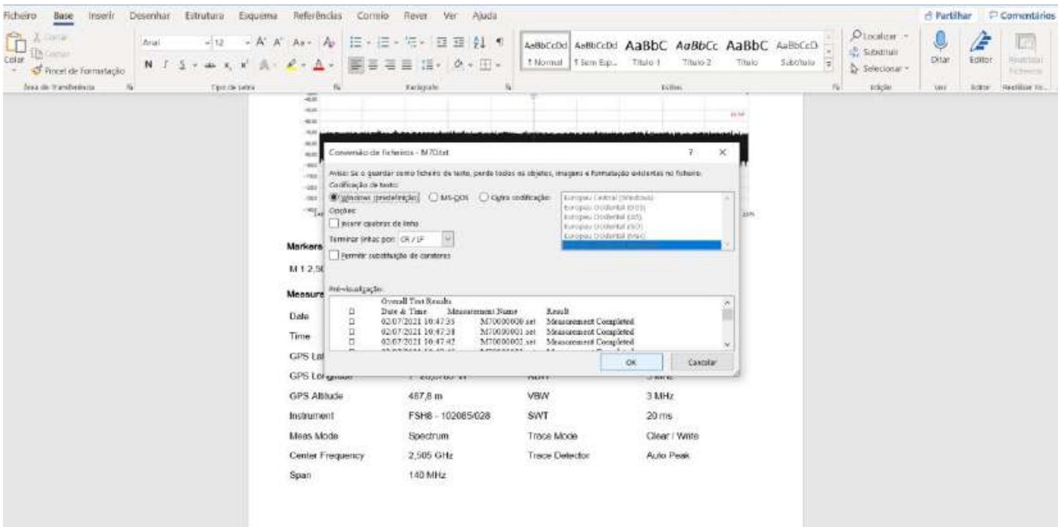

Figure C.5: TXT file recording

C.1 C++ Code for Power Extraction in TXT File

The following code extracts in each TXT file the receiver powers measured by the spectrum analyzer in columns parallel to the measurement time and, in other cases, the parallel columns of the coordinates provided by the GPS can be added.

C.2 Statistic Treatment

The mean, median, standard deviation, variance, standard error and carrier-to-interference ratio, respectively were calculated by [65]:

$$\bar{x} = \frac{\sum_{i=1}^{n} x_i}{N}, \quad \text{(C.1)}$$

$$S^2 = \frac{\sum_{i=1}^{n} (x_i - \bar{x})^2}{N-1} \quad \text{(C.2)}$$

$$\sigma = \sqrt{\frac{\sum_{i=1}^{n} (x_i - \bar{x})^2}{N-1}} \quad \text{(C.3)}$$

$$(\bar{x}_1 - \bar{x}_2) = \sqrt{\frac{\sigma_1^2}{N_1} + \frac{\sigma_2^2}{N_2}} \times z^* \quad \text{(C.4)}$$

where, N is the number of sample size (N = 30), $\bar{x}$ is mean, σ is standard deviation, and $(\bar{x}_1 - \bar{x}_2)$ is average of carrier-to.interference ratio. For significance number equal to 95 %, z^* is equal to 1.96.
The statistical data results from these formulas was used to produce the first group of graphics referred in Appendix D

```
#include <iostream>
#include <fstream>
#include <string>
#include <list>
using namespace std;
#include "Uteis.h"
#include "DADO.h"



void LerFicheiros()
{
    list<DADO *> *VFicheiro_DADOS[50];
    int MAX_FICHEIROS = 50;
    for (int Num_Ficheiro = 1; Num_Ficheiro < MAX_FICHEIROS; Num_Ficheiro++)
    {
        string st_Num_Ficheiro = Uteis::ConvertToString(Num_Ficheiro);
        string Ficheiro_OutPut = "SAIDA/S_" + st_Num_Ficheiro+".txt";
        string Nome_Ficheiro = "DADOS/M5" + st_Num_Ficheiro+".txt";
        string Tempo = "Time";
        string Markers = "Markers";

        list<DADO *> *Ldados = new list<DADO *>();
        VFicheiro_DADOS[Num_Ficheiro] = Ldados;
        ofstream FS(Ficheiro_OutPut);
        ifstream F(Nome_Ficheiro);
        if (F.is_open())
        {
            //cout << "Consegui Abrir o ficheiro " << Nome_Ficheiro << endl;
            int NL = 0;
            string linha_markers, linha_medicoes, linha_lixo, linha_time;
            while (!F.eof())
            {
                getline(F, linha_markers);
                //cout << "Linha[" << NL << "]=" << linha << endl;
                NL++;
                if (linha_markers.find(Markers) != std::string::npos)
                {
                    getline(F, linha_medicoes);
                    getline(F, linha_lixo);
                    getline(F, linha_lixo);
                    getline(F, linha_time);
                   // std::cout << "found!" << '\n';
                    //cout << "Linha[" << NL << "]=" << linha << endl;
                    vector<string> RES_TIME = Uteis::split(linha_time, '\t');
                    /*
                    for (int i = 0; i < RES_TIME.size(); i++)
                        cout << "RES_TIME[" << i << "]=" << RES_TIME[i] << endl;
*/
                    vector<string> RES_MED = Uteis::split(linha_medicoes, '\t');
                    /*
                    for (int i = 0; i < RES_MED.size(); i++)
                        cout << "RES_MED[" << i << "]=" << RES_MED[i] << endl;
*/
                    vector<string> RES_S = Uteis::split(RES_MED[2], ' ');
                    FS << RES_TIME[2] << "\t" << RES_S[0] << endl;
                    DADO *D = new DADO(RES_TIME[2], RES_S[0]);
                    Ldados->push_back(D);
                }
            }
        }
        else
            cout << "Erro no ficheiro " << Nome_Ficheiro << endl;
        F.close();
        FS.close();
    }

    list<DADO *> *Ldados = VFicheiro_DADOS[1];
    int NLinhas = Ldados->size();
    cout << "NLinha = " << NLinhas << endl;
    ofstream FG("Geral.csv");
    for (int Linha = 0; Linha < NLinhas; Linha++)
    {
        for (int Num_Ficheiro = 1; Num_Ficheiro < MAX_FICHEIROS; Num_Ficheiro++)
        {
            list<DADO *> *Ldados = VFicheiro_DADOS[Num_Ficheiro];
            list<DADO *>::iterator it = Ldados->begin();
            std::advance (it,Linha);
            FG << (*it)->Get_DATA() << ";" << (*it)->Get_VALOR() << ";";
        }
        FG << endl;
    }
    FG.close();
    for (int Num_Ficheiro = 1; Num_Ficheiro < MAX_FICHEIROS; Num_Ficheiro++)
```

```
    {
        list<DADO *> *Ldados = VFicheiro_DADOS[Num_Ficheiro];
        for(auto X : *Ldados)
            delete X;
        delete Ldados;
    }
}

int main()
{
    cout << "Ler/Escrever Ficheiros!" << endl;

    LerFicheiros();

    return 0;
}
```

```cpp
#include <iostream>
#include <fstream>
#include <string>
#include <list>
using namespace std;
#include "Uteis.h"
#include "DADO.h"



void LerFicheiros()
{
    list<DADO *> *VFicheiro_DADOS[50];
    int MAX_FICHEIROS = 50;
    for (int Num_Ficheiro = 1; Num_Ficheiro < MAX_FICHEIROS; Num_Ficheiro++)
    {
        string st_Num_Ficheiro = Uteis::ConvertToString(Num_Ficheiro);
        string Ficheiro_OutPut = "SAIDA/S_" + st_Num_Ficheiro+".txt";
        string Nome_Ficheiro = "DADOS/M5" + st_Num_Ficheiro+".txt";
        string Tempo = "Time";
        string Markers = "Markers";

        list<DADO *> *Ldados = new list<DADO *>();
        VFicheiro_DADOS[Num_Ficheiro] = Ldados;
        ofstream FS(Ficheiro_OutPut);
        ifstream F(Nome_Ficheiro);
        if (F.is_open())
        {
            //cout << "Consegui Abrir o ficheiro " << Nome_Ficheiro << endl;
            int NL = 0;
            string linha_markers, linha_medicoes, linha_lixo, linha_time;
            while (!F.eof())
            {
                getline(F, linha_markers);
                //cout << "Linha[" << NL << "]=" << linha << endl;
                NL++;
                if (linha_markers.find(Markers) != std::string::npos)
                {
                    getline(F, linha_medicoes);
                    getline(F, linha_lixo);
                    getline(F, linha_lixo);
                    getline(F, linha_time);
                   // std::cout << "found!" << '\n';
                    //cout << "Linha[" << NL << "]=" << linha << endl;
                    vector<string> RES_TIME = Uteis::split(linha_time, '\t');
                    /*
                    for (int i = 0; i < RES_TIME.size(); i++)
                        cout << "RES_TIME[" << i << "]=" << RES_TIME[i] << endl;
*/
                    vector<string> RES_MED = Uteis::split(linha_medicoes, '\t');
                    /*
                    for (int i = 0; i < RES_MED.size(); i++)
                        cout << "RES_MED[" << i << "]=" << RES_MED[i] << endl;
*/
                    vector<string> RES_S = Uteis::split(RES_MED[2], ' ');
                    FS << RES_TIME[2] << "\t" << RES_S[0] << endl;
                    DADO *D = new DADO(RES_TIME[2], RES_S[0]);
                    Ldados->push_back(D);
                }
            }
        }
        else
            cout << "Erro no ficheiro " << Nome_Ficheiro << endl;
        F.close();
        FS.close();
    }

    list<DADO *> *Ldados = VFicheiro_DADOS[1];
    int NLinhas = Ldados->size();
    cout << "NLinha = " << NLinhas << endl;
    ofstream FG("Geral.csv");
    for (int Linha = 0; Linha < NLinhas; Linha++)
    {
        for (int Num_Ficheiro = 1; Num_Ficheiro < MAX_FICHEIROS; Num_Ficheiro++)
        {
            list<DADO *> *Ldados = VFicheiro_DADOS[Num_Ficheiro];
            list<DADO *>::iterator it = Ldados->begin();
            std::advance (it,Linha);
            FG << (*it)->Get_DATA() << ";" << (*it)->Get_VALOR() << ";";
        }
        FG << endl;
    }
    FG.close();
    for (int Num_Ficheiro = 1; Num_Ficheiro < MAX_FICHEIROS; Num_Ficheiro++)
```

```
    {
        list<DADO *> *Ldados = VFicheiro_DADOS[Num_Ficheiro];
        for(auto X : *Ldados)
            delete X;
        delete Ldados;
    }
}

int main()
{
    cout << "Ler/Escrever Ficheiros!" << endl;

    LerFicheiros();

    return 0;
}
```

```
close all,
clear all;
clc;

R = 3;

PASSO_X =1;
PASSO_Y =1;
X = [-R:PASSO_X:R];
Y = [-R:PASSO_Y:R];
XX = [-R:1:R]; %%per la cdf


SCENARIO='femto-henb-al-centro';
TEST='SINR';
figure('Name','Analisi SINR','NumberTitle','on');

% RIUSO=2;
% AF=1;
%dati=load(strcat('../',SC3ENARIO,'/',TEST,'_riuso_',num2str(RIUSO),'_af_',num2str ↙
(AF)));
dati=importdata('Scenario_sala_49_new2');
SINR = make_sinr(dati, PASSO_X, PASSO_Y, R);
cdf_1 = make_cdf(dati, XX);
%subplot(2,2,1)

%dati=load(strcat('../',SC3ENARIO,'/',TEST,'_riuso_',num2str(RIUSO),'_af_',num2str ↙
(AF)));
ERR_dati=importdata('Scanario_Sala_Salomao_IC_95_new2');
ERR = make_sinr(ERR_dati, PASSO_X, PASSO_Y, R);
cdf_1 = make_cdf(ERR_dati, XX);
%subplot(2,2,1)


axes1 = axes('FontSize',20,'FontName','Times');
surferror(X,Y,SINR,ERR);
zlim([-85 -45]);
xlim([-R R]);
ylim([-R R]);
%title (strcat('RIUSO = ', num2str(RIUSO)),'FontSize',26,'FontName','Times New ↙
Roman');
ylabel('{\it y }[m]  ','FontSize',26,'FontName','Times New Roman' );
xlabel('{\it x }[m]  ','FontSize',26,'FontName','Times New Roman');
zlabel('Pr [dBm]','FontSize',26,'FontName','Times New Roman');
%colorbar('peer',axes1,'ZTickLabel','','ZTick',[0 0.5 1],'FontSize',2RIUSO=3;


% % subplot(2,2,4)
 % plot(XX,cdf_1,'b','LineWidth',1.7)
```

```
% % hold on
% % grid6
% % plot(XX,cdf_2,'r','LineWidPASSO_Xth',1.7)
% % plot(XX,cdf_4,'g','LineWidth',1.7)%
  %title (strcat('CDF of ', TEST),'FontSize',26,'FontName','Times New Roman');
  %xlabel('EESM [dB]','FontSize',26,'FontName','Times New Roman');
  %ylabel('CDF [%]','FontSize',26,'FontName','Times New Roman');
  %xlim([-10 40]);
% % legend('riuso 1', 'riuso 2', 'riuso 4','Location', 'SouthEast');
% % % subplot(2,2,4)

%
%  SCENARIO='femto-henb-al-centro';
% TEST='MCS';
% figure('Name','Analisi SINR'PASSO_X,'NumberTitle','on');
%
% XX = [0:0.001:30]; %%per la cdf
%
% RIUSO=3; %
% AF=1;
% %dati=load(strcat('../',SCENARIO,'/',TEST,'_riuso_',num2str(RIUSO),'_af_',num2str ↙
(AF)));
% dati=importdata('MCS_Freq_26_radius_0.6');
% SINR = make_sinr(dati, PASSO_X, PASSO_Y, R);
% cdf_1 = make_cdf(dati, XX);
% %subplot(2,2,1)
% % %axes1 = axes('FontSize',20,'FontName','Times');
% axes1 = axes('FontSize',20,'FontName','Times');
% surfc(X,Y,SINR)
% zlim([0 30]);
% xlim([-R R]);ylim([-R R])
% %title (strcat('RIUSO = ', num2str(RIUSO)),'FontSize',26,'FontName','Times New ↙
Roman');
% xlabel('{\it x} [m]','FontSize',26,'FontName','Times New Roman' );
% ylabel('{\it y} [m]','FontSize',26,'FontName','Times New Roman');
% zlabel('MCS','FontSize',26,'FontName','Times New Roman');
% %colorbar('peer',axes1,'ZTickLabel','','ZTick',[0 0.5 1],'FontSize',20,...
%   % 'FontName','Times New Roman');
%
% % % subplot(2,2,4)
% %   plot(XX,cdf_1,'b','LineWidth',1.7)
% % % % hold on
% % % % grid
% % % % plot(XX,cdf_2,'r','LineWidth',1.7)
% % % % plot(XX,cdf_4,'g','LineWidth',1.7)
% %   %title (strcat('CDF of ', TEST),'FontSize',26,'FontName','Times New Roman');
% %   xlabel('MCS','FontSize',26,'FontName','Times New Roman');
% %   ylabel('CDF [%]','FontSize',26,'FontName','Times New Roman');
% %  xlim([0 28]);
```

```
% %   set(gca,'XTick',[0:4:28])
% % % % legend('riuso 1', 'riuso 2', 'riuso 4','Location', 'SouthEast');
%
%
%
%
%
%
% TEST='TBS';
% figure('Name','Analisi TBS','NumberTitle','on');
% XX = [1:100:100000]; %%per la cdf
%
% RIUSO=3;
% AF=3;
% %dati=load(strcat('../',SCENARIO,'/',TEST,'_riuso_',num2str(RIUSO),'_af_',num2str
(AF)));
% dati=importdata('TBS_riuso_Freq_26_radius_0.6');
% SINR = make_tbs(dati, PASSO_X, PASSO_Y, R);
% cdf_1 = make_cdf(dati, XX);
% %subplot(2,2,1)
% %axes1 = axes('FontSize',20,'FontName','Times');
% surfc(X,Y,SINR/10^3)
% zlim([0 100]);
% xlim([-R R]);ylim([-R R])
% %title (strcat('RIUSO = ', num2str(RIUSO)),'FontSize',26,'FontName','Times New
Roman');
% xlabel('{\it x} [m]','FontSize',26,'FontName','Times New Roman');
% ylabel('{\it y} [m]','FontSize',26,'FontName','Times New Roman');
% zlabel('TBS [kbits]','FontSize',26,'FontName','Times New Roman');
% %colorbar('peer',axes1,'ZTickLabel','','ZTick',[0 0.5 1],'FontSize',20,...
% %    'FontName','Times New Roman');
%
%
% % % % subplot(2,2,4)
% %   plot(XX/1000,cdf_1,'b','LineWidth',1.7)
% % % % hold on
% % % % grid
% % % % plot(XX,cdf_2,'r','LineWidth',1.7)
% % % % plot(XX,cdf_4,'g','LineWidth',1.7)
% %  % title (strcat('CDF of ', TEST),'FontSize',26,'FontName','Times New Roman');
% %   xlabel('TBS [kbits]','FontSize',26,'FontName','Times New Roman');
% %   ylabel('CDF [%]','FontSize',26,'FontName','Times New Roman');
% %   xlim([1 100]);
% % % % legend('riuso 1', 'riuso 2', 'riuso 4','Location', 'SouthEast');
```

Appendix D

Results From the First Phase of Measurements

D.1 Spectrum Analyzer configuration Parameters

Based on the assigned license temporized from ICP-ANACOM, the spectrum analyzer was configured to measure the power received by the user at the central frequency of 2625 MHz. The other parameters are in the table below.

Table D.1: FSH8 spectrum analyzer configuration parameters.

Spectrum analyzer FSH8 parameters	
Start Frequency	2575 MHz
Center Frequency	2625 MHz
Stop Frequency	2675 MHz
Bandwidth	3 MHz
Span	100 MHz
Sweep Time	125 ms
Reference	-20 dBm
Range	100 dBm
Measure	30
Time interval	1s

Table D.2: Statistical distribution of P_r [dBm] in srsLTE scenario.

Statistical Measure	1 room	2 rooms	3 rooms
Sample Size	30	30	30
Mean	-60.6448	-70.2540	-70.8401
Median	-60.9150	- 70.5300	-70.8800
Min	-72.41	-72.2800	-72.69
Max	-44.84	-60.35	-68.28
SD	4.2913	1.3482	0.6494
CI	2.1992	0.6909	0.3328
Standard error	0.9834	0.2461	0.1185

The results of the normality tests are shown in table D.3.

D.2 Simulation Results in the 3.5 GHz Frequency Band

We have also obtained simulation results for the ESSM in the 3.5 GHz Frequency Band, as shown in Figure D.4.

Table D.3: Kolmogorov-Smirnov normality test results from SPSS.

Variable	Sig. 1 room	Sig. 2 rooms	Sig. 3 rooms
Point 1	0.000	0.200	0.200
Point 2	0.001	0.061	0.200
Point 3	0.000	0.200	0.200
Point 4	0.001	0.200	0.200
Point 5	0.000	0.200	0.200
Point 6	0.154	0.200	0.200
Point 7	0.001	0.021	0.200
Point 8	0.200	0.200	0.200
Point 9	0.057	0.200	0.200
Point 10	0.018	0.008	0.200
Point 11	0.000	0.200	0.200
Point 12	0.000	0.200	0.200
Point 13	0.000	0.200	0.200
Point 14	0.032	0.200	0.200
Point 15	0.020	0.200	0.200
Point 16	0.001	0.200	0.139
Point 17	0.000	0.200	0.200
Point 18	0.000	0.200	0.195
Point 19	0.001	0.193	0.000
Point 20	0.061	0.156	0.019
Point 21	0.000	0.200	0.200
Point 22	0.000	0.200	0.091
Point 23	0.000	0.010	0.016
Point 24	0.200	0.030	0.168
Point 25	0.000	0.199	0.134
Point 26	0.002	0.200	0.200
Point 27	0.000	0.200	0.200
Point 28	0.000	0.200	0.200
Point 29	0.000	0.048	0.200
Point 30	0.000	0.200	0.200
Point 31	0.000	0.200	0.200
Point 32	0.000	0.055	0.200
Point 33	0.000	0.39	0.200
Point 34	0.000	0.200	0.005
Point 35	0.000	0.200	0.200
Point 36	0.000	0.116	0.200
Point 37	0.200	0.080	0.200
Point 38	0.001	0.170	0.051
Point 39	0.000	0.200	0.200
Point 40	0.016	0.140	0.200
Point 41	0.000	0.200	0.200
Point 42	0.000	0.200	0.200
Point 43	0.000	0.200	0.200
Point 44	0.000	0.144	0.200
Point 45	0.000	0.000	0.200
Point 46	0.000	0.200	0.200
Point 47	0.013	0.197	0.044
Point 48	0.000	0.012	0.000
Point 49	0.000	0.200	0.200

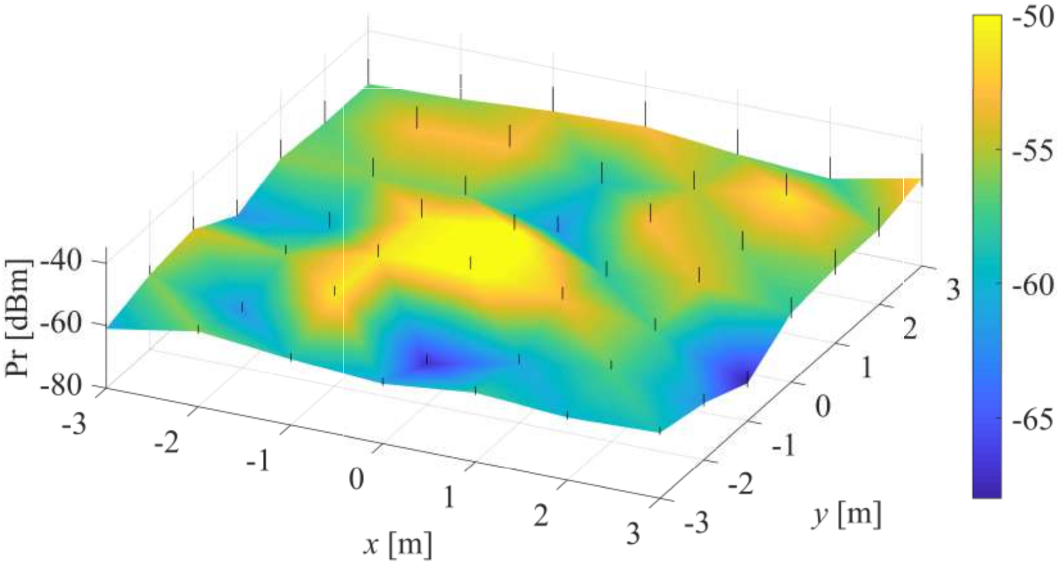

Figure D.1: Base station received power in the room 1

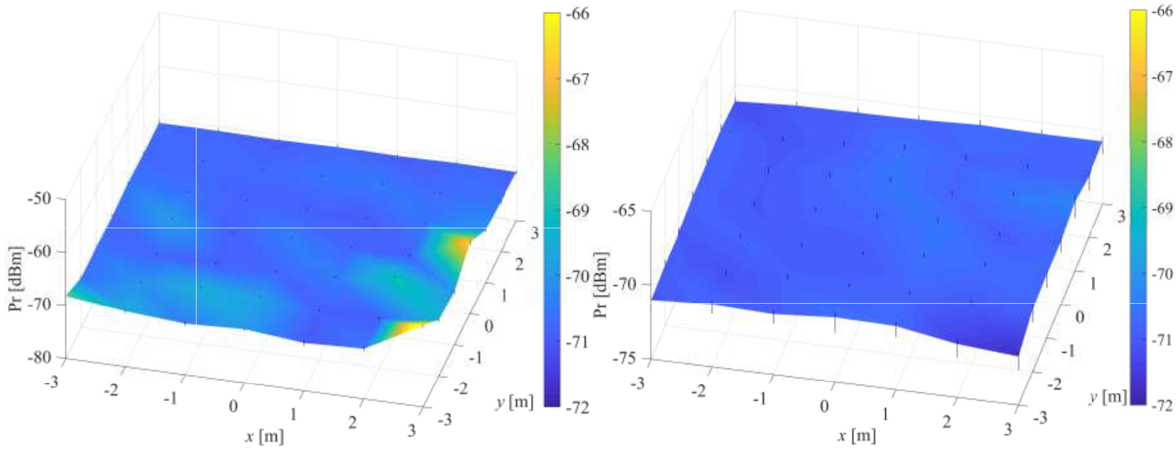

(a) 2 rooms (k=1)

(b) 3 rooms (k=2)

Figure D.2: Interferer power at 2.625 GHz frequency band.

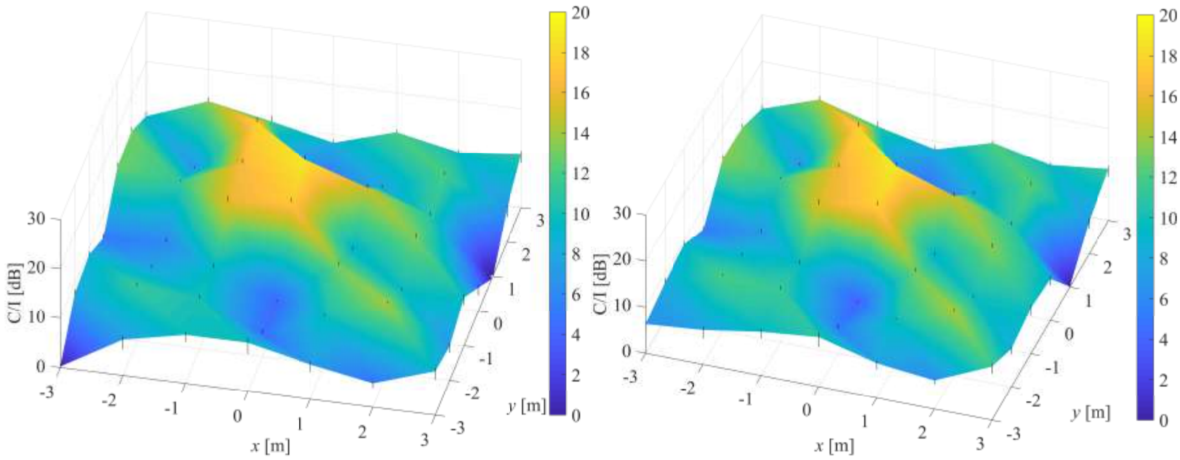

(a) 2 rooms (k=1)

(b) 3 rooms (k=2)

Figure D.3: C/I for interferer power at 2.625 GHz frequency band.

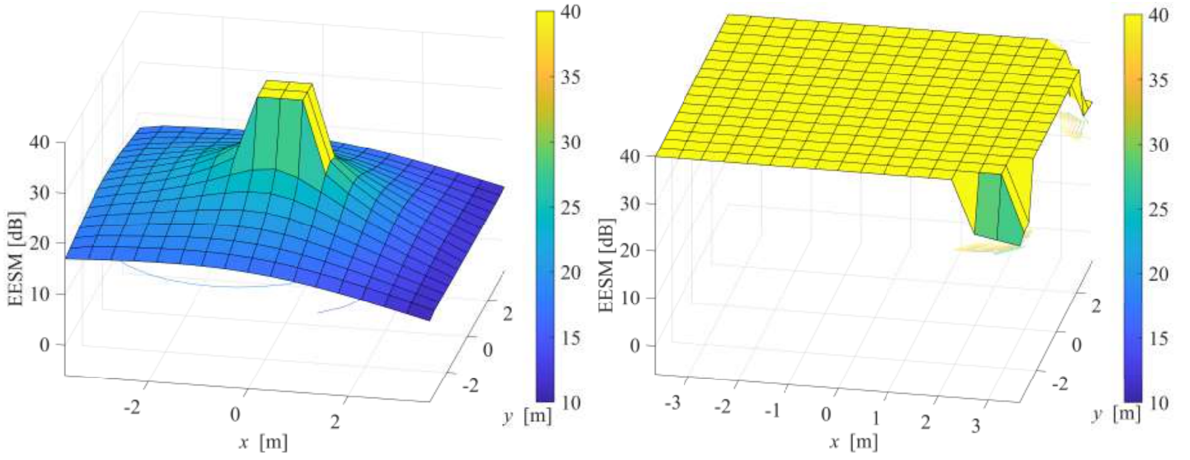

(a) 2 rooms (k=1)

(b) 3 rooms (k=2)

Figure D.4: EESM for a frequency band of 3.5 GHz with 20 MHz frequency bandwidth, (© 2020 by Rui R. Paulo, used with permission. All rights reserved).

D.3 Field Tests in the Urban Scenario at "Antigo Aeródromo da Covilhã"

As part of continuing to investigate the subject of this report, the Laboratório de Telecommunicações da Covilhã set up the towers at the former Covilhã aerodrome for experimental tests in the 2.6 GHz to 3.5 GHz bands. Figure D.5 shows the experimental setup for the research.

(a)

(b)

Figure D.5: Towers mounted on the antigo aeródromo da Covilhã to carry out tests at 2.6 GHz and 3.5 GHz frequencies bands.